GAS CHROMATOGRAPHY/MASS SPECTROMETRY AND NUCLEAR

MAGNETIC RESONANCE ANALYSIS OF

^{13}C LABELED FATTY ACIDS

By

ANTHONY WAYNE HARMON

Bachelor of Science
Bethany Nazarene College
Bethany, Oklahoma
1965

Master of Science
Purdue University
West Lafayette, Indiana
1967

Submitted to the Faculty of the Graduate College
of the Oklahoma State University
in partial fulfillment of the requirements
for the Degree of
DOCTOR OF PHILOSOPHY
May, 1979

GAS CHROMATOGRAPHY/MASS SPECTROMETRY AND NUCLEAR

MAGNETIC RESONANCE ANALYSIS OF

^{13}C LABELED FATTY ACIDS

Thesis Approved:

Louis P. Varga
Thesis Adviser

Thomas Whaley

E. J. Eisenbraun

George R. Waller

Norman N. Durham
Dean of the Graduate College

Name: Anthony Wayne Harmon   Date of Degree: May, 1979

Institution: Oklahoma State University Location: Stillwater, Oklahoma

Titel of Study: GAS CHROMATOGRAPHY/MASS SPECTROMETRY AND NUCLEAR
                 MAGNETIC RESONANCE ANALYSIS OF ^{13}C LABELED FATTY
                 ACIDS

Pages in Study: 147   Candidate for Degree of Doctor of Philosophy

Major Field: Chemistry

Scope and Method of Study: Carbon-^{13}C dioxide was supplied to the green
     algae <u>Chlorella</u> <u>pyrenoidosa</u> in order to biosynthesize a variety of
     fatty acids having a high ^{13}C content. Fatty acid methyl esters
     (FAMEs) were separated from the transesterified liquid extract
     using high-performance liquid chromatography.
          Gas chromatography-mass spectrometry was used to determine
     the total ^{13}C content of the FAMEs by taking repetitive scans as
     each GC peak eluted. The ion intensity data for each mass in the
     molecular ion cluster was least squares fitted to a skewed
     Gaussian curve. Computer programs were written to handle the data,
     correct for natural abundance ^2H, ^{17}O and ^{18}O, and calculate the
     mole % ^{13}C.
          ^{13}C nuclear magnetic resonance was used to determine the ^{13}C
     concentration at specific molecular sites. Paramagnetic shift
     reagents were used to eliminate some overlap of multiplets.

Findings and Conclusions: Due to an inverse isotope effect on the vapor
     pressure of the ^{13}C molecules, $^{13}C/^{12}C$ fractionation occurs on the
     GC column. Thus, an accurate determination of ^{13}C content requires
     that each molecular ion be integrated over the entire GC peak.
          Because the ^{13}C concentration in the carbon dioxide changed
     during the growth period and because the relative rates of fatty
     acid synthesis are dependent on nutrient concentration, each FAME
     exhibited a unique ^{13}C content. The FAMEs were uniformly labeled.

ADVISER'S APPROVAL _____ _Louis P. Varga_ _____

PREFACE

The objective of this study was to develop methods to fully characterize biosynthesized materials having a high ^{13}C content.

Appreciation is due Dr. Louis P. Varga, who served as major adviser, and members of the Advisory Committee. For various time periods Drs. G. R. Waller, S. E. Scheppele, E. J. Eisenbraun, H. A. Mottola, T. W. Whaley, C. T. Gregg and D. G. Ott served on the Advisory Committee. The assistance of Dr. Waller and Mr. Steven Young in obtaining GC-MS data is gratefully acknowledged. A special thanks is due Dr. Whaley for aid in editing the text. Mr. V. H. Kollman provided invaluable assistance with, and helpful discussions about, the culture of algae. Thanks to Drs. T. W. Whaley and R. E. London for helpful discussions about CMR spectrometry and for assistance in obtaining the CMR data. Instruction in the use of the LSMFT program was ably provided by Mrs. C. R. McInteer. The kind assistance of Mr. J. D. Caplinger and Mrs. D. Behrens in the final preparation of the manuscript was much appreciated. Los Alamos Scientific Laboratories generously provided equipment, laboratory space and computer time.

A special thanks is given to my wife, Ann, for her patience, understanding and support during this study. The encouragement of numerous friends was much appreciated.

This study was supported in part by Associated Western Universities, Salt Lake City, Utah. Additional support was provided by Continental

TABLE OF CONTENTS

LIST OF TABLES

LIST OF FIGURES

CHAPTER I

INTRODUCTION

The stable isotopes of carbon, oxygen, nitrogen, and sulfur (ICONS) are useful tracers for many applications where the use of radioactive tracers would be undesirable (e.g., medical or environmental studies). The ICONS program at Los Alamos Scientific Laboratories was initiated to provide quantities of separated stable isotopes at a reasonable cost so the use of these isotopes could be assessed in a variety of research areas (1). It was proposed that ^{13}C, as depleted and/or enriched compounds, could be used to study organic compounds in natural water systems. A literature search revealed that procedures had not been delineated for the isotopic analysis of compounds that are randomly labeled by living organisms. Such compounds may be produced with a high stable isotope content. This is desirable since highly enriched compounds provide increased sensitivity for detecting the tracer. Consequently, the thrust of the project was directed towards the analysis of biosynthetically labeled compounds.

In recent years the supply of the stable isotope ^{13}C has increased dramatically (1,2). The resulting decrease in cost has stimulated the use of ^{13}C as a label in chemical, biochemical and medical research. While most of the reported work has involved the production and/or use of specifically labeled compounds, there is increasing interest in the biosynthetic production of highly enriched compounds (3,4). Such

materials pose two analytical questions; i.e., the overall ^{13}C content

and the distribution of ^{13}C in the molecules.

Several analytical techniques may be used for ^{13}C analysis. The

counting of prompt gamma rays from the reactions $^{12}C(p,\gamma)^{13}N$ and

$^{13}C(p,\gamma)^{14}N$ has been used to assay ^{13}C content (5,6). However, the

method has a 20% variability and is most applicable to samples with a

low ^{13}C content. Infrared spectrometry has been used to measure the

^{13}C content of carbon monoxide (7), but this method is restricted to

simple molecules or gases (e.g., CO_2 from combustion).

Generally, mass spectrometry has been used to analyse stable iso-

topes, and in recent years, gas chromatography mass spectrometry (GC-MS)

has come into increasing use (8-10). The selected ion monitoring (SIM)

technique provides an accurate GC/MS measurement of isotope ratios (11).

However, the SIM method may be subject to error when an analysis of

large, highly-enriched molecules is required. So, spectral scans of

the molecular ion region were used in the present study. This procedure

provided no information about the location of the ^{13}C atoms; but, as

seen in Chapter IV, the complete spectral scan did not provide that

information either.

Since ^{13}C nuclear magnetic resonances are extremely sensitive to

the location of the ^{13}C atom in a molecule (4), the technique was used

to determine the label distribution.

Because of their biological importance and because their mass

spectra were well documented (see Chapter IV), fatty acid methyl esters

(FAMEs) were selected as model compounds for this study. The standard

notation is used to designate individual compounds; such that, the 18:2

FAME has a chain length of eighteen carbon atoms and contains two double bonds (methyl octadecadienoate).

Biosynthesis is the preferred method of preparing a variety of fatty acids that are multiply labeled with ^{13}C. Auxotrophic organisms require acetate, glucose or some other substrate as their source of ^{13}C. Even if such a substrate had been available, the expense would have been prohibitive. The autotrophic algae were selected for use in this study since the readily available carbon-^{13}C dioxide could be used as the carbon source.

Except as noted in the text, the data for this study is recorded in LA notebooks R-2361 and 18108. These notebooks are on file at the Report Library of Los Alamos Scientific Laboratories.

CHAPTER II

BIOSYNTHESIS OF ^{13}C LABELED FATTY ACIDS

Introduction

The first consideration was to select a species of algae, and
several factors had to be considered. A suitable fatty acid profile was
necessary; i.e., the species should produce fatty acids of several
chain lengths and several degrees of unsaturation. The blue-green algae
Anabaena cylindrica, A. flos-aquae, Spirulina platensis (12), Agmenellum
quadruplicatum, Plectonema terebrans, Oscillatoria williamsii (13),
Lyngbya aestuiri, Chroococcus turgidus (14), Nostoc muscorum, and
Chloragloea fritschii (15) all qualify. This requirement would also be
met by most of the green algae; for example, Bracteacoccus minor,
Chlorella vulgaris, C. fusia (16), C. ellipsoidea (17), Coelastrum
microsporum, Scenedesmus quadricauda, and Chlorella pyrenoidosa (14).

The selected species should also be easy to cultivate and have a
high growth rate. Of the numerous possibilities Chlorella pyrenoidosa
is outstanding in both characteristics (18-20). Also, a high tempera-
ture strain (Tx71105) which has a high rate of growth has been isolated
(21-23). Experimentally, the high culture temperature (37-39°C) is much
easier to maintain, since only part of the heat from light sources must
be dissipated. The growth inferred here is an increase in the number
of cells per unit volume, rather than an increase in cell size. Of

4

course, in a continuous culture both processes proceed concurrently.

In the preparation of labeled compounds an important consideration is the efficiency of converting a labeled substrate into the desired compound(s). For biosynthesis with algae this is a two part consideration; namely, the percent of the supplied carbon that is incorporated into cellular material and the percent of fatty acids in the cellular material. It has been shown that over 70% of the carbon supplied as carbon dioxide is converted into cellular material by Chlorella pyrenoidosa (24).

The amount of fatty acids in the cellular material correlates with the amount of total lipid and depends on environmental conditions (25). C. pyrenoidosa grown in a medium with low nitrogen concentration have a higher weight percent of lipid (26,27). It was also found that lipid accumulation was favored when nitrogen was supplied as ammonium rather than nitrate (26). Under low nitrogen conditions high light intensity favors the accumulation of lipid (26). This is likely due, at least in part, to the inhibitory effect of light on cell division (23). Also, C. pyrenoidosa produce more lipid with increasing age of the culture (26,27).

The fatty acid composition is dependent on the stage of growth and environmental conditions. In a synchronous culture of C. pyrenoidosa the amount of 16:0 and 18:2 fatty acids show a marked increase as the growth cycle proceeds toward cell division (28). Polyunsaturated fatty acids predominate in Chlorella grown in high-nitrogen medium, whereas 16:0 and 18:1 fatty acids are preferentially produced in low-nitrogen medium (16,26). As the culture temperature is increased from 22°C to 38°C Chlorella fatty acids show a decrease in the number of double bonds

per molecule and show a lower average chain length (29).

Culture Procedures and Results

Culture Medium

All algae production experiments were carried out aseptically in
a culture medium similar to media used previously for growing Chlorella
pyrenoidosa (24,30). The various nutrient concentrations are given
in Table I for the three media used. In all experiments carbon dioxide
was the carbon source. The high nitrogen concentration in these media
will produce a relatively low percent of cellular lipid, however the
growth of the algae is much faster than with lower nitrogen concentra-
tions so more lipid is produced in a shorter time (25,27).

Cell Culture in a Fermentor

Initially, an effort was made to produce algae in a New Brunswick
CF-250 Fermacell fermentor. The Fermacell fermentor has a stainless
steel vessel, so an internal light source was necessary. Figure 1
shows a sketch of the light source that was constructed for these
experiments. The light source was designed by C. T. Gregg and con-
structed by the Shops Department of Los Alamos Scientific Laboratories.
The discharge lamps are 250 watt General Electric Lucalox lamps
(LU 250/BD). The three lamps were wired individually, so any one or
any combination could be turned on as desired. At a distance of eleven
inches each lamp produced a light intensity of 16,000 lux. The lamp
ballasts were controlled by a powerstat, so the intensity of each lamp
could be controlled between 16,000 lux and 2000 lux.

TABLE I

NUTRIENT CONCENTRATIONS IN CULTURE MEDIA

	Medium A*	Medium B*	Medium C**
KNO_3	1.4 g/l	9.1 g/l	1.0 g/l
KH_2PO_4	2.5	3.0	-
K_2HPO_4	-	-	.25
$MgSO_4 \cdot 7H_2O$	5.0	5.7	.25
$CaCl_2$	.022	.034	.010
$NaCl$	2.0	2.0	.010
$FeCl_3 \cdot 6H_2O$	2.4×10^{-3}	1.9×10^{-2}	-
Iron Ammonium Citrate	-	-	5.0×10^{-3}
H_3BO_3	2.9×10^{-3}	5.7×10^{-3}	2.9×10^{-3}
$MnCl_2 \cdot 4H_2O$	1.8×10^{-3}	3.6×10^{-3}	-
$MnSO_4$	-	-	1.5×10^{-3}
$ZnSO_4 \cdot 7H_2O$	2.2×10^{-4}	4.4×10^{-4}	2.2×10^{-4}
$CuSO_4 \cdot 5H_2O$	7.9×10^{-5}	1.6×10^{-4}	7.5×10^{-5}
$Na_2MoO_4 \cdot 2H_2O$	3.2×10^{-5}	6.4×10^{-5}	-
$(NH_4)_6Mo_7O_{24} \cdot 6H_2O$	-	-	1.8×10^{-6}
$KCr(SO_4)_2 \cdot 12H_2O$	9.8×10^{-5}	2.0×10^{-4}	-
NH_4VO_3	2.3×10^{-5}	4.6×10^{-5}	-
$NaWO_4 \cdot 2H_2O$	1.8×10^{-5}	3.6×10^{-5}	-
$NiSO_4 \cdot 6H_2O$	4.5×10^{-5}	9.0×10^{-5}	-
$KTi(C_2O_4)_2 \cdot 2H_2O$	7.4×10^{-5}	1.5×10^{-4}	-
$Co(NO_3)_2 \cdot 6H_2O$	5.0×10^{-5}	1.0×10^{-4}	-
KOH	.28	.56	-
EDTA	.50	1.0	

*   Ref. (30)

** Ref. (24)
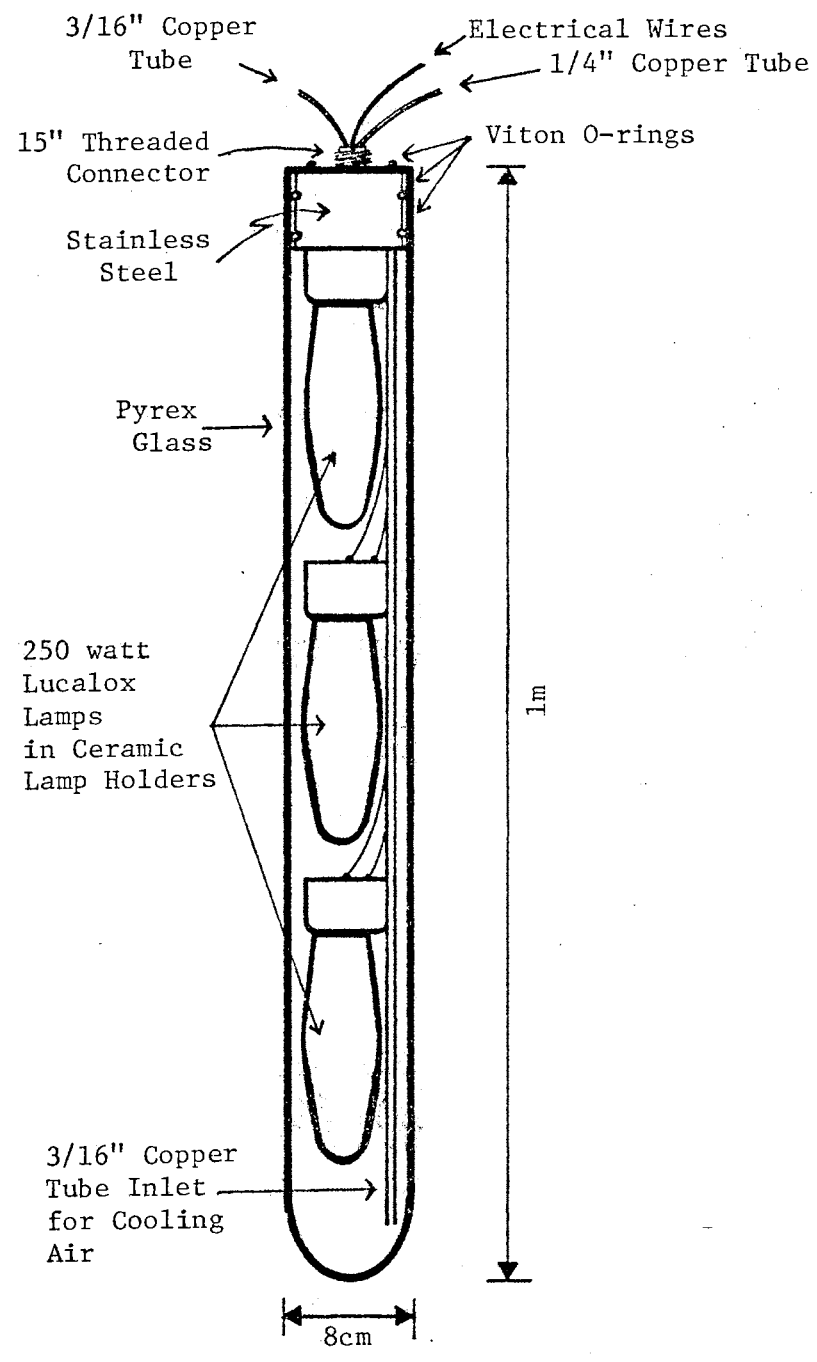
Figure 1. Light Source for Fermacell Fermentor

Agar slants of <u>Chlorella</u> <u>pyrenoidosa</u> (high temperature strain Tx-71105) were obtained from the Starr Collection, Department of Botany, Indiana University, Bloomington, Indiana. These slants were used to inoculate a 500 ml spinner flask. After about seven days of growth, the spinner flask was used to inoculate a fresh spinner flask and a 14 liter New Brunswick MF-114 Microferm fermentor. After 7 to 14 days of growth this small fermentor was used to inoculate the Fermacell fermentor. Standard fluorescent (cool white) and incandescent lamps were used to provide light for the spinner flasks and the Microferm fermentor.

Little or no growth was observed in the Fermacell fermentor whether using medium A, B or C. Cells in solution clumped badly and cells became caked on the light source, and on vessel walls and agitation baffles near the light source. Therefore, experiments with the fermentor were discontinued.

Cell Culture in a Polycarbonate Growth Chamber

The polycarbonate culture chamber (Figure 2) was designed by V. H. Kollman and built by the Shops Department of Los Alamos Scientific Laboratories. It is analogous to the lucite growth chamber described previously (24). The box was half-filled (20 liters) with medium and oscillated horizontally at 28 cpm. The curved ends of the box produced enough wave action to wash all interior surfaces. This insured uniform distribution of nutrients, aided temperature control and maximized cell exposure to light in dense cultures.

Light was provided by very high-intensity natural-outdoor fluorescent lamps (Sylvania) mounted above and below the culture box. Only one lamp was used to start each batch, and then additional lamps were
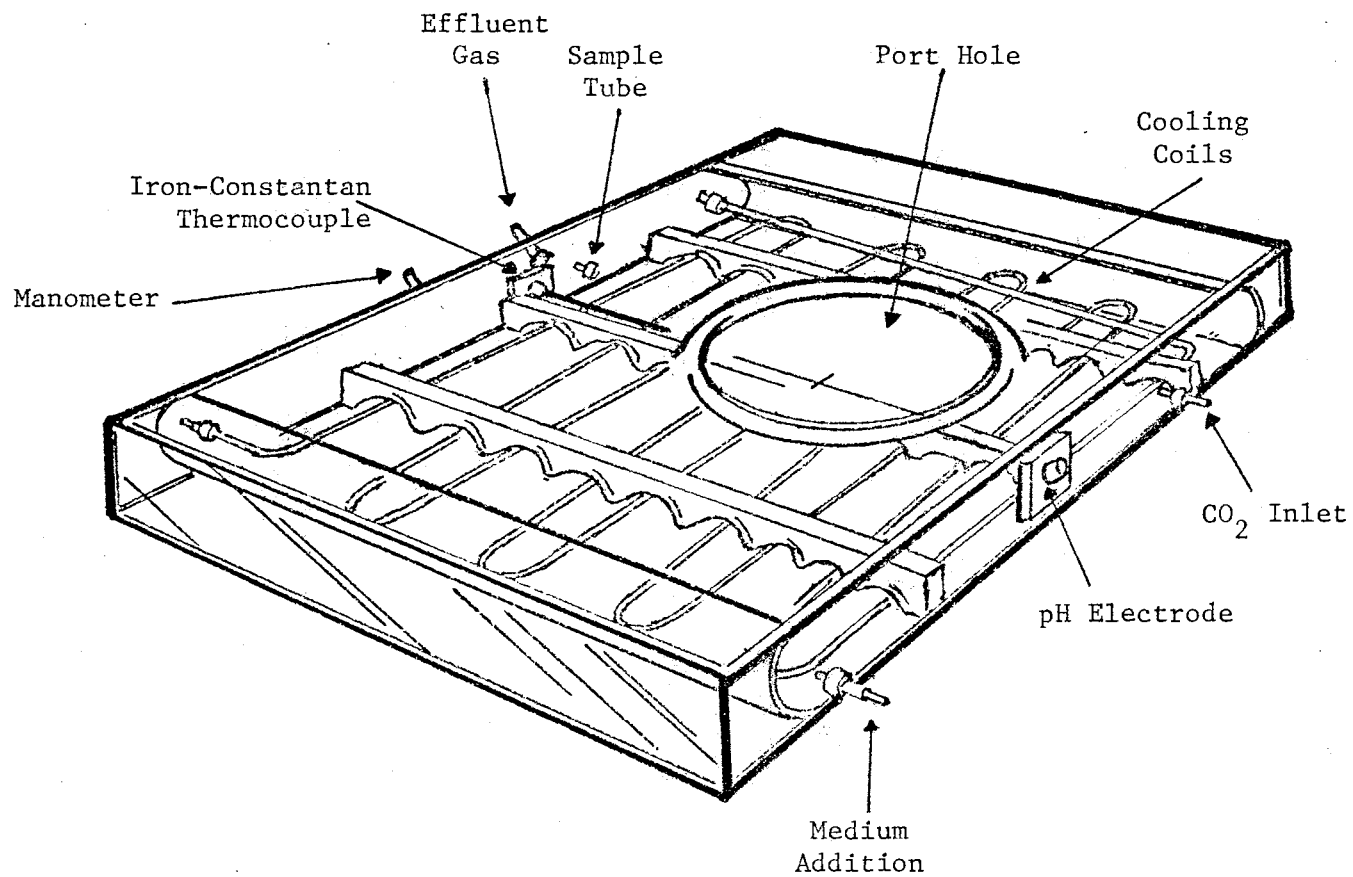
Figure 2.   Polycarbonate Culture Chamber

turned on until the light intensity was 70,000 lux at the surface of the box. The heat produced by the lamps was dissipated by fans externally and by cooling coils internally. A temperature controller operated a solenoid valve which regulated the flow of ethanol-water coolant (at $0^{o}C$) from a refrigerated bath to maintain the medium temperature ($37^{o}C$).

A pH controller automatically added carbon dioxide to maintain the pH. When nitrate (rather than ammonium) was used as the nitrogen source, CO_2 fixation caused an increase in pH. When the pH reached 7.4 carbon dioxide was added until the pH of the medium was reduced to 7.2. Excess gas was vented through gas-washing bottles filled with sodium hydroxide in order to recover unused carbon-^{13}C dioxide.

The C. pyrenoidosa culture was started in a small spinner flask as described in the previous section. The small spinner flask was used to inoculate a large spinner flask (2 liter) which in turn was used to inculate the culture box. Medium C was used throughout this procedure. Since optical density is a linear function of the number of cells per volume (31), cell growth was monitored by measuring the absorbance at 550 nm (A_{550}) on a Bausch and Lomb Spectronic 20 spectrophotometer.

Several batches of algae were grown with natural abundance carbon dioxide using the polycarbonate culture chamber. The first batch was inoculated from a spinner flask, and successive batches were inculated by leaving about two liters of algal suspension in the culture chamber at the time of harvest (LA notebook R-2538, pp. 6-21). The inoculum for the batch grown on carbon-^{13}C dioxide had an A_{550} of 5.11 au. As seen in Figures 3 and 4 there was a period of exponential growth followed by a period of nearly linear growth. This behavior is characteristic of cultures that change from light-saturated growth to
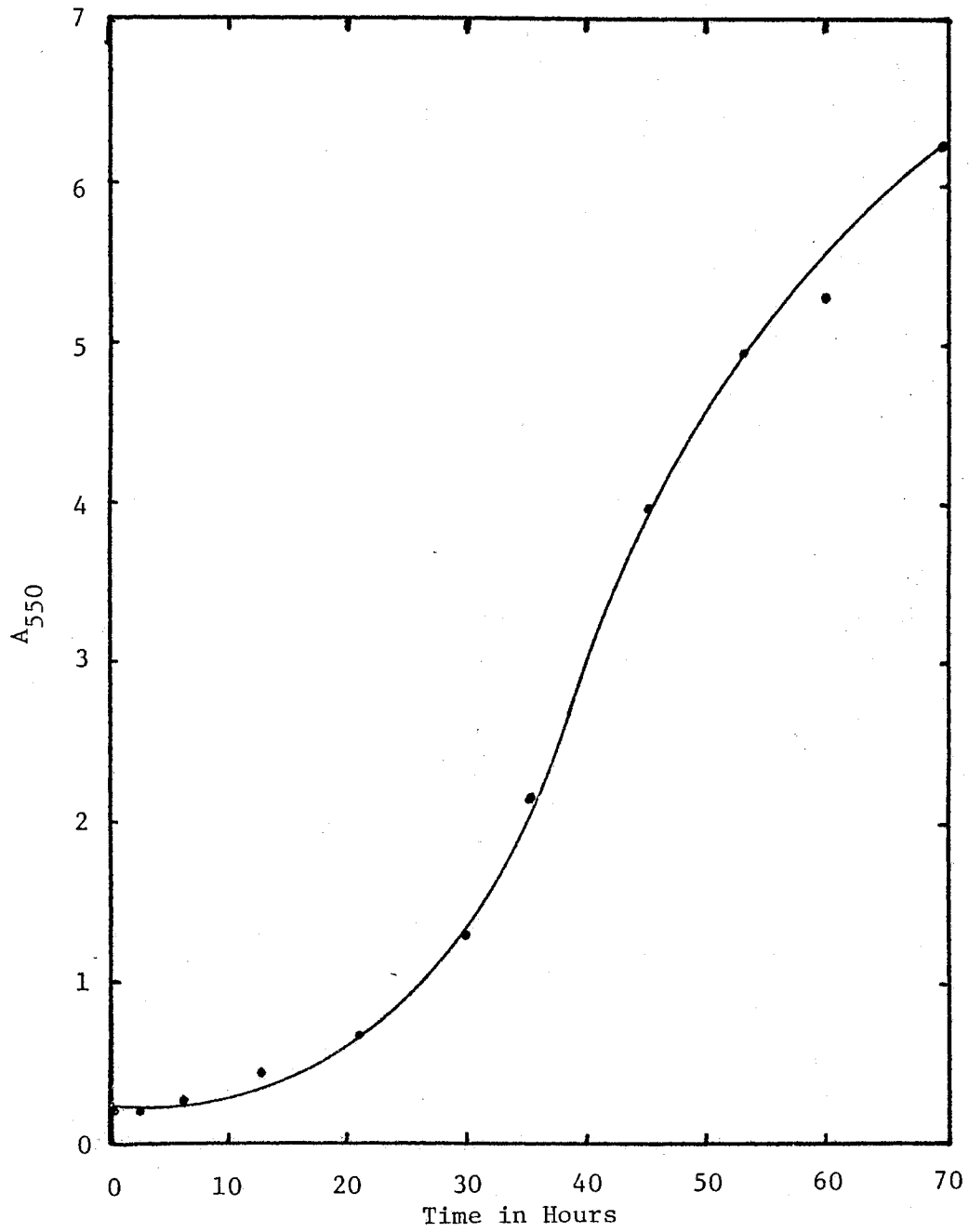
Figure 3. Algal Growth Curve
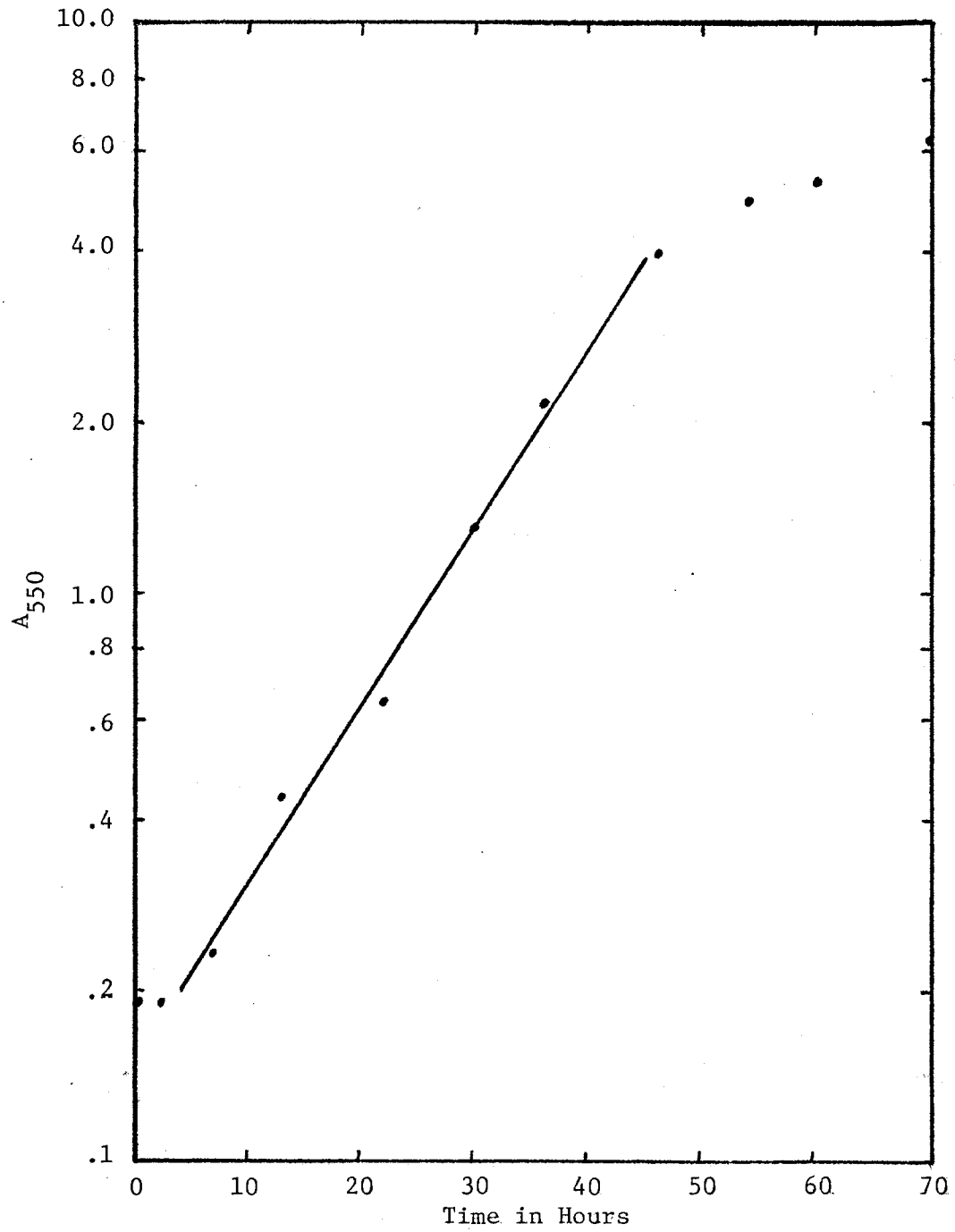
Figure 4. Semi-logarithmic Plot of Algal Growth

light-limited growth as the optical density of the culture increases

(32). For the purposes of this study the period of slower growth was

beneficial since older cells have a higher lipid content (26,27).

Based on the initial and final absorbance values, the growth of this

^{13}C-enriched batch progressed through 5.0 generations. During exponen-

tial growth the cell generation (doubling) time was 9.6 hours.

In order to minimize the various processes (respiration, autoxida-

tion, etc.) that might affect the fatty acid composition, the algae were

harvested directly into 24 liters of 2 $\underline{N}$ saline and ice. The cells were

separated from this solution by centrifugation using a Sharples Model

16 open-type continuous-flow supercentrifuge. The temperature after

centrifuging was 4°C. The cells were frozen, lyophilized and stored at

-20°C. The harvest produced 2.6 g (dry weight) of cells per liter of

medium.

The ^{13}C content of the administered carbon-^{13}C dioxide was 91.2

mol % (LA notebook R-2538, p. 19). The ^{13}C content of the cells was

82.7 $\pm$ .4 mol % (LA notebook R-2538, p. 20).

CHAPTER III

ISOLATION OF PURE FATTY ACID METHYL

ESTERS FROM ALGAE

Extraction of Lipids

Evaluation of Extraction Methods

Although many solvents and solvent systems have been used to ex-
tract lipids from algae, 2:1 (v/v) chloroform/methanol is the solvent

system used most often. When any justification is offered, the work of

Folch, Lees and Sloane-Stanley (33) and/or Bligh and Dyer (34) is

usually cited. However, these investigators did their work with animal

tissues. While chloroform/methanol extracts more lipid from algae than

other solvents (35), particularly nonpolar solvents (36), reports on

the completeness of lipid extraction* are not in agreement. Gellerman

and Schlenk (35) report that treatment of extracted cells (Ochromonas

danica) with alkali "released an additional amount of fatty acids

equal to that obtained via the initial extraction." However, Chuecas

and Riley (36) used the same method to evaluate the completeness

of extraction and obtained a quantitative extraction of "a composite

---

*
 Fatty acid content was used as a measure of the amount of lipid
 extracted.

15

sample of phytoplankton" by repeated extraction until the extract became
colorless. Nichols and Appleby (37) report that chloroform/methanol
extracted 75 percent of the total lipids from Monodus subterraneus,
as compared to treating the extracted cells with 6 N HCl and again
extracting with the same solvent. However, it is true that the ease
with which lipids are extracted depends on the particular species.
Lipid extraction is particularly difficult from Cyanidium caldarium
(38), Chlorella pyrenoidosa (25,39), Achromonas danica (35), and
Monodus subterraneus (37). Not only does the extracting solvent effect
the amount of lipid,* but using a nonpolar vs a polar solvent may alter
the fatty acid range and even alter which fatty acids are major com-
ponents (36).

One way of improving the speed and completeness of extraction is
to mechanically break the cell walls by grinding, homogenizing, or
sonicating. However, if the lipids are to be separated into classes
prior to fatty acid analysis, this procedure is not recommended. Allen,
Good and Holton (38) report finding "appreciable quantities of lysolipids
and fatty acids indicative of enzymatic degradation" when homogenization
was used.

An alternative to lipid extraction is to heat the wet cells with a
KOH/methanol/water solution to directly saponify the lipids. However,
even this does not assure complete removal of fatty acids from some
algae, notably Chlorella (40,41). Besides, the use of concentrated base
and/or prolonged heating poses the danger of isomerizing polyunsaturated

---

*Fatty acid content was used as a measure of the amount of lipid
  extracted.

acids (42).

It must be concluded that no one extraction procedure has been shown to be generally applicable. Therefore, each worker is obliged to determine the procedure best suited to the species studied and to the purpose of the investigation.

Algae Extraction

As noted above, the extraction of lipids from Chlorella is difficult so exhaustive extraction in a Soxhlet apparatus was used. A chloroform-methanol mixture was selected as solvent, since it has been shown to be the best solvent for several classes of lipids (43,44). A chloroform-methanol ratio of 3.5:1 (by volume) was used since this azeotropic composition has a low boiling point (45). In order to further reduce the extraction temperature, the apparatus in Figure 5 was designed. All standard taper joints were Clear-Seal® joints (Wheaton Scientific) or had teflon sleeves, so the extraction could be carried out at a reduced pressure. Thus, the maximum temperature during extraction was $40^{\circ}C$.

The condenser design combines high-flux capacity in the lower portion with high efficiency in the upper portion. A refrigerated bath supplied water ($10^{\circ}C$) to the condenser. The three-way teflon stopcock was connected to a vacuum controller (Conodyne Corporation Model H20LV) through one arm and a nitrogen supply through the other arm. At the beginning of an extraction the pressure was reduced and the apparatus back-filled with nitrogen several times to establish an inert atmosphere. The reflux temperature was set by adjusting the vacuum controller. The boiling flask was heated with a water bath.
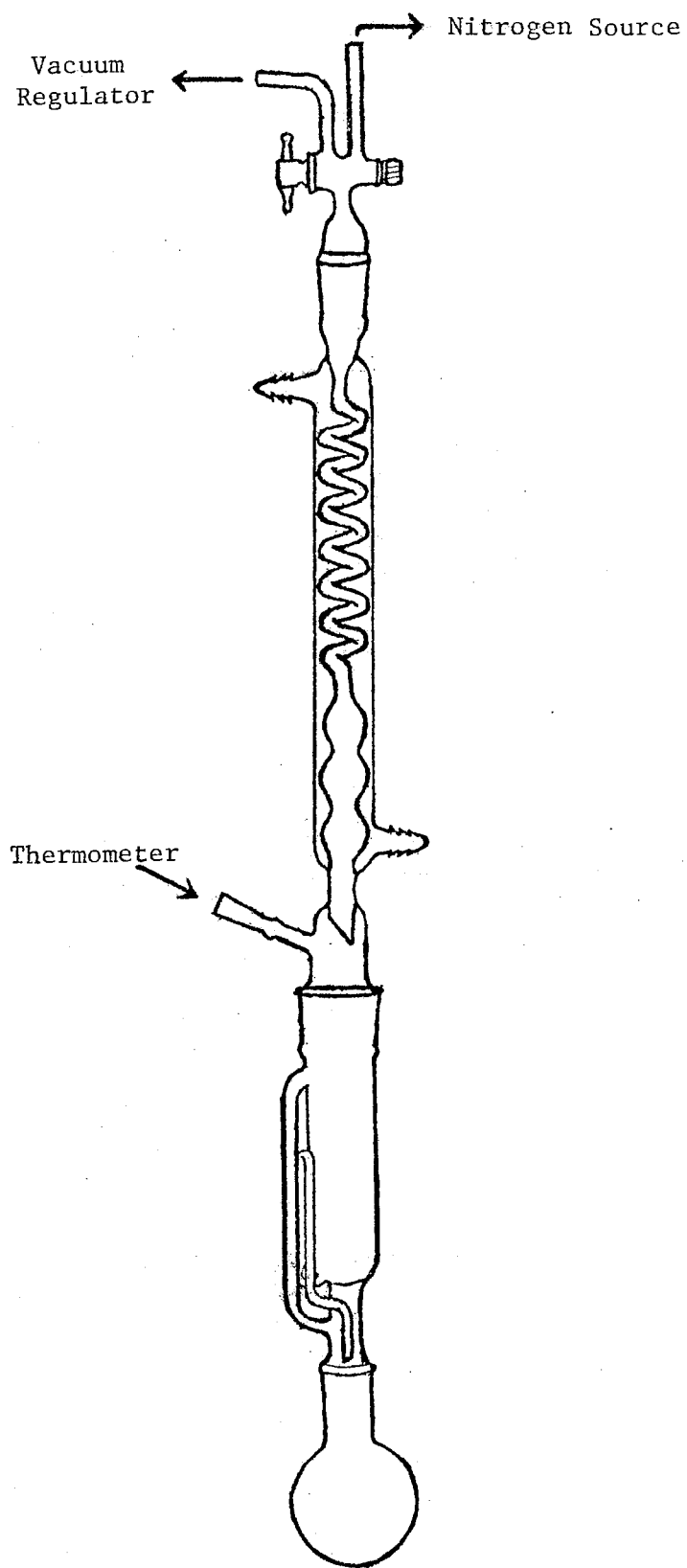
Figure 5. Extraction Apparatus

An extraction of 3.4 g of natural abundance <u>Chlorella</u> yielded 20.1%
lipid. An extraction of 3.2 g of ^{13}C-enriched <u>Chlorella</u> yielded 21.8%
lipid. No attempt was made to determine the percent of fatty acids.
The natural abundance extract was used to develop the separation methods
described later.

Esterification

Workers in the area of algal lipids have shown a decided preference
for the use of diazomethane in the preparation of methyl ester deriva-
tives of fatty acids. This is doubtless because the reaction is quite
rapid in ether solution. As described by Schlenk and Gellerman (46),
this method is quantitative, does not produce artifacts, and does not
require aqueous extractions for the removal of reagents. The explosion
and toxicity hazards are minimal when this procedure is used for small-
scale preparations. It has been shown that there is no significant
loss of polyunsaturated acids during esterification with diazomethane
(47). While the esterification step is fast, it must be preceded by
a saponification process which is time-consuming (48).

A second widely used esterification method involves boron trifluo-
ride as a catalyst. A 12 to 14% solution of BF_3 in methanol completely
esterifies fatty acids in 2 minutes (49). The procedure of Metcalfe,
Schmitz and Pelka (50) has received the approval of the Instrumental
Committee of the American Oil Chemists Society (51). However, it has
been reported that aged reagent, a prolonged reaction time, or a high
BF_3 concentration (e.g., 50%) produces artifacts (48,52,53). Lough (54)
identified the artifact from the methylation of oleic acid as a methoxyl

substituted ester. Since the reaction time is relatively long (e.g.,

25 min for triglycerides) for the transesterification procedure of

Morrison and Smith (53), artifact production is more likely, and this

procedure has received little acceptance. Consequently, a saponification

process must precede the use of BF_3 in methanol.

Since saponification poses the danger of double bond isomerization

in polyunsaturated acids (42), a transesterification procedure was deemed

more desirable than either of the above methods. Either 1 to 2% sulfuric

acid or 5% hydrochloric acid in anhydrous methanol can be used to trans-

esterify lipids without producing artifacts (48). Several workers have

used 2,2-dimethoxypropane to scavenge water, and hence assure a quanti-

tative reaction (55-57).

In this study a modification of the procedure of Mason and Waller

(56) was used for up to 100 mg of lipid. To each lipid sample was

added:

> 4.0 ml benzene (AR, dried over sodium)
>
> 0.1 ml 2,2-dimethoxypropane (Dow Chemical Company,
>
> > redistilled)
>
> 0.5 ml 3% HCl in Lipopure methanol (Applied Science
>
> > Laboratories)

After sitting overnight at room temperature, the solvent and HCl were

removed under a stream of nitrogen. The residue was dissolved in

carbon disulfide for analysis by gas chromatography.

Autoxidation

In the extraction and subsequent handling of lipids and fatty

acids care must be taken to avoid loss of polyunsaturated acids due to autoxidation, i.e., oxidation by atmospheric oxygen (58). In order to increase the length of the induction period and to decrease the rate of oxidation, the temperature should be kept low and exposure to oxygen should be minimized (59,60). Autoxidation has been discussed in depth by Scott (61).

While it is best to minimize the time between extraction and analysis, sample storage is sometimes necessary. In which case, the samples should be kept in the cold either in a petroleum ether solution under nitrogen (35,62-64) or in vacuum-sealed vials (35). Several workers advise adding antioxidants to the solvents used (36,37,65).

In accordance with the observation of others (36,60), no loss of polyunsaturated acids was observed prior to separation from the naturally occurring antioxidants in the crude extract. Individual FAME were purified as near the time of analysis as practicable, and stored under nitrogen until analysis.

High-Performance Liquid Chromatography

Introduction

Only a few years ago, liquid chromatography was used for analysis as a last resort. While the method was potentially applicable to any liquid or solid mixture, it required considerable time, had low reproducibility and inadequate monitors for the column effluent. Today, high-performance liquid chromatography (HPLC) is the method of choice for a wide range of separation problems. This renaissance has been the

result of concomitant advancements in three areas: column packing

materials, instrumentation and detectors.

Column efficiency in all modes of liquid chromatography (absorp-

tion, liquid partition, ion exchange and gel permeation) has increased

dramatically as a result of three developments in column packing mater-

ials. First, surface coated (pellicular) packings were developed to

provide faster mass transfer (66-68). These packings have an "active"

layer on the surface of a solid bead. So the diffusion path in the

pores of the packing material is much shorter, and equilibrium of the

solute between the mobile phase and the stationary phase is more rapid.

This rapid equilibration minimizes band spreading and greatly increases

column efficiency. However, since these packings have a very limited

surface area, they have a small sample capacity.

A second development in packing materials was very small, totally

porous beads having diameters of less than 50 μm (69). Columns packed

with microspheres of 5- and 10-μm-diam particles are now commercially

available (70). Not only are these microspheres at least 10 times more

efficient than pellicular packings, but their surface area is up to

100 times greater (71,72). This increased surface area provides efficient

separation of much larger samples.

The third major advance in packing materials was the development

of chemically bonded stationary phases (73-75). These packings are

prepared by allowing an alcohol or alkoxysilane to react with the sur-

face of a pellicular or microsphere packing material. By incorporating

various functional groups it is possible to obtain a wide range of

polarity for the stationary phase. The most common functional groups

are sulfonate, amino, cyano, phenyl and octadecyl (in order of decreas-
ing polarity). These packings are used with solvents ranging in polarity
from water to fluorocarbons for both normal and reversed phase separa-
tions. In a reversed phase separation the mobile phase is more polar
than the stationary phase.

Inherently, a narrow-bore column packed with one of the small-
diameter packings has a high resistance to flow, so a 1000- to 5000-psi
pump is necessary to obtain an adequate flow rate (76,77). Several
types of pumps have been developed for HPLC (78,79), but the small
displacement, reciprocating pumps have several advantages. First, they
provide a continuous flow of solvent without stopping for a periodic
refill as is required for a syringe pump. This is significant in
preparative separations. Second, a continuous- or step-gradient may be
produced in the solvent reservoir that feeds the pump. Third, the
problem of gas bubbles in the detector cells is minimized, since a
pressurized gas does not interface with the solvent. Also, the positive
displacement of a piston pump makes it possible to easily reproduce
flow rates from one day to the next. Finally, with a small-displacement
piston pump, it is possible to accomplish difficult separations by the
recycle technique.*

A number of detectors have been developed (81), but the differen-
tial refractometer (ΔRI detector) and the ultraviolet absorption detector
are considered standard equipment with most HPLC systems. Both detectors
have small cell volumes ($\leq$ 10 µl), are convenient to use, and are

---

*
In the recycle technique the eluent emerging from the detector is re-
turned to the pump and again through the column (80). This effectively
increases the column length without increasing back pressure and with-
out investing in additional columns.

moderate in cost. Typically, a ΔRI detector has a full-scale sensitivity of ΔRI = 1×10^{-5}, and a UV detector has a full-scale sensitivity of 0.1 o.d. unit. The combination of sensitivity and small cell volume give a detection limit of about 10^{-6} grams for the ΔRI detector and about 10^{-8} grams for the UV detector (82). On the other hand, by using large columns and attenuating the detectors, samples of several grams may be monitored and fractions collected. While each detector suffers the disadvantage of not responding equally to various components, dual UV-ΔRI detection can successfully monitor components of a very complex mixture (83). Recently, the use of the fluorescence and variable wavelength detectors has increased significantly.

Since a narrow-bore column filled with microspheres has a small interstitial volume, HPLC provides very rapid analysis. Whereas thin-layer and column chromatography have relatively long separation times (thirty minutes to days), HPLC separations usually require less than thirty minutes. The separation conditions of those methods are a useful guide in choosing the conditions for HPLC (84). While separations are developed on an analytical scale, the separation may be scaled up to achieve the same degree of resolution for preparative work (83).

Theory

A separation may be evaluated by determining the resolution between two components. As shown in Figure 6, resolution is usually defined as the distance between the peak centers divided by the average base width of the peaks. From this simple concept of resolution may be derived an equation that relates resolution to the three fundamental
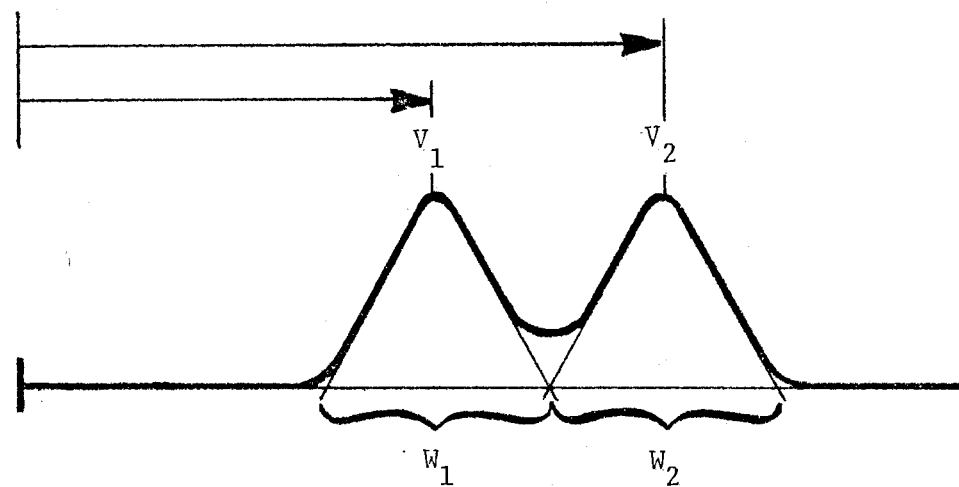
$$R = \frac{V_2 - V_1}{1/2(W_1 + W_2)}$$

Figure 6. Resolution Between Chromatographic Peaks

parameters of a chromatographic separation (85); namely,

$$R = 1/4 \ \sqrt{N} \left(\frac{\alpha - 1}{\alpha}\right) \left(\frac{K_2'}{1 + K_2'}\right)$$

The three parameters are defined in Figure 7, where V_o is the void volume of the system. The number of theoretical plates, N, indicates the column efficiency, which is determined by the physical characteristics of the packing material and the solvent (86). Pellicular packings will typically produce 3000 theoretical plates/meter, while microspheres can attain efficiencies of 10,000 theoretical plates/25cm (72). The selectivity, α, depends on the chemical interactions between the solute and the two chromatographic phases (87). The retention, K', (or capacity factor) is a measure of the rate of migration and is determined by the partitioning between the mobile phase and the stationary phase. Figure 8 illustrates the effect these parameters have on resolution.

Since the height equivalent to a theoretical plate (HETP = N/column length) is a function of the linear velocity (μ) of the mobile phase, there is a trade-off between column efficiency and separation speed. The van Deemter plot in Figure 9 diagrams this trade-off for both gas and liquid chromatography (88). In the van Deemter equation

$$HETP = A + B/\mu + C\mu$$

the A term is a measure of eddy diffusion, the B/μ term is the result of molecular diffusion of the solute in the mobile phase, and the $C\mu$ term is the consequence of slow mass transfer of solute between the mobile and stationary phases. For HPLC the molecular diffusion term
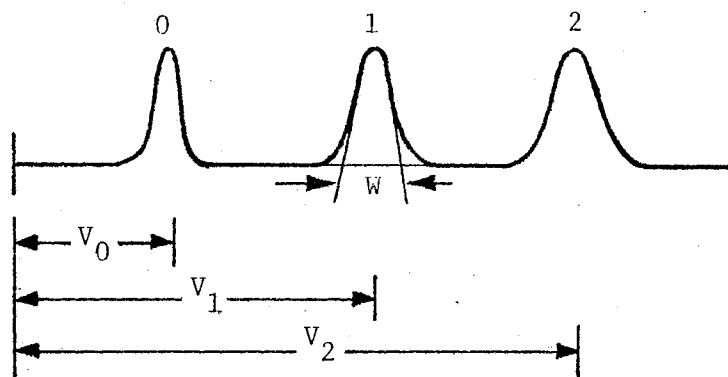
Retention, $K_1' = \dfrac{V_1 - V_0}{V_0}$

Selectivity, $\alpha = \dfrac{K_2'}{K_1'} = \dfrac{V_2 - V_0}{V_1 - V_0}$

Plates, $N = 16 \left(\dfrac{V_1}{W}\right)^2$

Figure 7.   Fundamental Parameters of
Chromatography
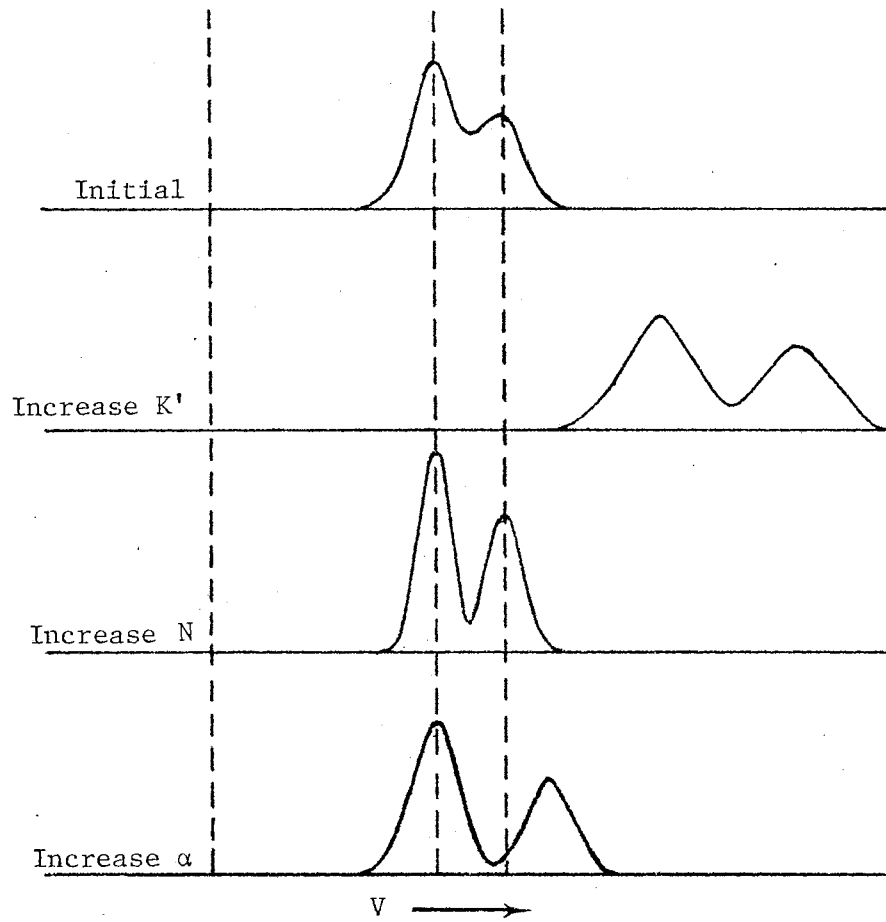
Figure 8. Effect of Fundamental Parameters on Resolution
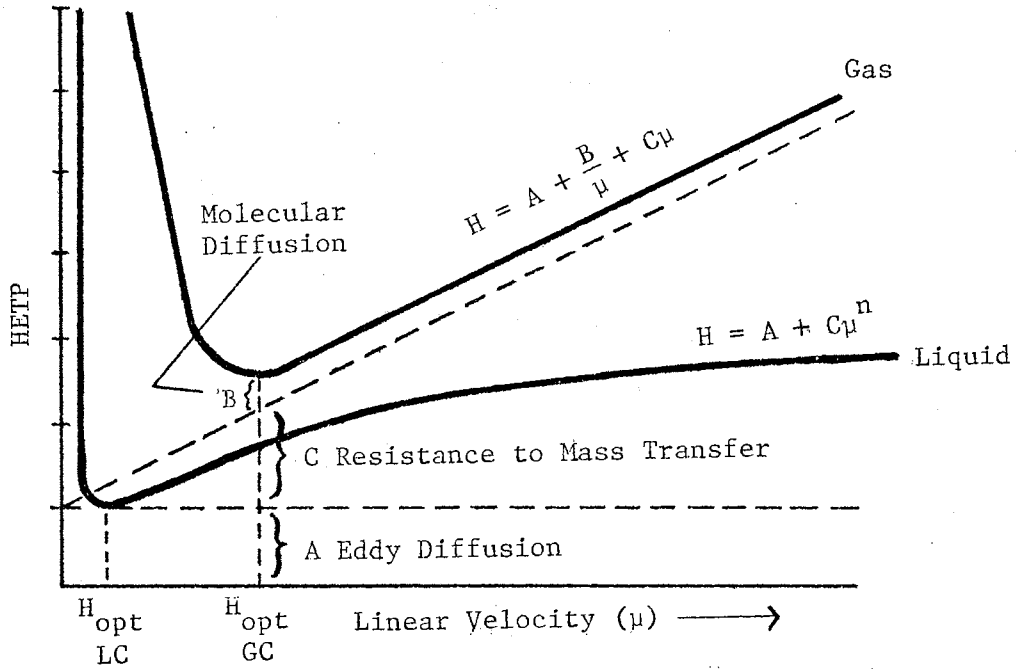
Figure 9. Relationship Between Column Efficiency (HETP)
and Linear Velocity of Mobile Phase

is usually negligible (89). Empirically, it has been shown that for the mass transfer term the linear velocity has an exponent (90). So, for HPLC the van Deemter equation reduces to

$$HETP = A + C\mu^n$$

where n < 1. The value of n ranges from .50 to .75 for porous particles smaller than 40 μm (91).

The practical result of this equation is very low HETP values, limited by eddy diffusion. Thus, the column has a high efficiency; i.e., a large number of theoretical plates. Also, the linear velocity can vary over a rather wide range with only a small sacrifice in efficiency. So HPLC is normally performed at a linear velocity well above that of maximum efficiency (μ_{opt}). For example, μ_{opt} for a μBondapak-C_{18} column (water/acetonitrile mobile phase) corresponds to a flow rate of about 0.2 ml/min (92), whereas the normal operating flow rate is 1-2 ml/min. At this μ_{opt} the column exhibits an HETP of about .03 mm (92).

FAMEs for GC/MS Analysis

Instrument and Supplies

The solvents used in this section were analytical reagent grade and were used without further purification except for hexane. Hexane from several sources exhibited significant UV absorption. The UV-absorbing impurities were removed by passing the hexane through a 3 x 20 cm column filled with 200 mesh silica gel (MC/B, activated at 220°C). Pesticide grade hexane from MC/B was free of UV-absorbing impurities.

Reference FAMEs (99+% pure) were obtained from Applied Science
Laboratories.

All of the columns shown in Table II were evaluated for FAME
purification. Only the first six will be discussed in this section.
Except for the Poragel 60Å column these columns were dry packed using
the tap-fill method (93). Frits having a 10 μm porosity were used to
hold the packing material in place. The Poragel 60Å column was obtained
prepacked. The Vydac CX column was converted to the silver form by pump-
ing 100 ml of 0.01 $\underline{N}$ AgNO$_3$ through the column. Distilled water was then
pumped through the column until the effluent remained clear when HCl was
added.

The work reported in this section was performed on a Chromatec
Model 3100 liquid chromatograph with a differential refractometer
(Waters Associates Model 401) connected to the outlet of the UV detector
(254 nm). For analytical samples a stop flow/septum injection system
was used, and for preparative samples a valve loop injector was used.
The pump was a reciprocating piston type rated at 1000 psi. The flow
rate was controlled by adjusting both the pump stroke frequency and
stroke length.

The pump system was modified in three ways. As an aid for trouble-
shooting, a pressure gauge was inserted between the pump and injector.
The 1/4 inch stainless steel tubing connecting the solvent reservoir to
the pump was replaced with 1/8 inch tubing (2 mm i.d.) to permit faster
solvent change-over. The rubber ring-seal of the piston seal assembly
was removed so that only teflon and stainless steel were in contact with
the solvent. This permitted chloronated solvents to be used.

TABLE II

HPLC COLUMNS

| Packing Material | | Column Dimensions | | Particle |
Name	Type	Length(cm)	i.d.(mm)	Size (μm)
1. Vydac Reverse Phase	octadecyl bonded to pellicular silica	61	2.1	30-44
2. Permaphase-ETH	ether bonded to pellicular silica	61	2.1	30
3. Poragel 60Å	styrene/divinyl benzene copolymer	122	7.0	37-75
4. Porasil T	porous silica	61	2.1	25-37
5. Corasil I	pellicular silica	61	3.0	37-50
6. Vydac CX	pellicular strong cation exchange	91+91*	3.0	30-44
7. Fatty Acid Analysis	(proprietary)	30	3.9	10
8. Porasil A	porous silica	122+122*	7.8	37-75
9. μBondapak-C18	octadecyl bonded to porous silica	30	3.9	10
10. μBondapak-C18	octadecyl bonded to porous silica	30	7.8	10

* Two columns connected with a low dead-volume connector.

The pump system imposed several restrictions on the HPLC experiments. Since there was no pulse damping devise, "pump noise" limited the ΔRI detector to its less sensitive settings. The flow rate was sensitive to back pressure changes caused by a solvent change or even a change in room temperature. Only a small part of the rather large cylinder volume ($\geq$ 2 ml) was displaced by each piston stroke, and there was a relatively large volume between the solvent reservoir and the injection system. This precluded use of the recycle technique and use of gradient elution.

Separation Methods

The first type of separation required is to separate the FAMEs from the crude lipid extract. Results from thin-layer and column chromatography have shown that absorption on silica is an effective method for this separation (35,94-98). The principles of absorption chromatography have been discussed in depth by Snyder (99). As was discussed earlier, pellicular packings provide high efficiency but have a limited sample capacity. So, a column of totally porous silica (Porasil T) was connected in series with a column of pellicular silica (Coracil I). The Porasil T column provides the capacity for a preliminary separation of up to 20 mg of crude lipid extract. The Corasil I column then provides a rapid final separation. The benefit of using a porous packing in series with a pellicular packing has been demonstrated (100). For a mobil phase of hexane/chloroform (95/5) the FAMEs have a K' of about 1, as seen in Figure 10. Most of the pigments were adsorbed strongly on the silica and were flushed from the column with chloroform.
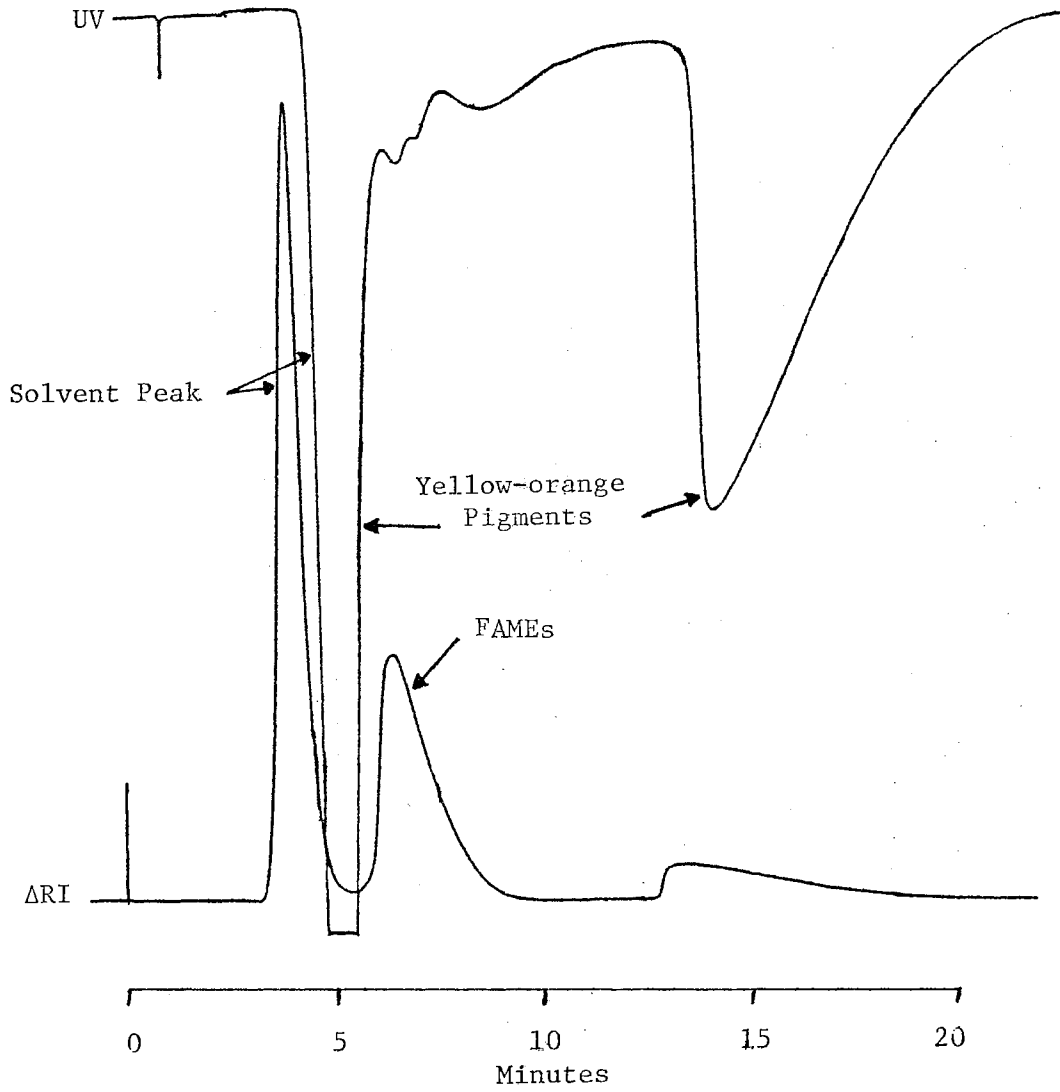
Figure 10. Separation of Crude Lipid Extract

The second type of separation required is much more difficult than the first; namely, the isolation of pure, individual FAME. Since the FAME mixture varies in chain length and degree of unsaturation, and even contains some methyl substituted FAME, it represents a virtual continuum of chemical and physical properties. Preparative gas-liquid chromatography (GLC) cannot adequately separate the components of a complex FAME mixture. For example, Korn (101) was able to obtain 29 peaks by GLC of the total fatty acid esters of Euglena gracilis, but by using other fractionation techniques and structure analysis in combination with GLC he identified 51 fatty acid esters. So, the FAME mixture requires some form of preliminary separation prior to GC/MS analysis.

GLC analysis of fractions collected during the separation of the crude lipid extract indicated some fractionation of the FAME mixture according to the degree of unsaturation. So the FAME mixture was chromatographed using a mobile phase of hexane/chloroform (99/1). As seen in Figure 11 a significant fractionation was obtained. However, since recycle was not possible, the silica columns could not provide the necessary preliminary separation of the FAME mixture.

The separation of small molecules by gel permeation chromatography has been reported for Bio-Beads and Sephadex LH-20 (102,103) and for Poragel (104,105). A Poragel 60$\overset{o}{\text{A}}$ column (see Table II) was evaluated with tetrahydrofuran, chloroform and toluene as the mobile phase. A small degree of fractionation by chain length was observed. However, several more columns plus recycle would have been necessary to achieve a useful preliminary separation.
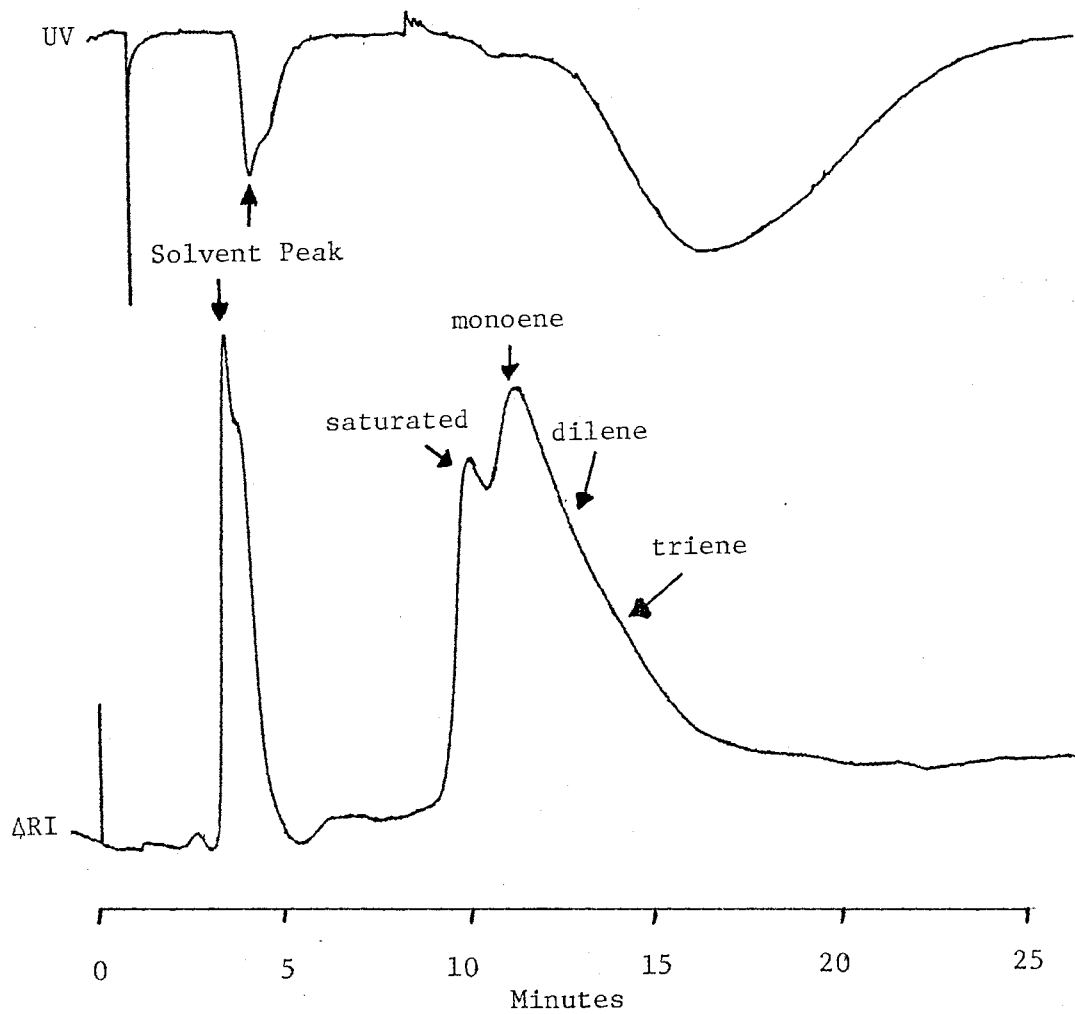
Figure 11. Fractionation of FAMEs on a Silica Column

Reverse phase, liquid-liquid chromatography has been used to separate FAMEs. Two approaches have been used. Some workers have used a solid stationary phase such as powdered rubber (106,107) or hydrophobic Sephadex (108). These materials concentrate the nonpolar component of the mobile phase to form a lipophilic gel. The FAMEs are partitioned between the gel and the polar mobile phase. Alternatively, a liquid stationary phase such as hexane (109) or silicone oil (35,110) can be coated on a solid support. A polar mobile phase such as methanol/water or acetonitrile/water is used with such columns. These later columns are analogous to HPLC packings having chemically bonded stationary phases. Of course, the pellicular packings have a much higher efficiency. Using methanol/water as the mobile phase, an attempt was made to separate various FAMES on a Vydac Reverse Phase column and a Permaphase-ETH column. A satisfactory separation was not found at that time, however. As will be seen later in this chapter, reverse-phase HPLC proved to be the method of choice for the preparative separation of a FAME mixture.

The well known complex formed between silver ion and unsaturated compounds is the basis of argentation chromatography. In this technique the absorbent (silica, silicic acid or Kiesilgel) is modified by the addition of silver nitrate, which retards the migration of unsaturated FAMEs (111). The resulting separation is based on the degree of unsaturation irrespective of chain length (112). The separation of isomers is possible, since the silver complexes with _cis_-isomers are more stable than those with _trans_-isomers (113). Positional isomers may also be separated (114).

Ion exchange resins have also been used as a support for silver ions. Such columns can be used to separate cis- and trans-isomers (115), as well as to separate mixtures according to the degree of unsaturation (116). An advantage of this approach is that polar solvents may be used without leaching silver from the column. Because of the high efficiency of pellicular ion exchange packings this method appeared promising. So a Vydac CX column (see Table II) was converted to the silver form, and a number of solvent systems were evaluated for use in separating a FAME mixture. The results from several useful solvent systems are shown in Table III.

TABLE III

RETENTION OF FAMES ON VYDAC CX-AG$^+$ COLUMN

Mobile Phase	K' values for FAMEs			
	saturated	monoene	diene	triene
hexane/chloroform, 9/1	.24	.61	1.1*	NE
chloroform	.08	.16	.65	~1.6*
chloroform/acetone, 9/1	.05	.13	.38	~2.0*
chloroform/methanol, 95/5	<.05	<.05	.22	.41

* indicates incomplete elution and considerable tailing.
NE indicates that this FAME is not eluted by this mobile phase.

To accomplish a separation for a complex FAME mixture, first the trienes were separated using chloroform/methanol (95/5) as a mobile

phase. The other FAMEs were collected near the solvent front. Next, the dienes were separated using chloroform as the mobile phase. Finally, the monoenes were separated from the saturates using a mobile phase of hexane/chloroform (9/1). Since Chlorella pyrenoidosa produce primarily 16- and 18-carbon chain fatty acids, this argentation separation produces pairs of FAMEs. As will be discussed later, the monoene fraction contained a methyl substituted FAME which co-chromatographed with the 16:1 FAME. These separations provided 5 to 50 micrograms of FAMEs in each fraction.

FAMEs for CMR Analysis

Instruments and Supplies

The solvents used for the separation in this section were all "distilled in glass" solvents from Burdick & Jackson Laboratories. Before use the solvents were filtered through a 0.45 μm pore-size filter in an all-glass filter apparatus from the Millipore Corporation. Reference FAMEs (99+% pure) were obtained from Applied Science Laboratories.

The columns used in this section were obtained prepacked from Waters Associates, and are columns seven through ten described in Table II.

Two types of chromatographs were used. Work with the fatty acid analysis column was performed on a Waters Associates Model ALC/GPC-202/R-401 with a Model 6000 pump. All other separations were performed on a Waters Associates Model ALC/GPC-244 with a Model 6000A solvent delivery system and a Model 660 solvent programmer. Both instruments

provide UV detection at 254 nm, and both have a Model 401 differential refractometer. The pumps for both systems are rated at 6000 psi. The second instrument provides the option of gradient elution and/or flow programming.

Separation Methods

Since several milligrams of a pure FAME was desired for CMR analysis, a larger scale separation was necessary compared to the separations described above. This was straightforward for separating the FAMEs from the crude lipid extract. The Porasil A column described in Table II was used with a mobile phase of hexane/chloroform (3/7). At a flow rate of 4.0 ml/min the elution of FAMEs required 34 minutes. As before (see page 33), the pigments were flushed off the column with chloroform.

The Porasil A column was also evaluated for a preliminary separation of the FAME mixture. The recycle technique was used on 83 mg of FAME mixture, and the sample was passed through the column fifteen times. On each pass after the fourth, fractions were "shaved" from the front and back of the FAME peak. On the final pass several fractions were collected as the FAME peak eluted.

The results of the GLC analysis of these fractions indicated that a dual mechanism of separation might be involved when using the above mobile phase. As expected for an adsorption process, the FAMEs were fractionated according to molecular polarity. So, the C-16 FAMEs were eluted in the order 16:0, 16:1, 16:2 and 16:3, and the C-18 FAMEs analogously. There also appeared to be fractionation according to

molecular size, in that a C-18 FAME was eluted before the analogous

C-16 FAME. For example, the 18:2 FAME was concentrated in the fractions

shaved from the front of the HPLC peak, while the 16:2 FAME was con-

centrated in fractions shaved from the back of the peak. As a result of

this dual mechanism the two major components (16:0 and 18:2) were not

separated, but these two were separated from most of the other FAMEs.

On the fifteenth pass the front of the peak was enriched in the 18:2 FAME.

Fractions containing primarily 16:0 and 18:2 FAMEs were pooled.

The mobile phase was changed to 6/4 (hexane/chloroform) so the adsorption

mechanism would dominate, and the pooled sample was injected. Hexane/

chloroform (6/4) was pumped for 110 minutes and then the ratio was

changed to 3/7. This produced two incompletely resolved peaks, the

first being primarily 16:0 FAME and the second being primarily 18:2 FAME.

The overlap region between the two peaks was a composite of several

FAMEs. It was concluded that the Parasil A column could not produce the

high purity FAMEs needed for CMR analysis.

The argentation column used in the previous section had a very

limited sample capacity. Even for the micro-preparative separations

already described, there were occasional problems with column overload.

Using longer columns with a larger i.d. might increase the capacity by

a factor of 10, but a factor of 100 was needed. Besides, such a large

column would have been prohibitively expensive.

A Fatty Acid Analysis column (see Table II) was evaluated for

separating the FAME mixture. This column was developed for the separa-

tion of free fatty acids using an acetonitrile/water/tetrahydrofuran

mixture as the mobile phase (117). A number of solvent ratios were tried in isocratic runs; however, without gradient elution it proved impossible to find the necessary solvent composition.

At this point reverse phase chromatography was reevaluated for two reasons. About this time the Waters chromatograph capable of gradient elution was made available for use. Also, three reports of FAME separations with reverse-phase packings were published. Several mixtures of standards were separated using methanol/water as the mobile phase (118), however these analytical separations were not adequate for use with a complex FAME mixture. They did show the potential of using reverse-phase chromatography for FAME separations. The first paper by Scholfield (119) was an analytical study using a pellicular packing (C18/Corasil) and the second (120) was a preparative study using C18/Porasil. Based on his earlier work with counter-current distribution, he used acetonitrile/water as the mobile phase. Neither the analytical nor the preparative columns showed the resolution necessary to separate the FAME mixture from Chlorella.

Columns packed with μBondapak-C18 were used in preference to those above. As discussed earlier, microspheres have a higher efficiency and sample capacity than pellicular packings. While its sample capacity is less than that of C18/Porasil, its efficiency is much higher. About 20 mg of FAME mixture could be separated on this column. Because its viscosity is lower than that of methanol, acetonitrile allows faster mass transfer (higher efficiency) and was used for these separations.

If the compounds in a mixture are similar, their relative retention in reverse phase chromatography is determined by their relative solubility

in the mobile phase (121). This fact has two results. For members of a homologous series the solubility in a given liquid varies in a regular manner with chain length. Thus, analogous to GLC, a plot of log corrected retention volume vs chain length is linear. This was observed in this study for the saturated FAMEs and has been reported previously (119). Results indicate that the slope is insensitive to small changes in the acetonitrile/water ratio, but a shift in the ordinate is observed.

In addition to chain length, the degree of unsaturation determines solubility. In early reverse phase work this resulted in "critical pairs" (e.g., 16:1 and 18:2 FAMEs) which were inseparable (35,109,110). Thus, adding a double bond was equivalent to shortening the chain by two carbons. The effect of chain length and the degree of unsaturation are both seen in Figure 12. This figure shows that the critical pairs are indeed separable using HPLC and high efficiency column packings. A pair may not be completely resolved if one of the FAMEs is a major component of the sample. In such a case recycle may be used to separate the pair.

<center>Gas-Liquid Chromatography</center>

FAME Identification by GLC

GLC was used in this study to analyze the FAME content of various HPLC fractions. While GLC is the generally accepted method for the routine analysis of FAME mixtures, several considerations are necessary to ensure accurate identification. Some workers have "identified" algal fatty acids by direct comparison with the retention times of standard compounds. While this may be adequate for major components or simple
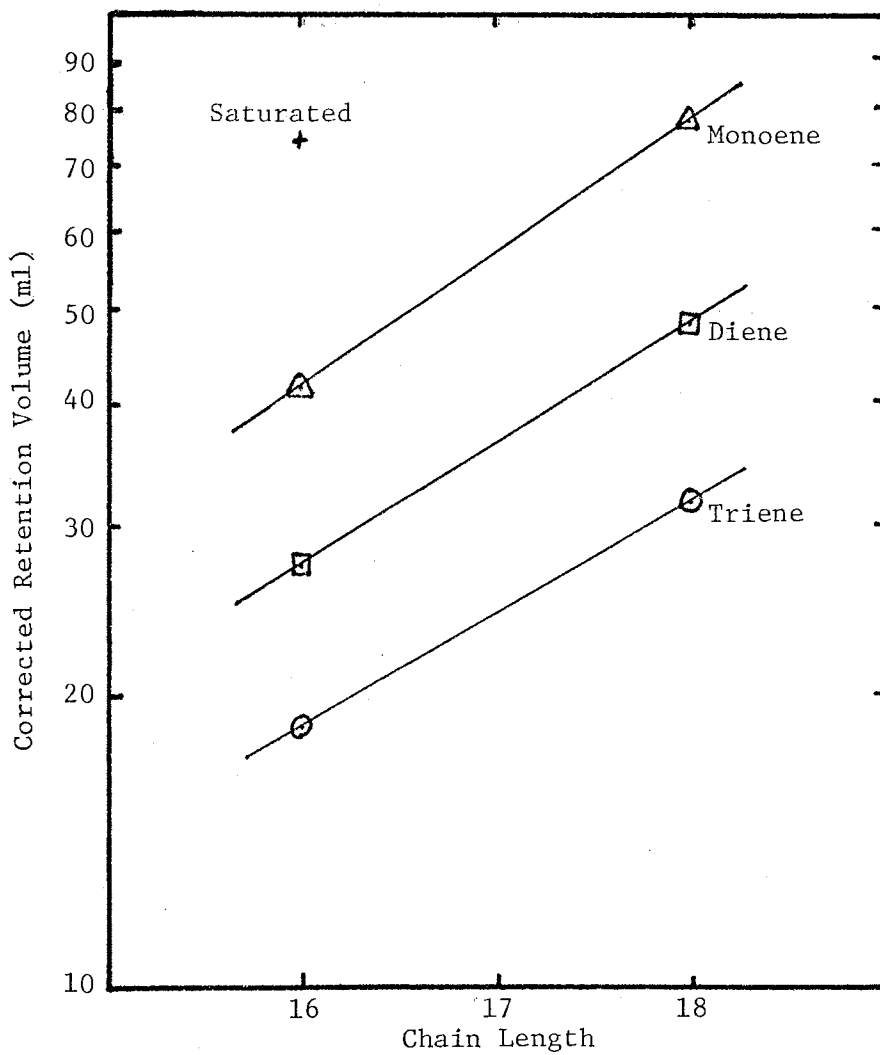
Figure 12. Effect of Chain Length and Degree of
Unsaturation on Retention Volume
in Reverse Phase Chromatography

FAME mxitures, it is not satisfactory for minor components or complex

FAME mixtures, since some pairs of esters are inseparable on certain

stationary phases (see below). The pitfalls of identifying esters by

the direct comparison of retention times can be illustrated by an example

from the work of Korn (101). A symmetrical peak having the same reten-

tion time as methyl oleate was actually composed of five different com-

ponents, and methyl oleate was only 10 percent of the total.

While polar stationary phases (e.g., diethylene glycol succinate

or Silar 10C) provide the best overall resolution of a FAME mixture,

analysis on a nonpolar phase (e.g., Apiezon L or SE-30) can aid identi-

fication. When a polar phase is used, the saturated ester of a given

chain length is followed by the unsaturated esters in the order of in-

creasing number of double bonds (122). This may cause a particular

component to be overlapped by esters having shorter chains and more

double bonds [e.g., 18:1, 17:2, and 16:3 esters may not be separated

(101)]. Landowne and Lipsky have outlined how to distinguish between

unsaturated and branched FAMEs using a polar phase (123). The order of

elution is reversed on a nonpolar phase, so the unsaturated esters

are eluted in the order of decreasing number of double bonds and prior

to the corresponding saturated esters (124). However, the polyunsatu-

rates are usually unresolved or only partially resolved by a nonpolar

phase (122). While these different elution patterns may aid identifica-

tion, there is likely to be some ambiguity involved when a complex

mixture is analyzed.

Identification is much simpler when capillary columns are used,

since these columns provide much greater resolutions (124-127). In

fact, capillary columns are capable of separating isomers (124,128-131).
However, analysis time is long (up to several hours), and hence not
suitable for screening a large number of HPLC fractions.

Since plots of log retention time <u>vs</u> the chain length are linear
for the members of a homologous series, they are useful for identifying
a component when the particular reference compound is not available
(36,62,101,132). However, there was some question as to which of the
many unsaturated isomers actually constituted a homologous series.
Using his own data and that of others, Ackman (132) showed that retention
data for esters with the same number of double bonds and the same "carbon
end chain" (the number of carbon atoms from the terminal methyl end to
the first double bond) produced a linear semilog plot. His conclusion
applies to a wide range of polar supports (122). Of course, this method
of identification is only as good as the resolution and precision of the
GLC data.

Since the absolute retention time is so dependent on operating con-
ditions, it is best to convert to some relative number. The equivalent
chain length (ECL) described by Miwa <u>et al</u>. (133) has been widely used.
The "carbon number" developed independently by Woodford and van Gent
(134) is identical to ECL. The basis of this system is the straight-
line plot of the logarithm of retention time versus the number of carbon
atoms for the normal, saturated esters. The ECL of any other ester is
read from this plot using its retention time measured under identical
conditions. The analogy to the Kovats retention indices is obvious
(135). The ECL indicates the elution sequence characteristic of the
particular stationary phase, but there is rather close agreement between

similar stationary phases [i.e., nonpolar (134) or polar (122)].

GLC Analysis

The gas chromatograph used in this study was an Aerograph Hy-Fi Model 600-D equipped with a Model 328 temperature control module. A 1/8"x8' column packed with 10% Silar-9CP on 100/120 mesh Gas-Chrom Q (Applied Science) was used with nitrogen as carrier gas. A Brooks Model 8744A flow controller was used to maintain a 20 cm^3/min flow rate during temperature-programmed analyses. The flow rate was monitored by an inline Gow-Mac flow meter that was calibrated against a bubble meter. An Aerograph electrolytic hydrogen generator supplied the flame ionization detector (FID). Reference FAMEs (99+% pure) were obtained from Applied Science Laboratories.

The solvent was removed from the HPLC fractions with a stream of nitrogen. The residue was dissolved in carbon disulfide for GLC analysis. Carbon disulfide was used because of its very low response in a FID and because it does not tail into early-eluting peaks. However, it is a poor solvent for FAMEs, and occasionally a few drops of chloroform were added to clear a turbid solution.

Optimum resolution of the FAME mixture (see Figure 13) was obtained by temperature programming from $180^{\circ}C$ to $210^{\circ}C$ at a nominal rate of $4^{\circ}C$ per minute. The program was initiated two minutes after injection. However, this procedure required about 15 minutes per sample. So HPLC fractions were routinely screened isothermally at $210^{\circ}C$, and only 8 min were needed per sample. As seen in Figure 14 the main loss of qualitative information is with regard to the 16:1 FAME.
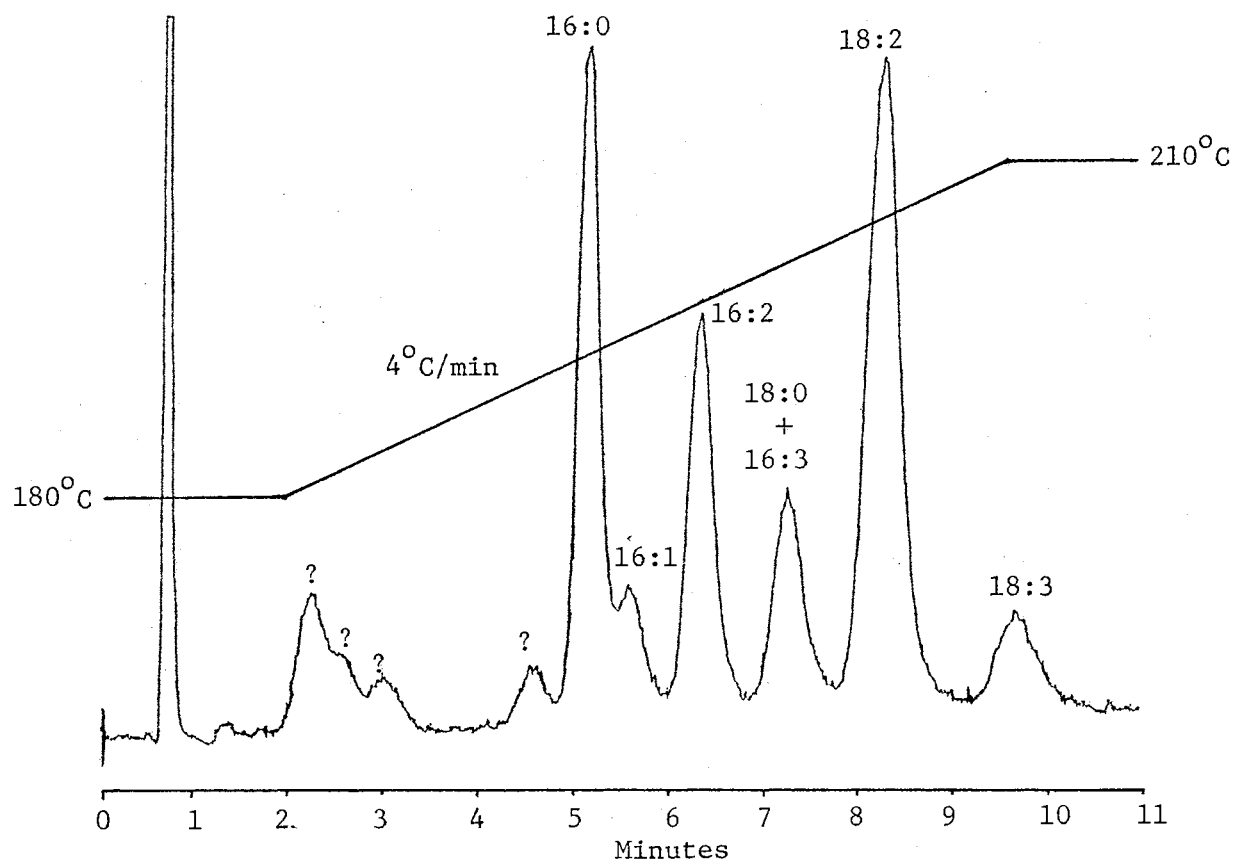
Figure 13. Temperature Programmed GLC Separation of
FAME Mixture
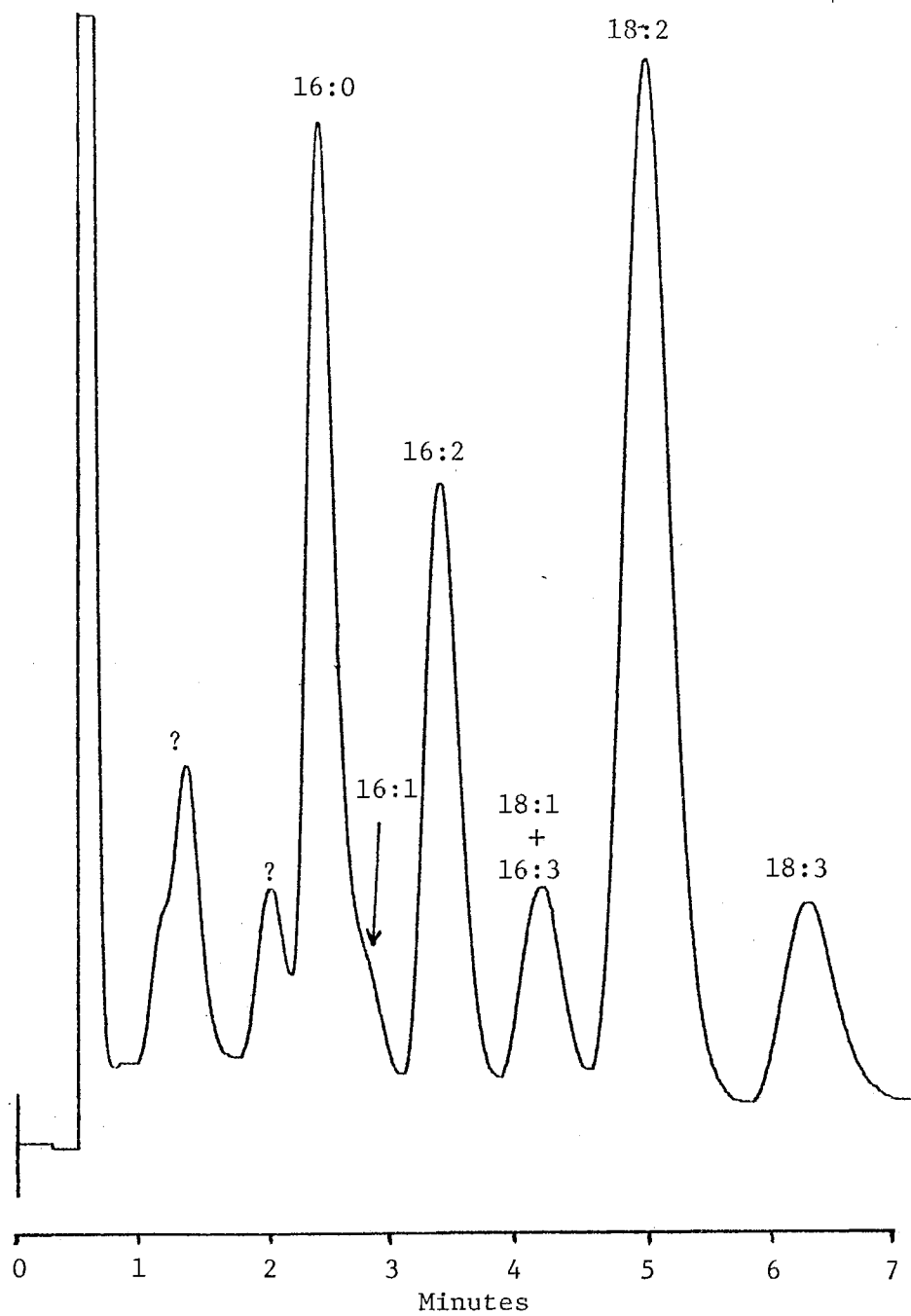
Figure 14.   Isothermal (210°C) GLC Separation of
FAME Mixture

On Silar-9CP the 18:1 FAME and 16:3 FAME are not separated. When injected separately they exhibit a small difference in retention time, but when they are co-injected only one peak is observed. Also, there is poor resolution between the 16:0 and 16:1 FAMEs. Thus, the Silar-9CP column could not provide an accurate quantitative analysis.

CHAPTER IV

DETERMINATION OF ^{13}C CONTENT USING GAS

CHROMATOGRAPHY/MASS SPECTROMETRY

FAME Identification

By combining the separation efficiency of gas chromatography with
the structural elucidation capabilities of mass spectrometry, a powerful
tool has been created for the analysis of complex biological samples.
The utility of gas chromatography/mass spectrometry (GC/MS) for lipid
analysis is evidenced by numerous reviews (e.g., 136-139). For the
identification of FAMEs the GC/MS simultaneously provides the retention
time and the molecular ion, and fragmentation patterns (including some
metastable ions), which indicate the number of carbons, degree of unsatu-
ration and position of branching.

One difficulty in early work was the high background caused by the
liquid phase bleeding into the mass spectrometer (139). This problem
has been substantially reduced by the replacement of polyester phases
with the more thermally stable silicone phases (140). In the present work
SILAR-5CP provided separations comparable to polyester phases and exhib-
ited negligible column bleed.

In addition to the molecular ion $(M^{+\cdot})$ the fragmentation pattern of
saturated, straight-chain FAMEs is characterized by four types of ions

(141). The base peak (peak of greatest intensity) results from the McLafferty rearrangement (142) and appears at m/z 74. The acylium ion (M-31) corresponds to the loss of the methoxy group. The higher mass range of the spectrum is dominated by a series of ions (m/z 87, 101, 115, 129, etc.) resulting from chain cleavage and having the general formula $[CH_3OCO-(CH_2)_n-]^+$. A series of hydrocarbon ions (m/z 69, 83, 97, etc.) are prominent in the low mass range.

The well understood fragmentation pattern just discussed can readily be extrapolated to describe isotopically enriched material, if the material can be accurately characterized mathematically (e.g., binomial distribution, known percent ^{13}C at certain sites, etc.). However, the FAMEs in this study exhibit a nondescript enrichment cluster. As seen in Figure 15 the expected binomial distribution is skewed on the low mass end and there is a small amount of natural abundance material. In comparing Figure 15 to Figure 16 it is obvious that each FAME has a different enrichment cluster, and this will be discussed later. The pertinent consideration here is that the mass spectrum of the labeled FAMEs cannot be predicted in detail from the corresponding natural abundance spectrum. So, retention time and the molecular ion for the small amount of natural abundance material served as the primary basis for FAME identification. Then the general features of the fragmentation pattern were compared to published spectra.

Due to the high level of enrichment, the major ions for methyl hexadecanoate (methyl palmitate) are correlated to the published spectrum (137,141) by adding one unit for each carbon (except methoxy) in the fragment. So, the molecular ion appears at m/z 286 (m/z 270 + 16
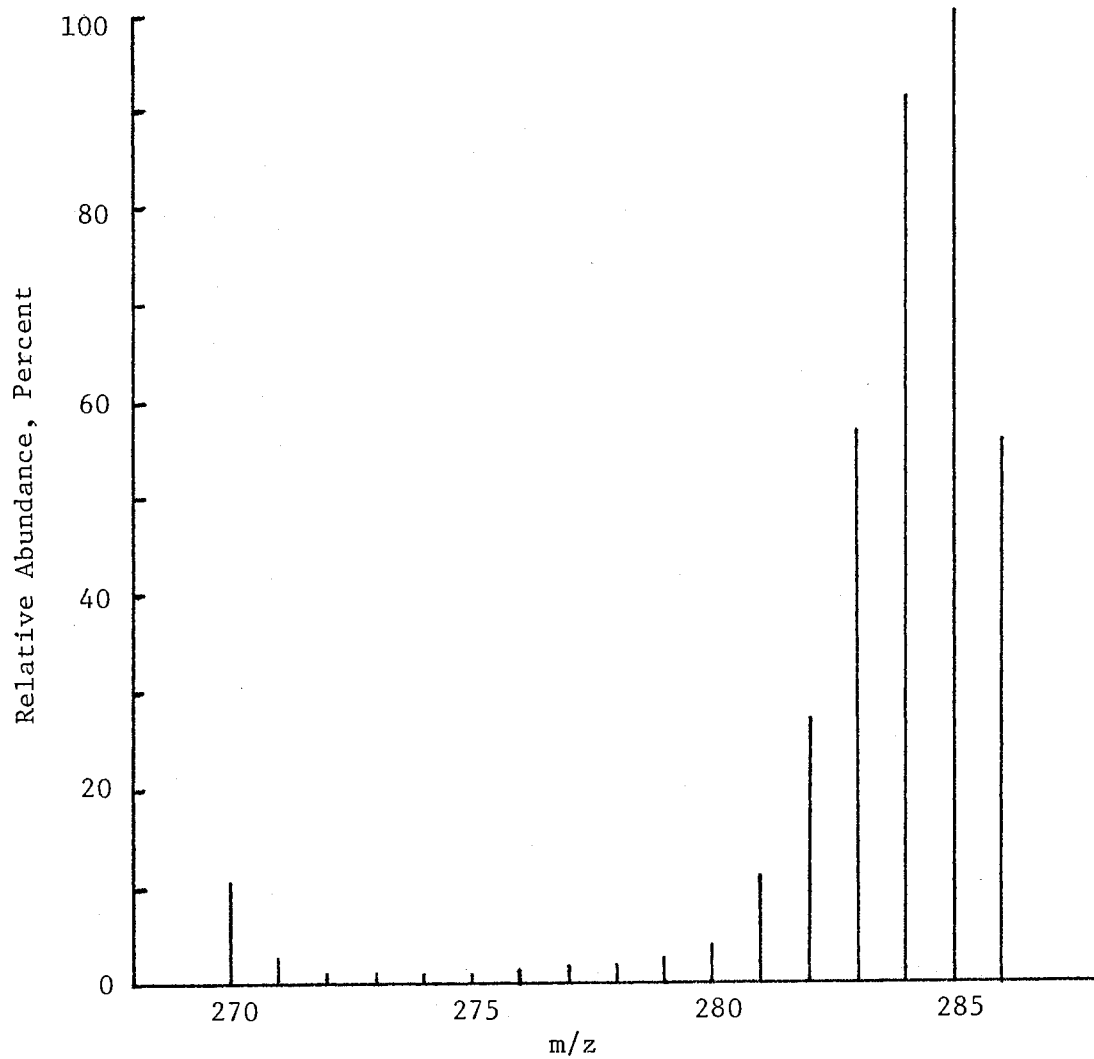
Figure 15. Normalized Spectrum of Molecular Ions for
^{13}C Enriched 16:0 FAME
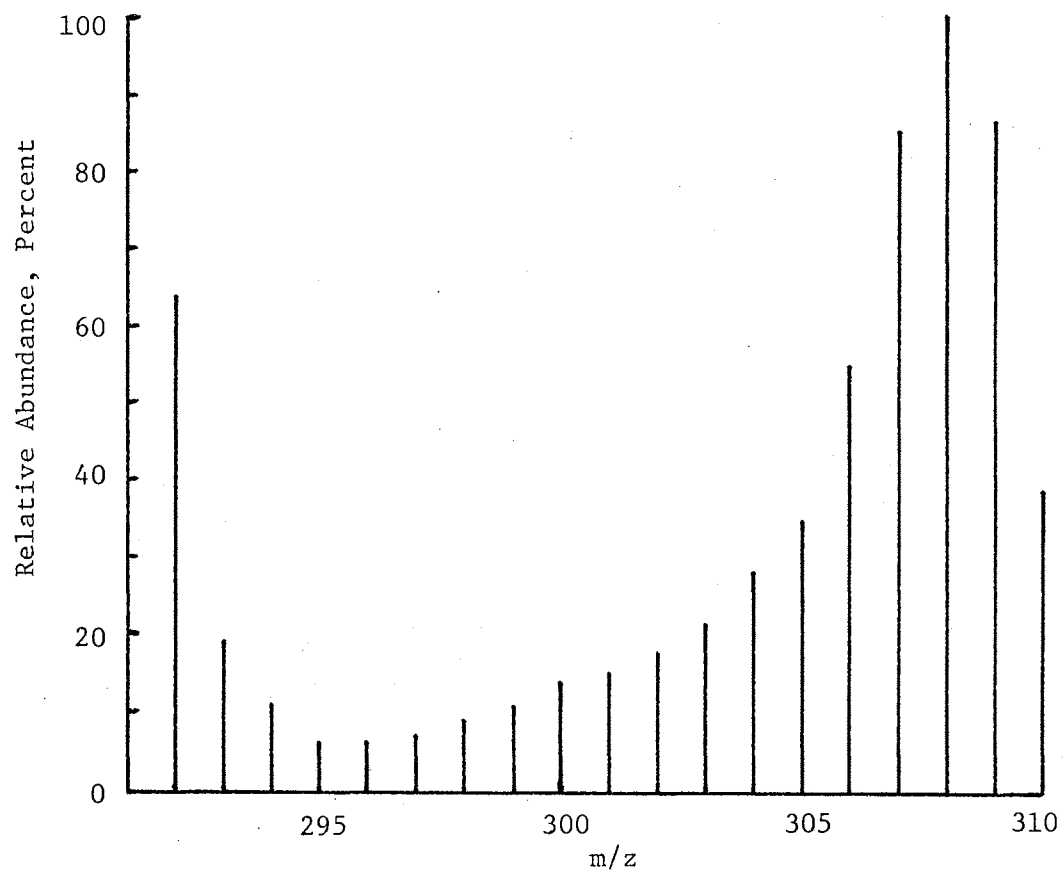
Figure 16. Normalized Spectrum of Molecular
Ions for ^{13}C Enriched 18:3
FAME

^{13}C atoms), and the McLafferty rearrangement ion appears at m/z 76

(m/z 74 + 2 ^{13}C atoms). Since the methoxy carbon contains natural

abundance ^{13}C, the acylium ion still appears at M-31 (i.e., m/z 286 -

31 = 255). Loss of an ethyl group is also M-31 and the resulting ions

are indistinguishable from the acylium ion. Also, the two series of

ions are spaced 15 units apart. For each of the ions mentioned, the

mass number cited is the highest m/z value in a cluster, which has a

size and relative intensity according to the number of carbon atoms the

ion contains. See Figures 17 and 18 for a comparison of the natural

abundance spectrum and the ^{13}C enriched spectrum for 16:0 FAME.

In the spectra of unsaturated FAMEs (140,143) the hydrocarbon

series of ions becomes more prominent as the number of double bonds

increases. The tropylium ion ($C_7H_7^+$) also increases with increasing

unsaturation. Diagnostically, the $M^{+\cdot}$, $(M-32)^+$ (base peak), $(M-74)^+$

and m/z 55 ions are prominent in the spectra of monoenes. For dienes

the m/z 67 (base peak), 81 and 95, $(M-31)^+$ and $M^{+\cdot}$ are characteristic

peaks. The important peaks for trienes are m/z 79 (base peak), 95 and

108, $(M-69)^+$, $(M-56)^+$, $(M-31)^+$ and $M^{+\cdot}$. As discussed earlier, each of

these peaks is converted into an enrichment cluster with higher mass

numbers because of the high ^{13}C content.

As mentioned in Chapter III (see page 39) the reverse phase HPLC

separation produced a FAME whose retention on Silar 9CP was nearly

identical to 16:1 FAME. The equivalent chain length (approximately 16.6

atoms, see page 46) indicated a methyl substituted FAME (122). By com-

parison to published spectra of methyl substituted FAMEs (144) the

compound was identified as methyl 15-methylhexadecoate (iso-17 FAME).

The McLafferty rearrangement peak (base peak) was observed at m/z 76,
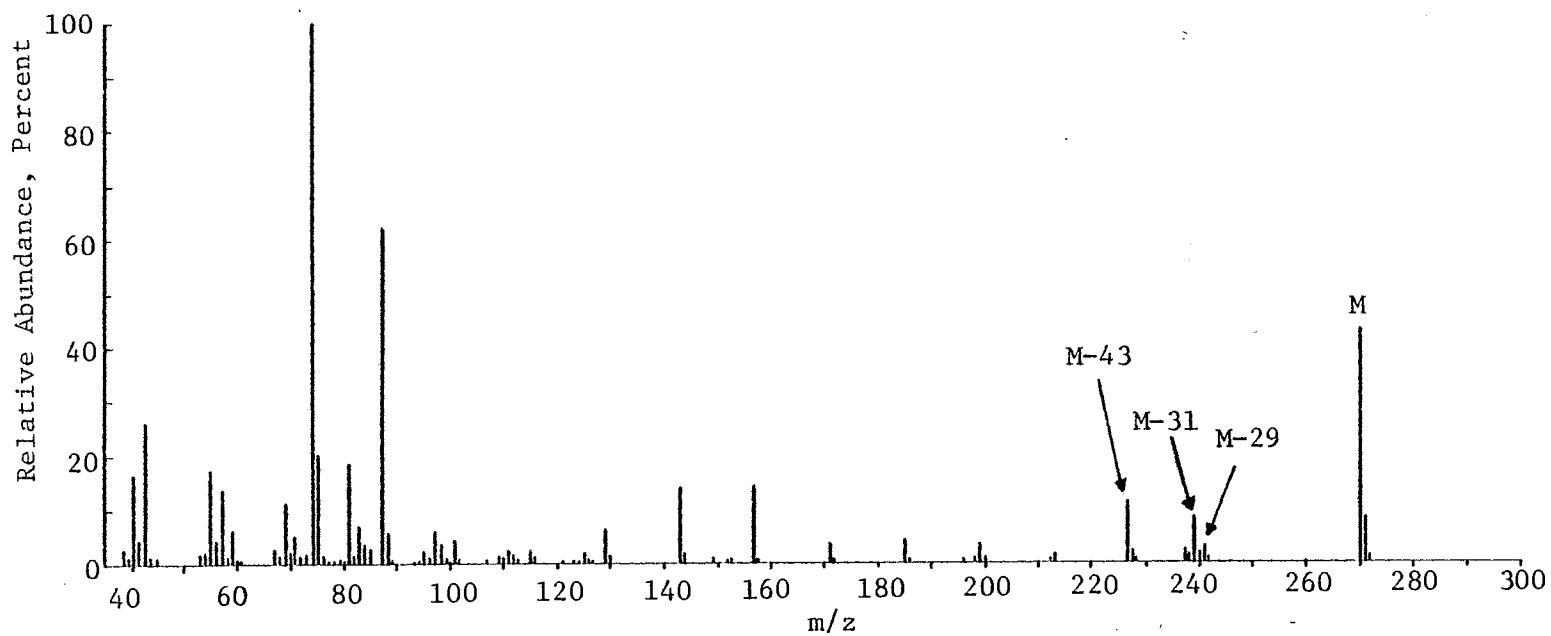
Figure 17. Normalized Spectrum of 16:0 FAME
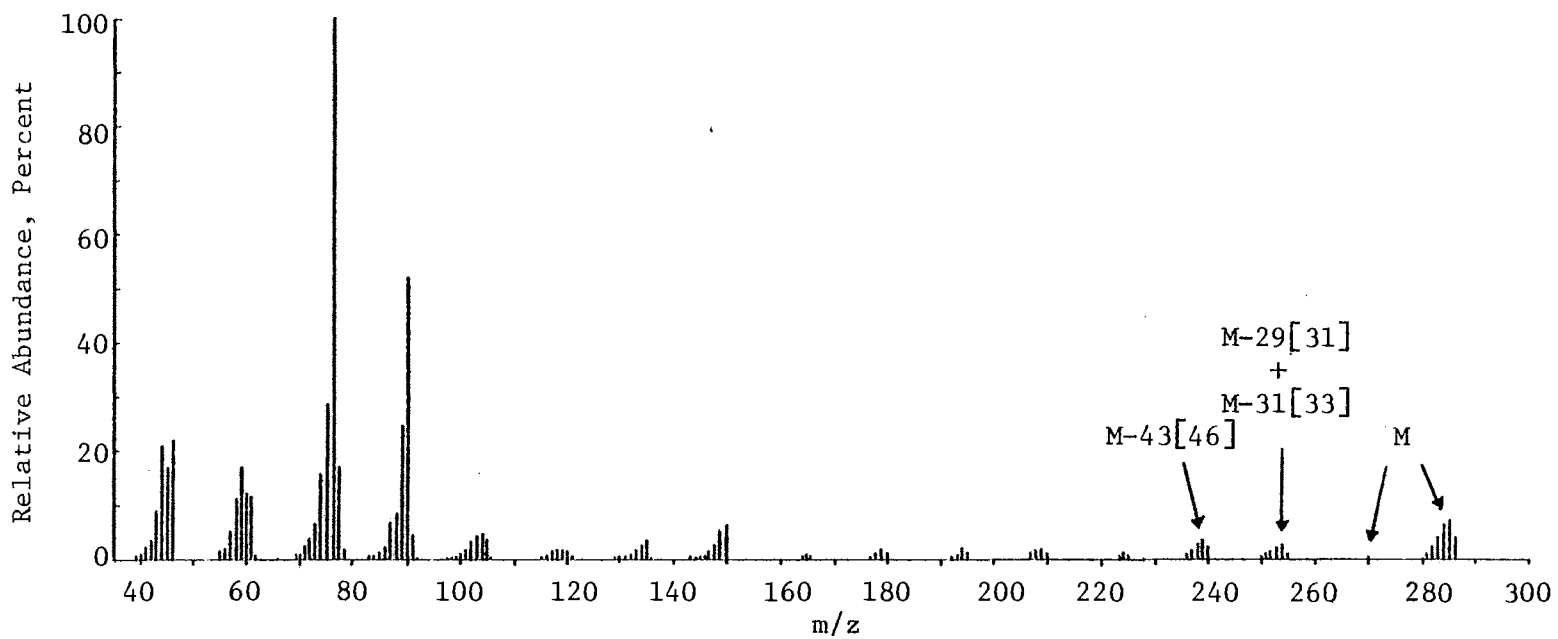
Figure 18. Normalized Spectrum of ^{13}C Enriched 16:0 FAME

so there was no substitution at the C-2 position. Methyl substitution in the middle of the chain would result in cleavage on either side of the methyl group and produce prominent peaks 30u apart. Such peaks were absent from the spectrum. Substitution at position 14 (anteiso-17 FAME) would produce significant peaks at M-31 and M-61 for loss of ethyl and butyl groups (^{13}C enriched), but this was not observed. The loss of propyl group, $(M-46)^+$, was prominent and the fragmentation pattern at lower mass numbers was very similar to 16:0 FAME. The presence of anteiso-17 FAME in Chlorella lipids has previously been reported (145), but that assignment was based on GLC retention data rather than the GC/MS fragmentation pattern.

Data Acquisition

The methyl substituted FAME was identified from spectra obtained on a Hewlett Packard Model 5980A GC/MS with a Model 5934A data system. The first column in Table IV was used with this instrument. The data system of this instrument supplied normalized, hard-copy spectra.

TABLE IV

GAS CHROMATOGRAPHY COLUMNS USED IN GC/MS EXPERIMENTS

Column Description	Packing Material*	Instrument
8' x 1/8" o.d., stainless steel	10% SILAR-9CP on 100/120 mesh Gas-Chrom Q	Hewlett Packard Model 5984A
6' x 4 mm i.d., glass	3% SILAR-5CP on 100/120 mesh Gas-Chrom Q	LKB 9000 Prototype
6' x 4 mm i.d., glass	3% OV-1 on 100/120 mesh Gas-Chrom Q	LKB 9000 Prototype

*Applied Science Laboratories

Except as noted, GC/MS experiments were performed on a prototype of the LKB 9000 (146). See Table IV for a description of the two columns used with this instrument. The helium carrier gas was set at 27 ml/min. The temperature of the column oven was calibrated (see Figure 19) with a thermometer which had been checked for accuracy by comparison to a precision platinum resistor (Dimensional Standards Laboratory, Los Alamos Scientific Laboratories). Spectral data was recorded by means of a light beam oscillograph recorder using Kodak Linagraph Direct Print paper, Type 2022.

Spectra used for FAME identification were obtained near the maximum of the GC peak. The ion abundance was quantitated using a millimeter scale, and normalized using a program written for a Hewlett Packard 9810A programmable calculator.

Isotope fractionation was initially observed using the Selected Ion Monitoring (SIM) system to compare the ^{12}C molecular ion with the totally labeled molecular ion. The SIM chart speed was calibrated by marking the chart at several timed intervals. The time intervals and ion abundance values were measured from oscillograph traces using a vernier caliper.

Repetitive scans of the GC peaks were made over a limited mass range that included the molecular ion enrichment cluster. The scans were initiated manually at fixed intervals. The time from T_o (retention time corresponding to void volume) to the first scan was measured from the total ion current chart with a vernier caliper. The ion abundance values on the oscillograph traces were digitized using an OSCAR Model K Oscillograph Analyzer and Reader (Benson-Lehner Corporation, Santa Monica, California), which was directly connected to an IBM Kepunch Type 024.
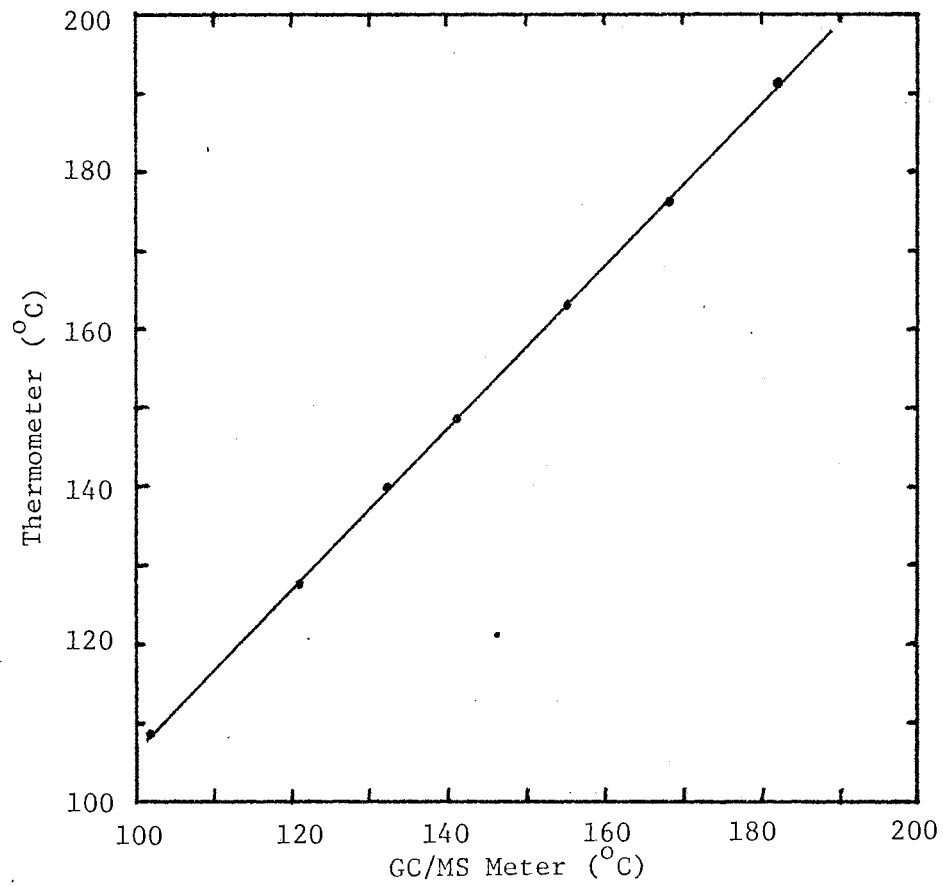
Figure 19. Temperature Calibration of GC/MS
Column Oven

Computations

In order to accurately determine the retention time for isomers of
a particular mass, the SIM data (ion abundance <u>vs</u> time) was least squares
fitted to a skewed Gaussian equation

$$Y = \left[\frac{P_1}{\sqrt{2\pi}\ P_2}\ \exp\left(-\frac{1}{2}\left(\frac{X-P_3}{P_2}\right)^2\right)\right]\left[1. - \frac{P_4(X-P_3)}{2P_2}\left(1. - \frac{(X-P_3)}{3P_2}\right)\right]$$

where P_1 is the area under the curve, P_2 is sigma, P_3 is the mean,
P_4 is the skew factor which adjusts to asymmetry in peak shape, X is
the time and Y is the ion abundance. A standard deviation (σ_i) for
each parameter (P_i) was also calculated. The computer program (LSMFT)
used to accomplish this data fitting was provided by the Statistics
Group at Los Alamos Scientific Laboratories (LASL), and is on file in
the LASL program library. The operation of LSMFT is explained briefly
in Appendix A.

The repetitive scans provided ion abundance <u>vs</u> time data for each
mass number in the molecular ion cluster. The data for each mass
number was fitted to a skewed Gaussian equation as described above. A
weighted average of the skew factors for all the mass numbers in the
molecular ion cluster was calculated using $1/\sigma_4$ as the weighting factor.
The data for each mass number was again fitted with the average skew
factor being held constant. This was done for each GC peak.

The least squares curves were used for "smoothing" the data in that
ion abundance values used for further calculations were taken from the
curves. The area under the curve (P_1) for each mass number was added

to the data matrix. These areas were treated in the same manner as an individual spectral scan in order to calculate an integrated value for mol % ^{13}C. The mean (P_3) for a given mass number is the retention time for the isomers of that mass number, and one way to observe isotope fractionation is to compare the retention times for the various mass numbers in the molecular ion cluster.

The smoothed data was corrected for natural abundance ^{2}H, ^{17}O and ^{18}O, and for ^{13}C in the methoxy carbon. Beginning with the abundance for the molecular ion containing no ^{13}C atoms ($M^{+ \cdot}$), the $(M + 1)^{+ \cdot}$ and $(M + 2)^{+ \cdot}$ abundance values due to heavy isotopes (other than ^{13}C) were calculated from the elemental composition and known values for natural abundance (147). These calculated abundance values were then subtracted from the observed abundance values at M + 1 and M + 2. This correction procedure is analogous to that used by Boone, Mitchum and Scheppele (148). In turn, the abundance values of each mass number were corrected; i.e., the corrected abundance of $(M + 1)^{+ \cdot}$ was used to calculate corrections for $(M + 2)^{+ \cdot}$ and $(M + 3)^{+ \cdot}$, etc. until the entire molecular ion cluster had been corrected. The corrected ion intensities were used to calculate the mol % ^{13}C for each spectral scan and for the integrated GC peak (149).

A Fortran program was written to move data into and from the LSMFT program and to perform the calculations described above. A listing of this program is in Appendix B. All calculations were performed on a CDC 7600 computer at the Central Computing Facility of the Los Alamos Scientific Laboratories.

^{13}C Content of FAMEs

The initial values for mol % ^{13}C (calculated from complete spectral scans taken at random on the GC peak) showed significant variability. This posed the possibility of ^{13}C/^{12}C fractionation on the GC column. This was investigated using the SIM system of the GC/MS. Figure 20 shows the obvious difference in retention time of the totally labeled species. An isotope fractionation was observed in this manner for 16:0, 16:2, 16:3 and 18:3 FAMEs on the 6-ft Silar-5CP column. Similar results were obtained on a 3% OV-1 column (5 ft, 200°C) for 16:0 FAME using a Finnigan GC/MS (150).

Because of the ^{13}C/^{12}C fractionation, an accurate determination of ^{13}C content requires that the entire GC peak be integrated for all molecular ion species. This was accomplished by making repetitive scans as described in the previous section. Figure 21 through Figure 37 show the data points and fitted curves for 16:0 FAME on Silar-5CP at 158°C. For m/z 270 and the highly enriched isomers (m/z 280 to 286) the data points fit the curves very closely, so the curve parameters have small standard deviations. For low enrichment isomers the ion intensity was quite low, so the data points are scattered about the fitted curve and the curve parameters have large standard deviations. Obviously, more spectral scans for a given GC peak will more precisely define the fitted curve and provide more precise values for ^{13}C content.

The results of a number of experiments are summarized in Table V and illustrate two general considerations. First, the FAMEs of highest purity (i.e., 16:0, 18:2 and 18:3) give the most consistent values for
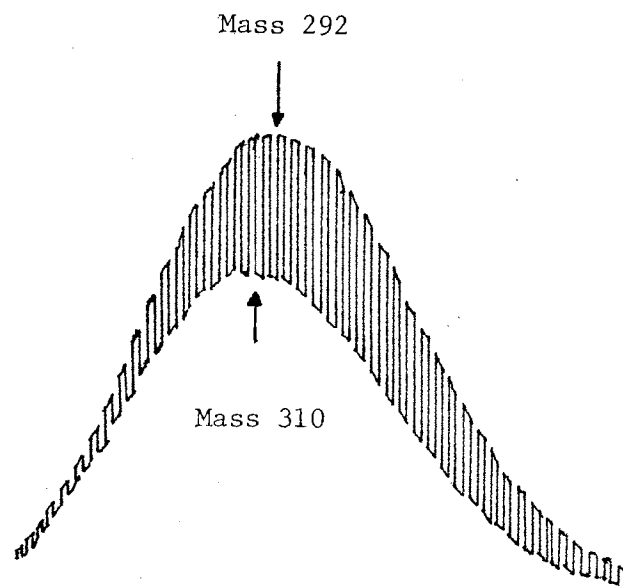
Figure 20. Chart Record of SIM Experiment for ^{13}C Enriched 18:3 FAME (Silar-5CP, $168^{\circ}C$)

Figure 21.   Elution of Mass 270 for ^{13}C Enriched
16:0 FAME (Silar-5CP, 158°C)
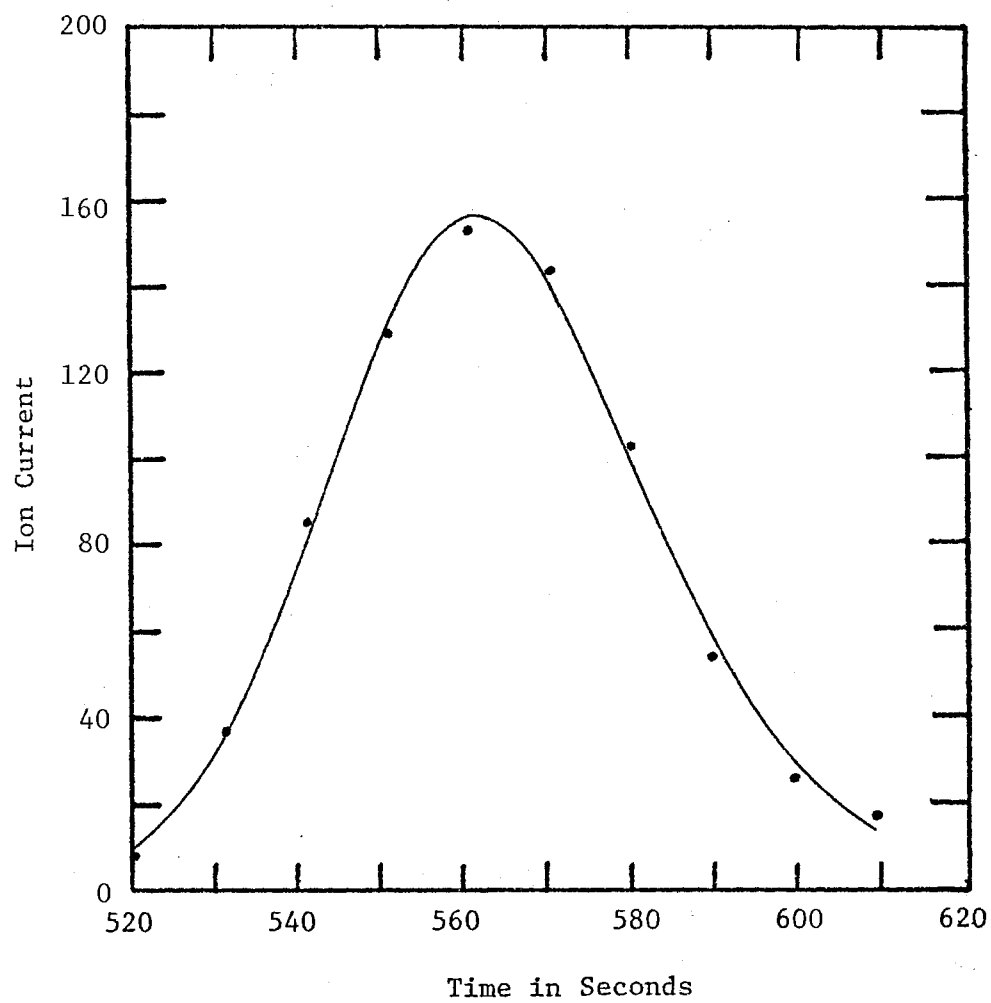
Figure 22. Elution of Mass 271 for ^{13}C Enriched 16:0 FAME (Silar-5CP, 158$^{\mathrm{O}}$C)
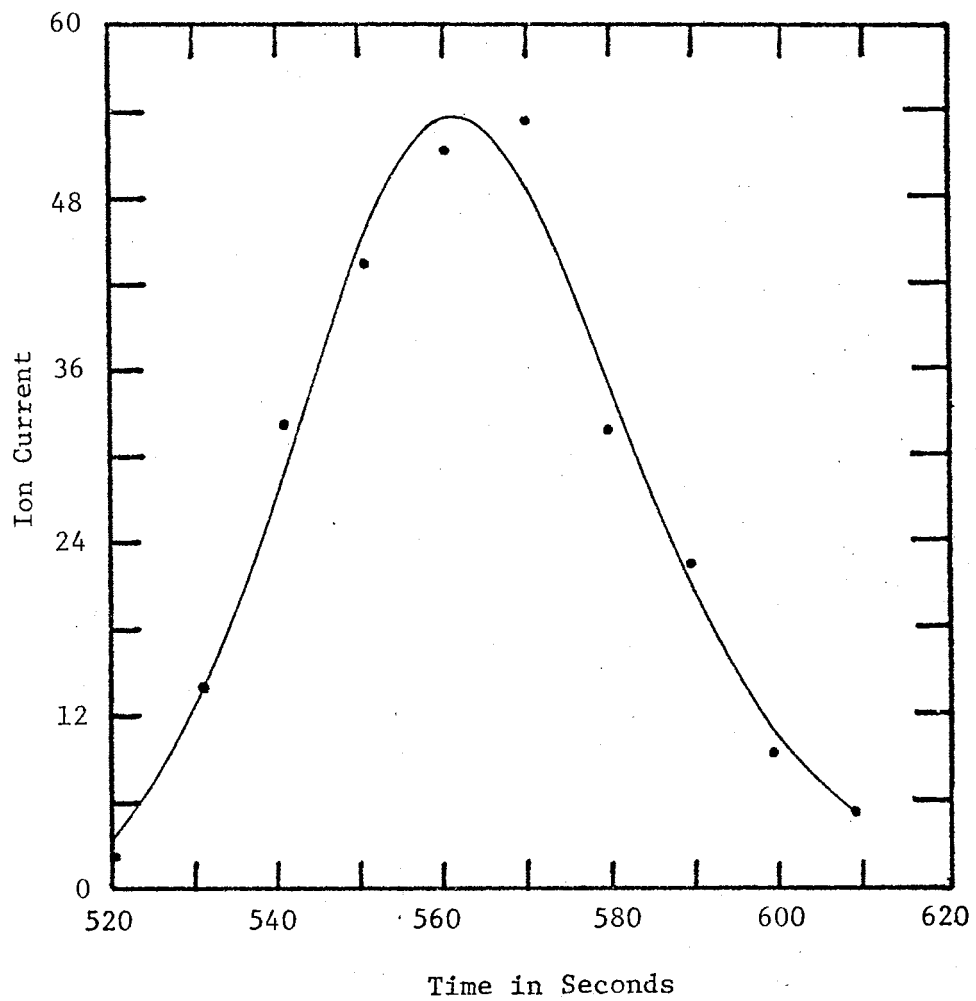
Figure 23. Elution of Mass 272 for ^{13}C Enriched 16:0 FAME (Silar-5CP, 158°C)
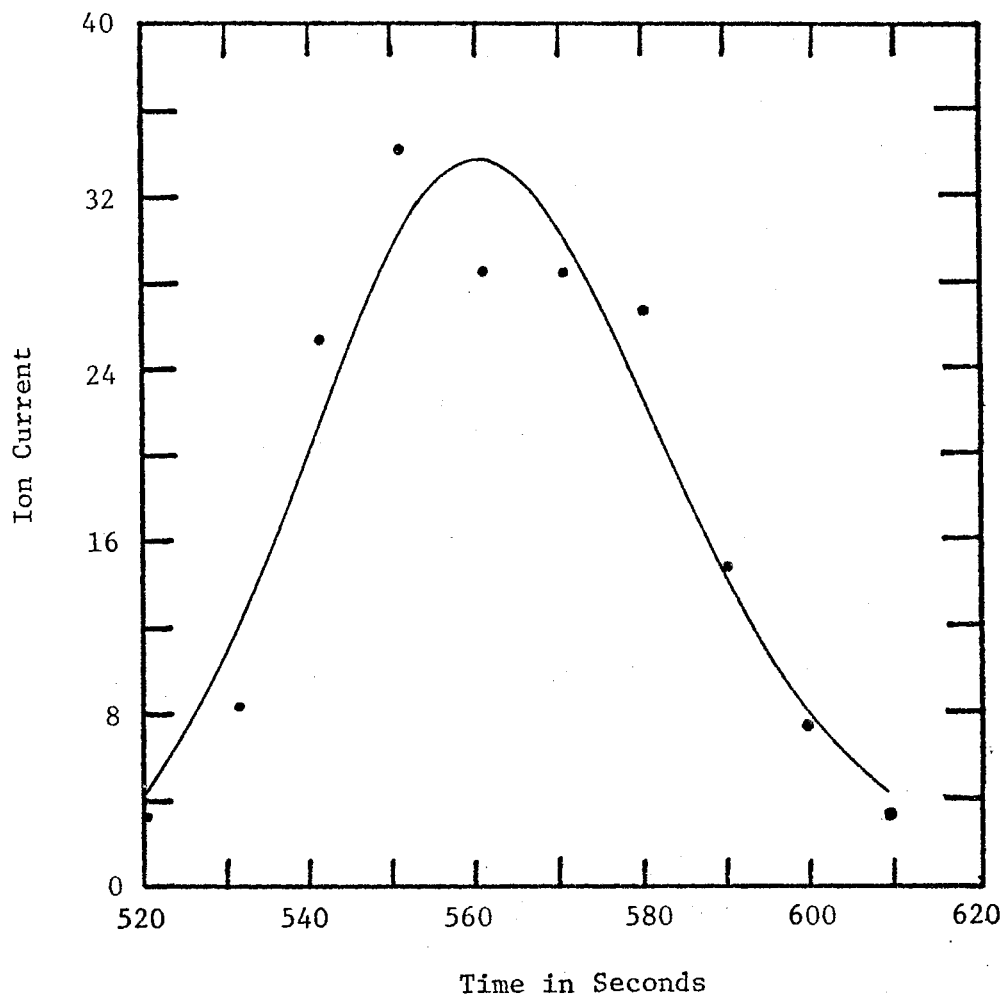
Figure 24. Elution of Mass 273 for ^{13}C Enriched
16:0 FAME (Silar-5CP, 158°C)
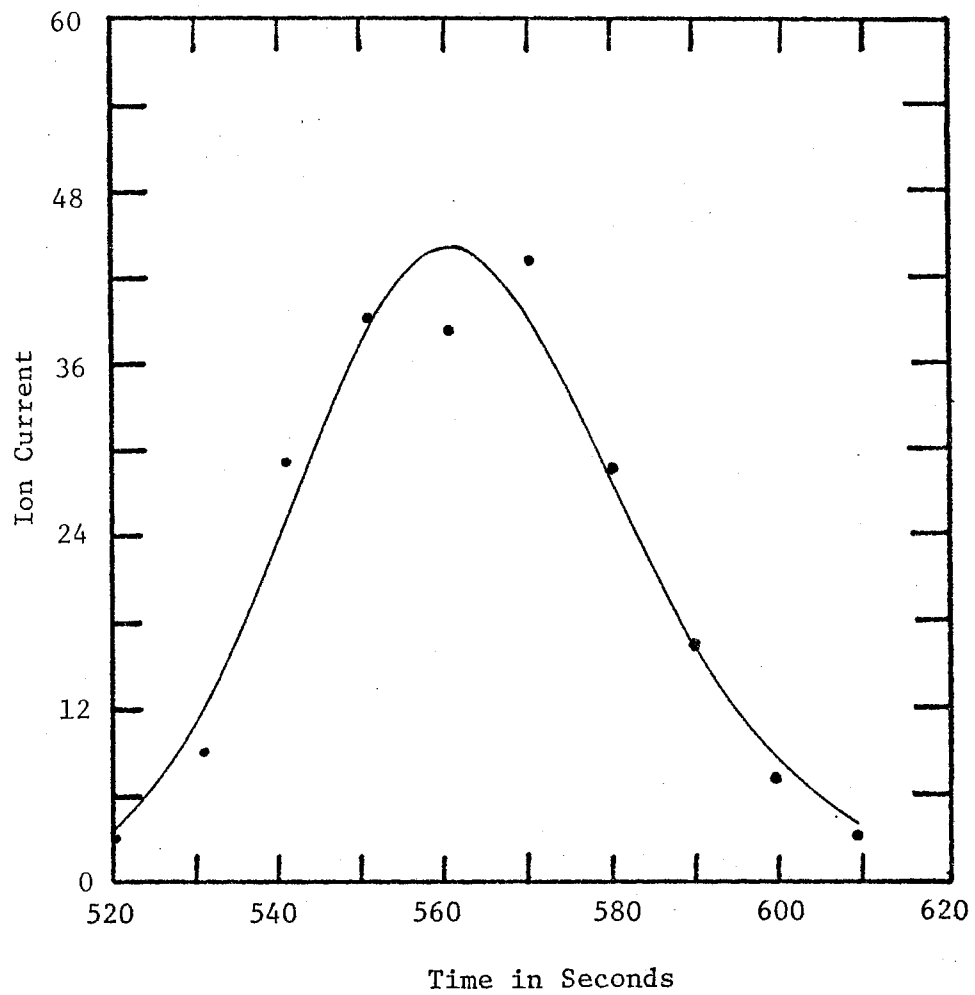
Figure 25. Elution of Mass 274 for ^{13}C Enriched 16:0 FAME (Silar-5CP, 158°C)
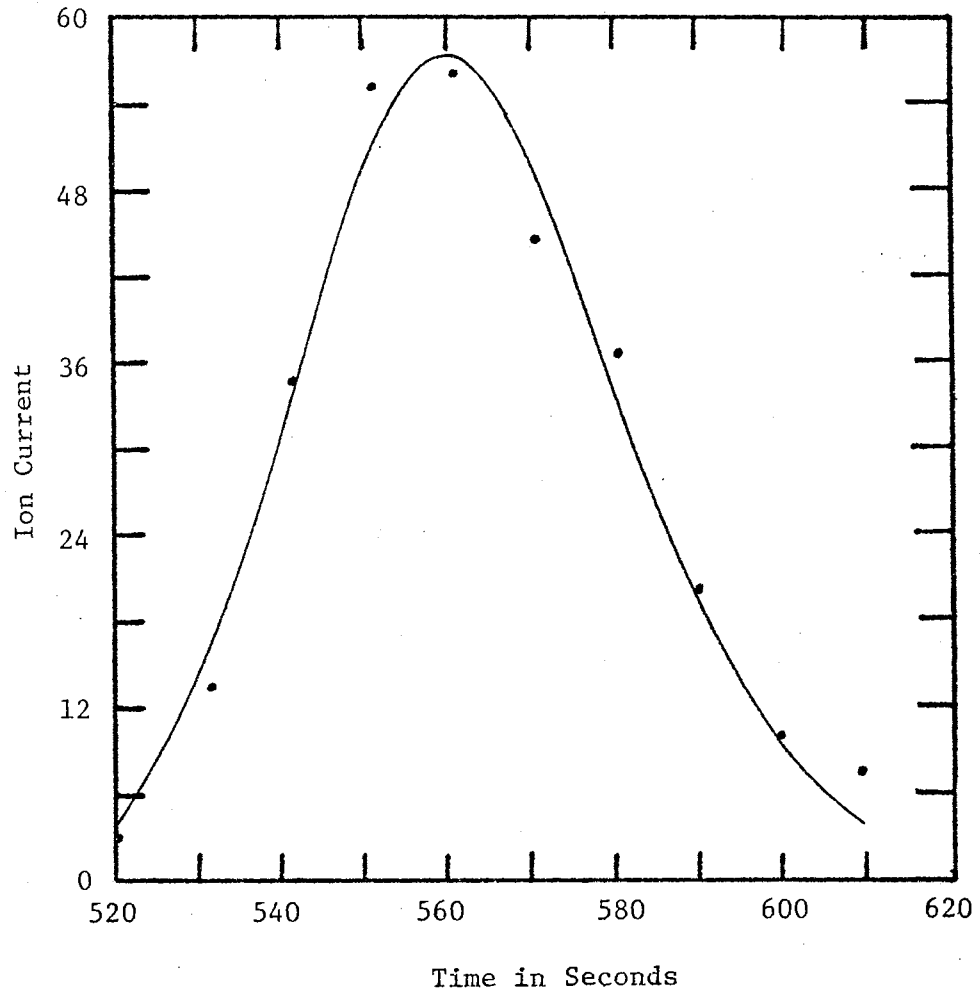
Figure 26. Elution of Mass 275 for ^{13}C Enriched 16:0 FAME (Silar-5CP, 158°C)
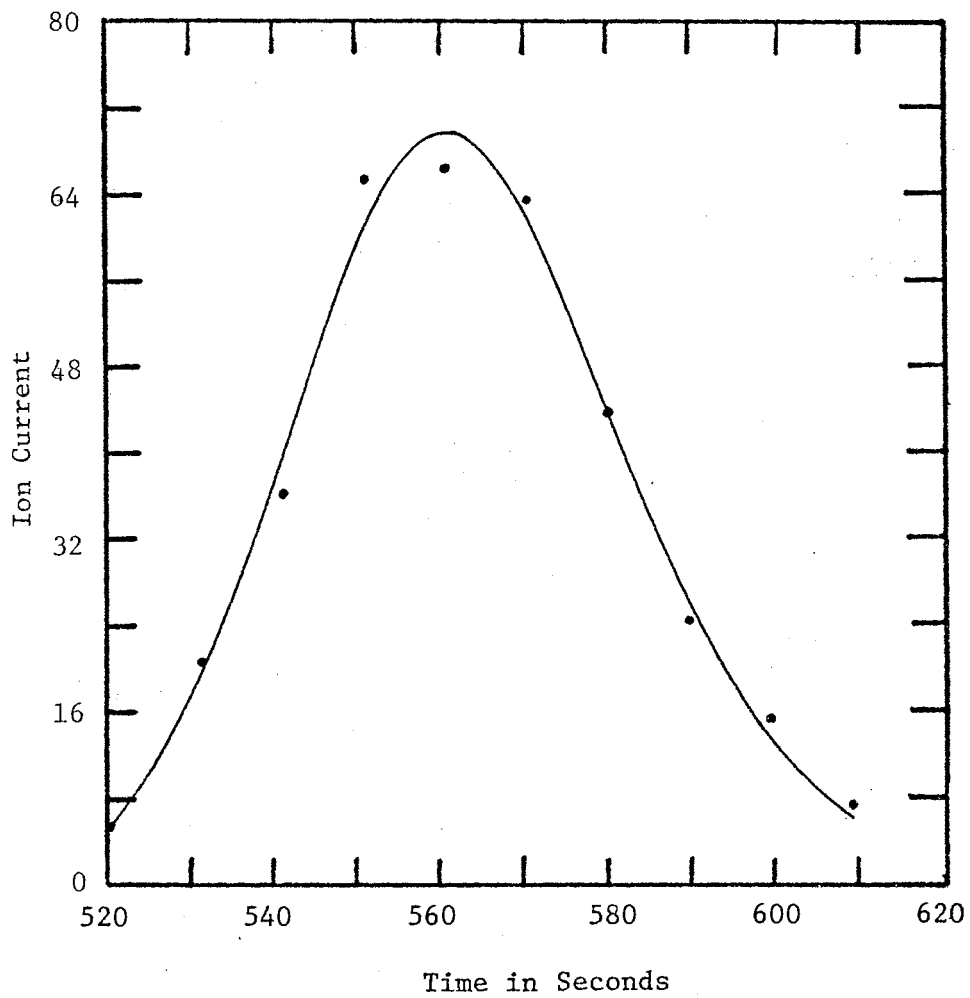
Figure 27. Elution of Mass 276 for ^{13}C Enriched 16:0 FAME (Silar-5CP, $158^{o}C$)
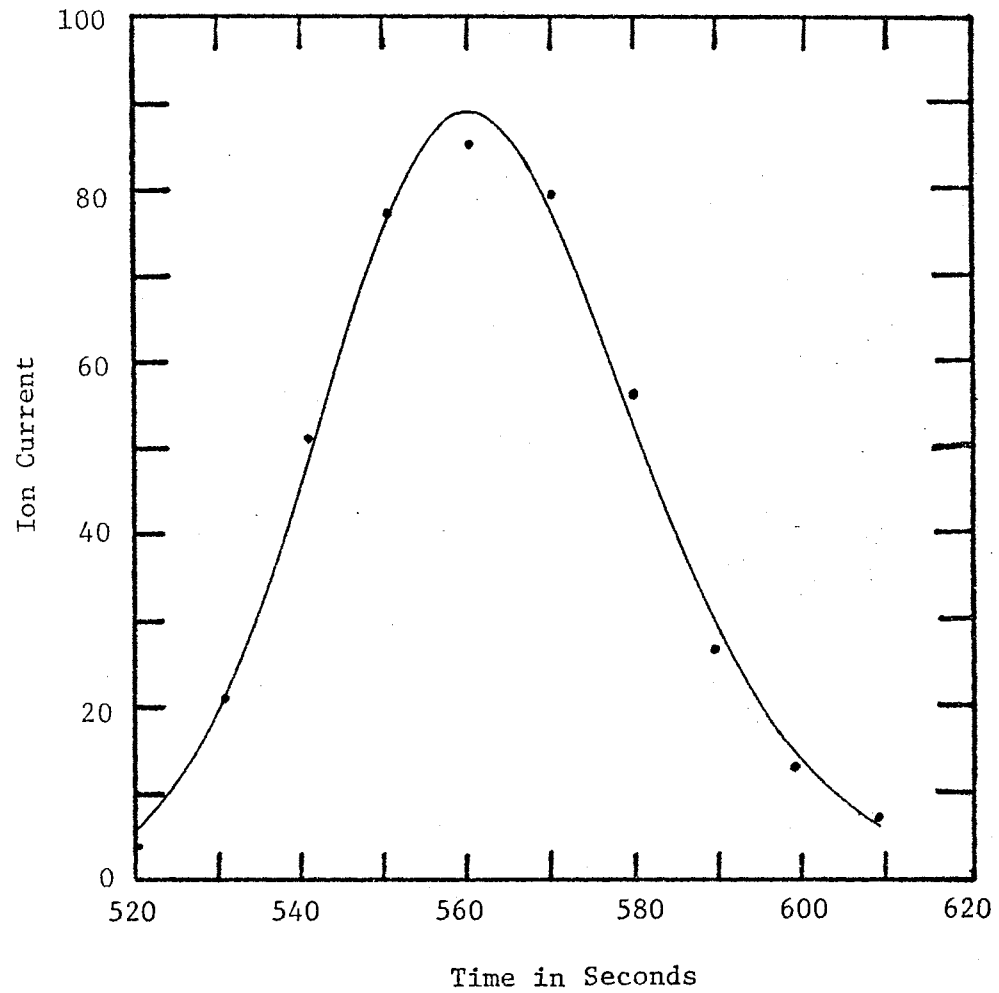
Figure 28. Elution of Mass 277 for ^{13}C Enriched 16:0 FAME (Silar-5CP, 158°C)
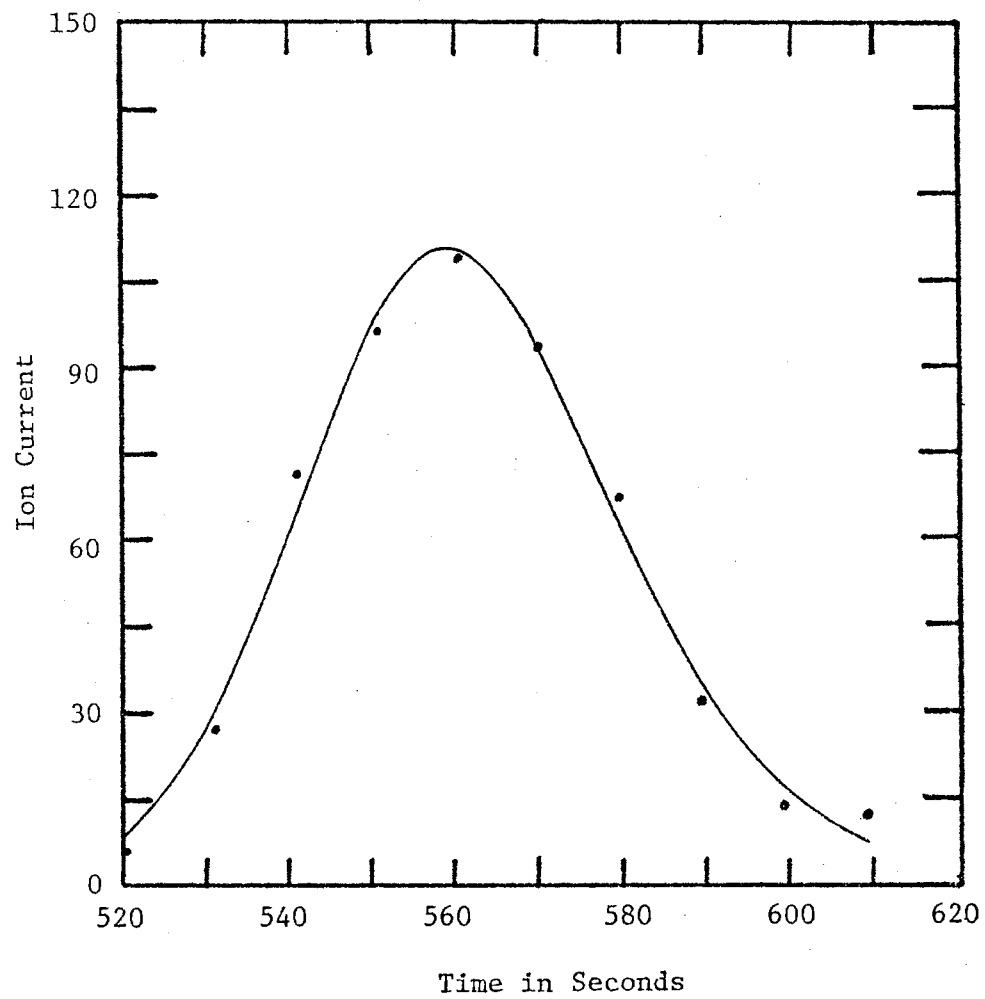
Figure 29. Elution of Mass 278 for ^{13}C Enriched
16:0 FAME (Silar-5CP, 158°C)
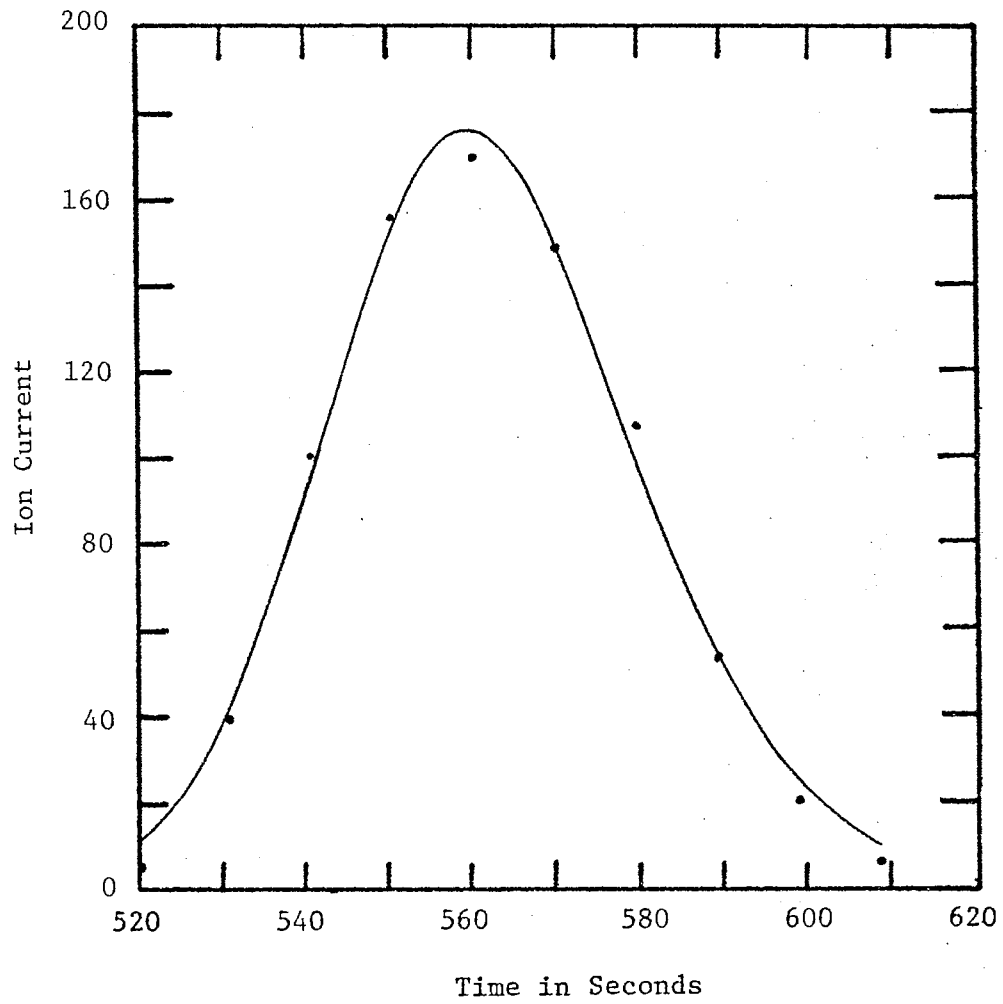
Figure 30. Elution of Mass 279 for ^{13}C Enriched 16:0 FAME (Silar-5CP, 158°C)
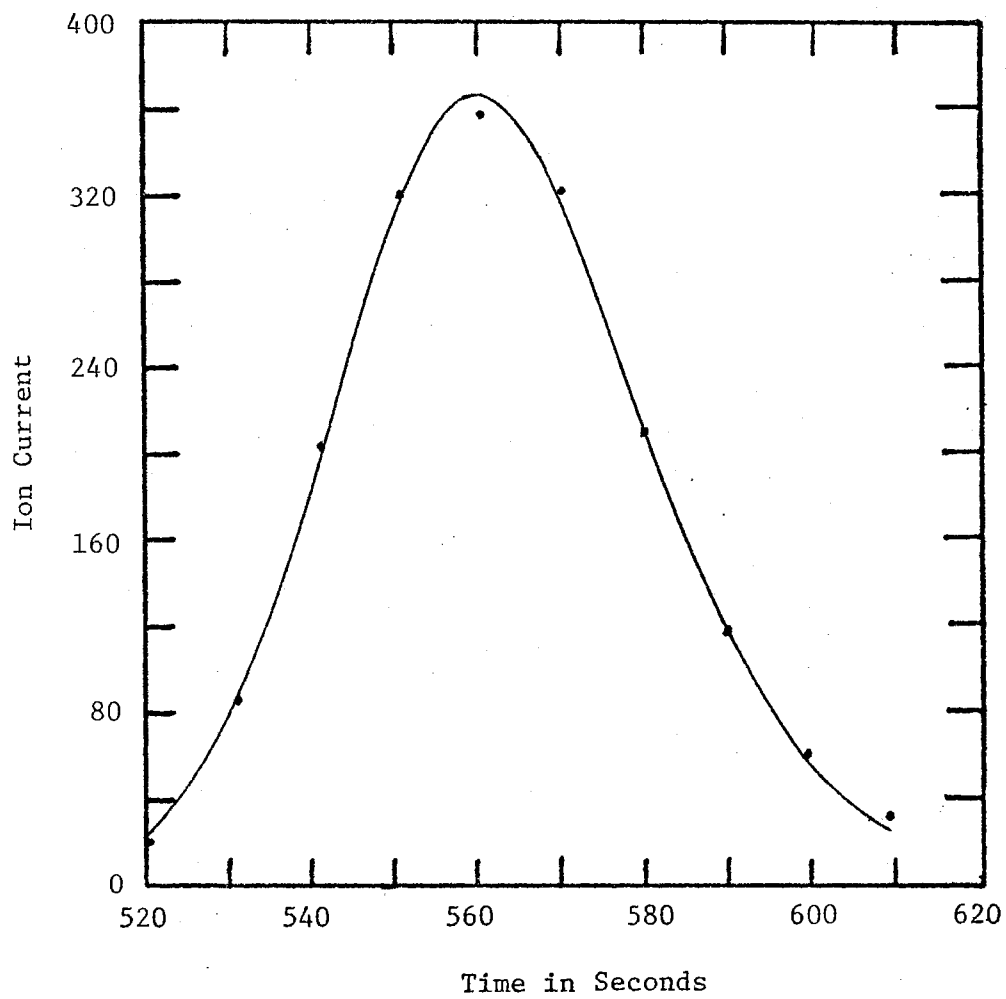
Figure 31. Elution of Mass 280 for ^{13}C Enriched
16:0 FAME (Silar-5CP, 158°C)
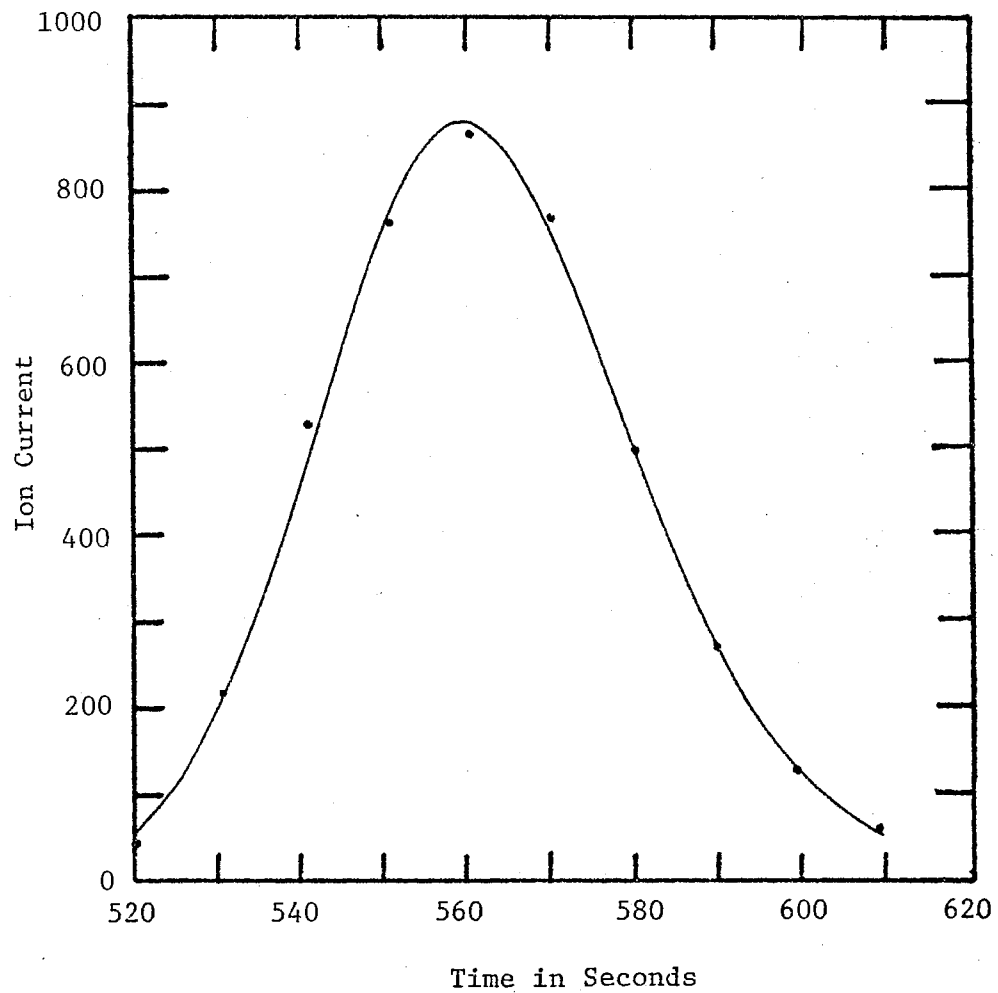
Figure 32. Elution of Mass 281 for ^{13}C Enriched
16:0 FAME (Silar-5CP, 158°C)
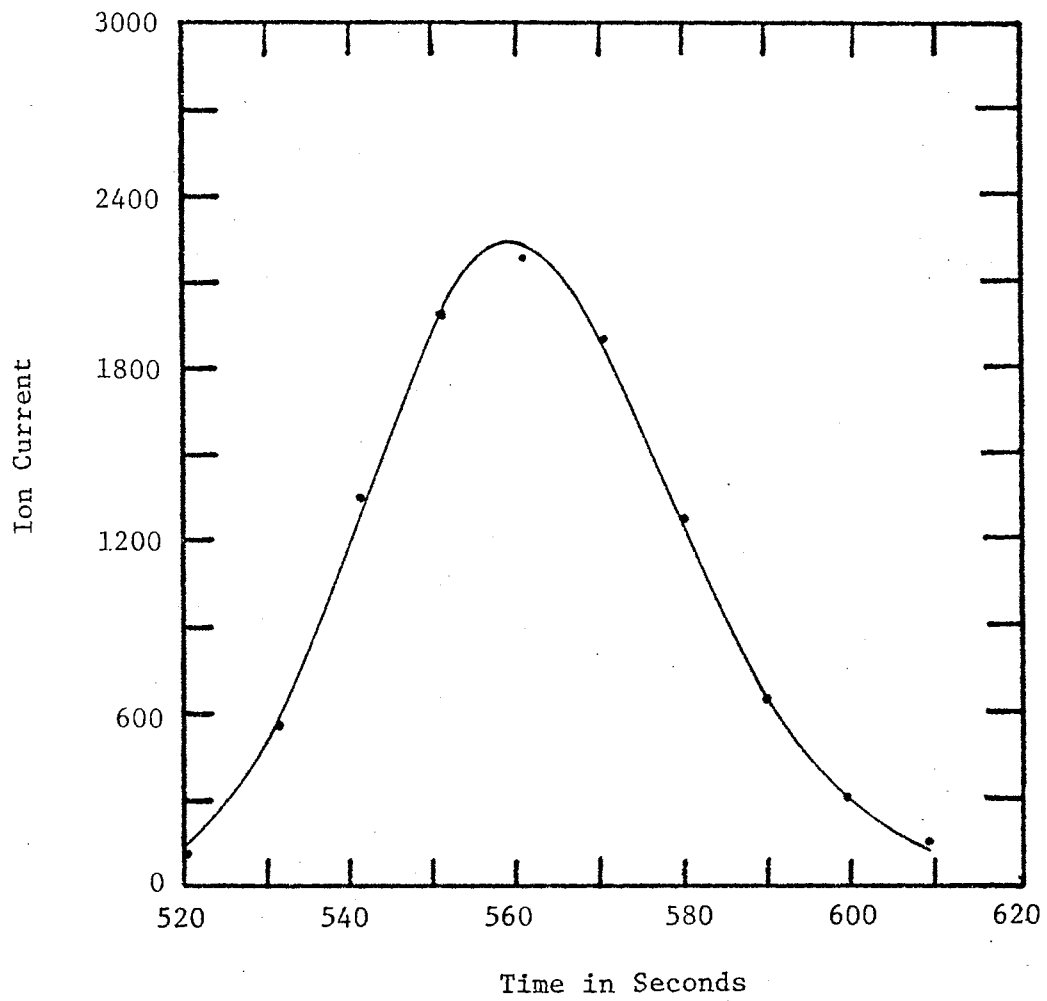
Figure 33. Elution of Mass 282 for ^{13}C Enriched
16:0 FAME (Silar-5CP, 158°C)
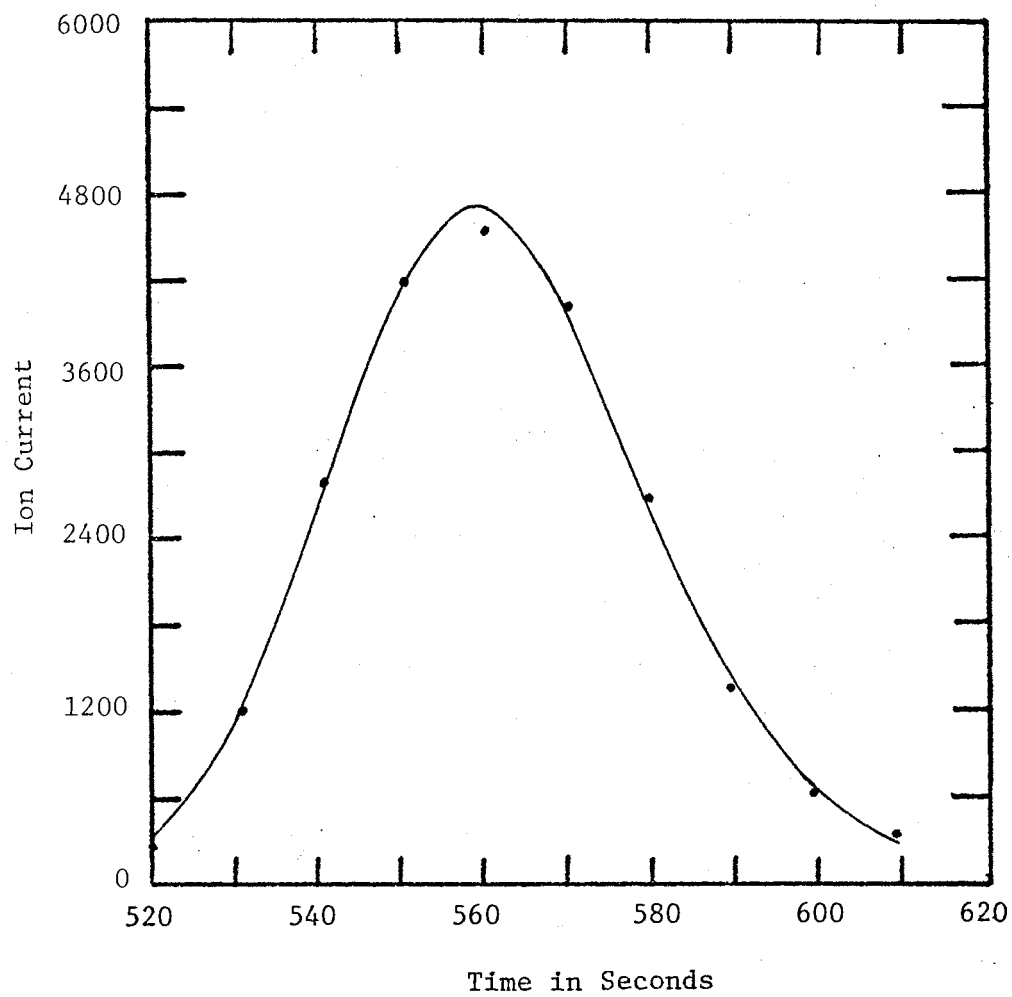
Figure 34. Elution of Mass 283 for ^{13}C Enriched
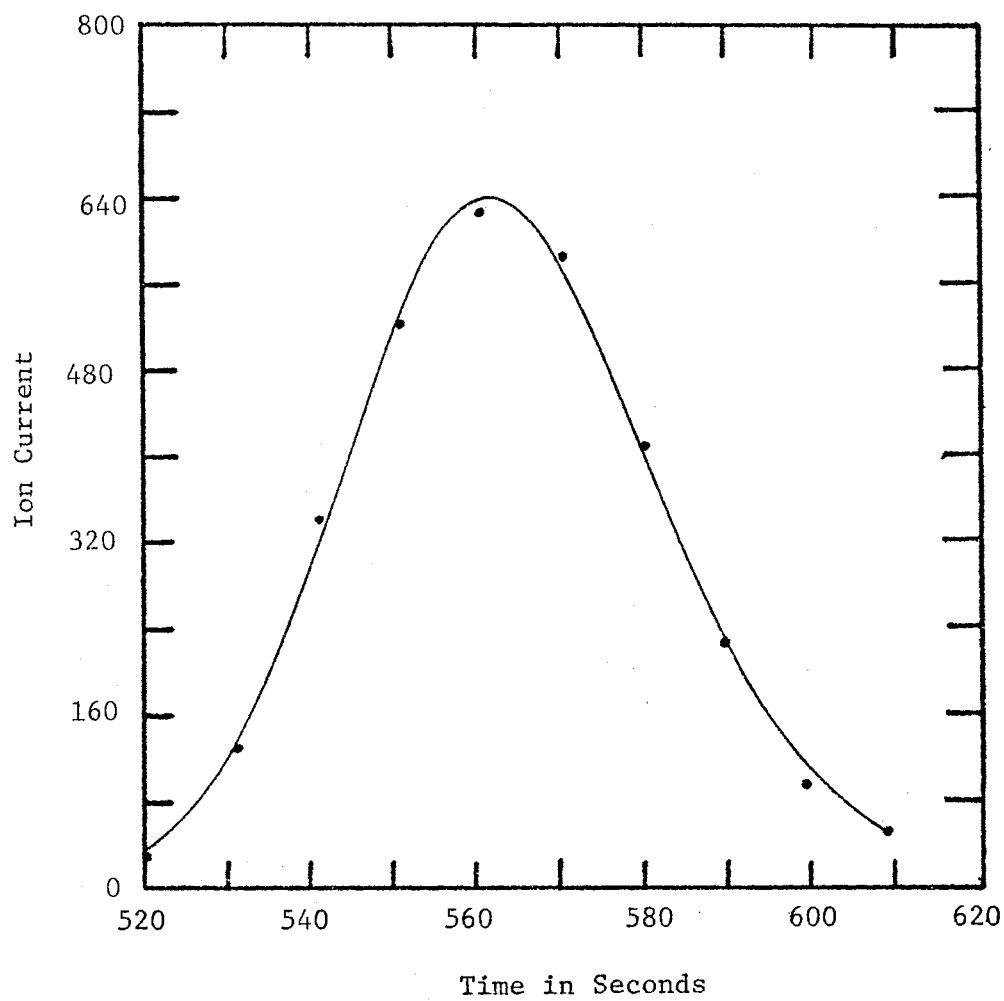16:0 FAME (Silar-5CP, 158°C)
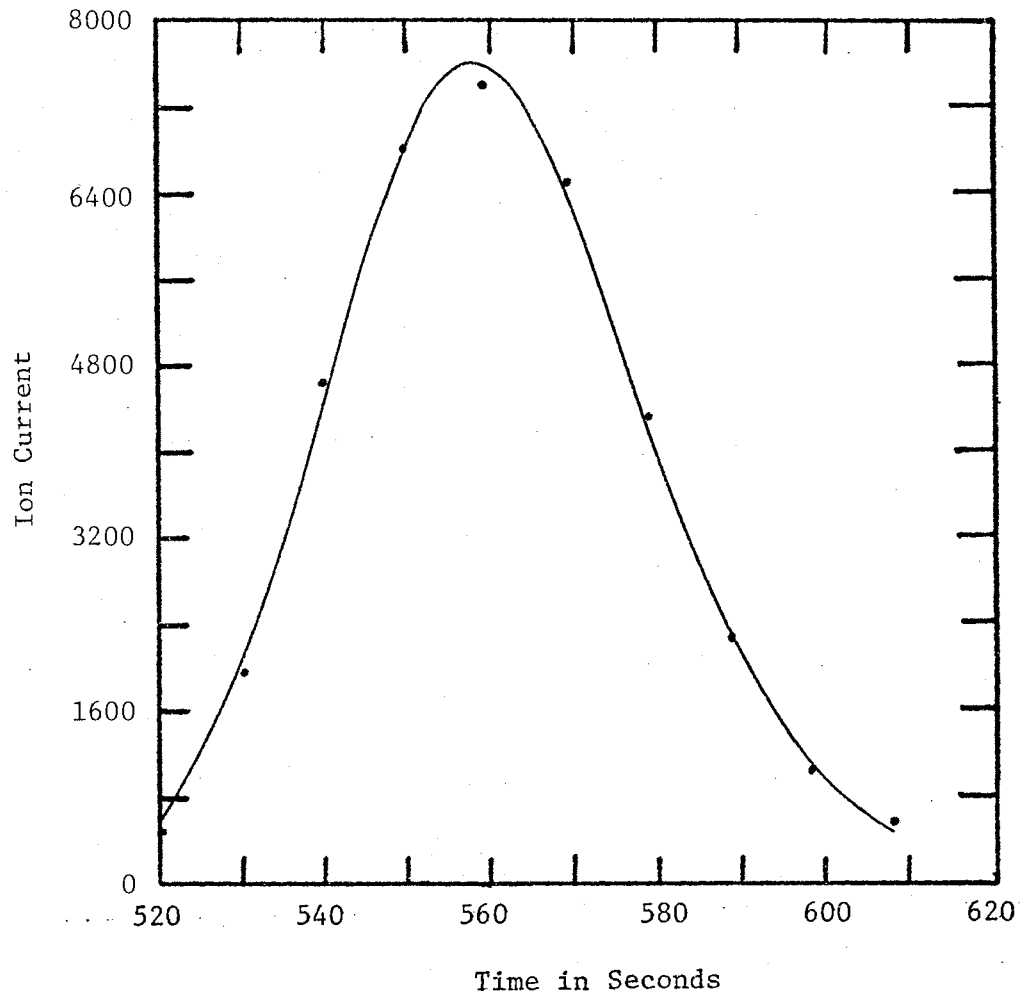
Figure 35. Elution of Mass 284 for ^{13}C Enriched
16:0 FAME (Silar-5CP, 158°C)
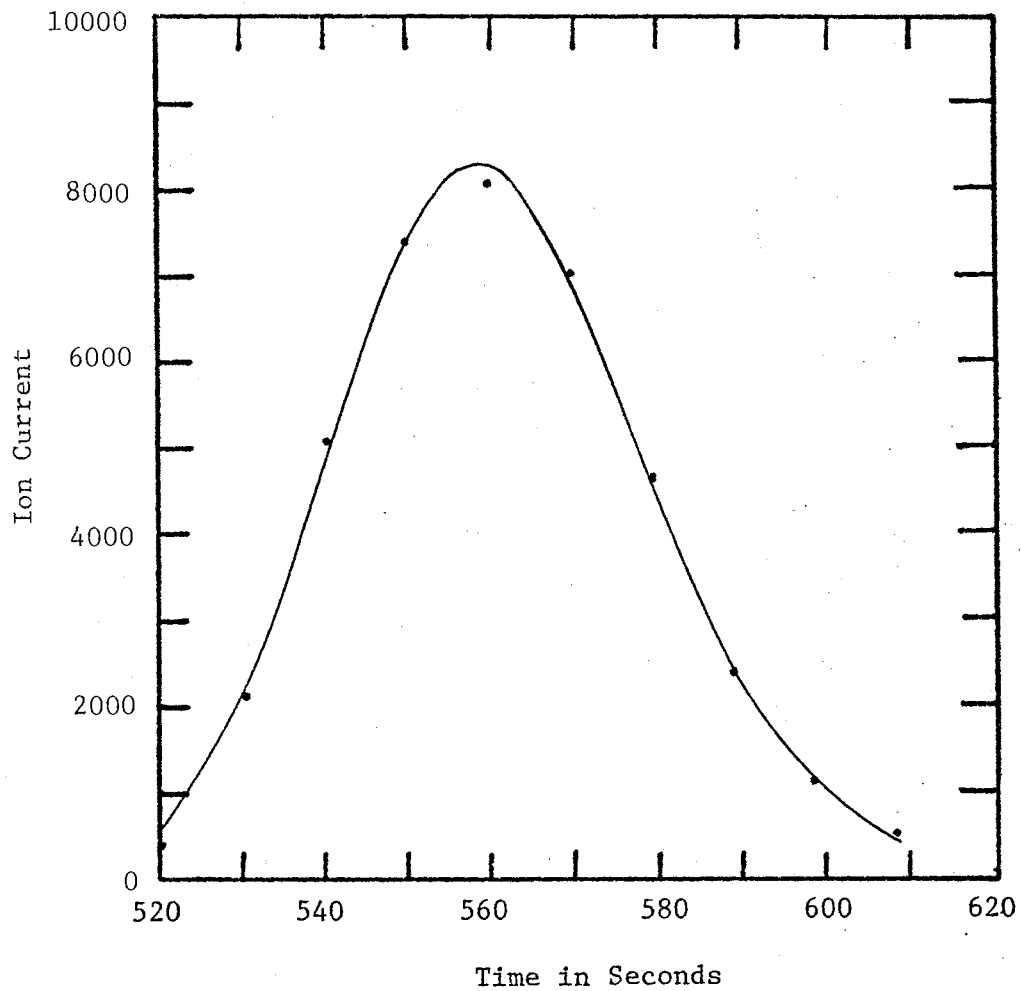
Figure 36. Elution of Mass 285 for ^{13}C Enriched 16:0 FAME (Silar-5CP, 158°C)
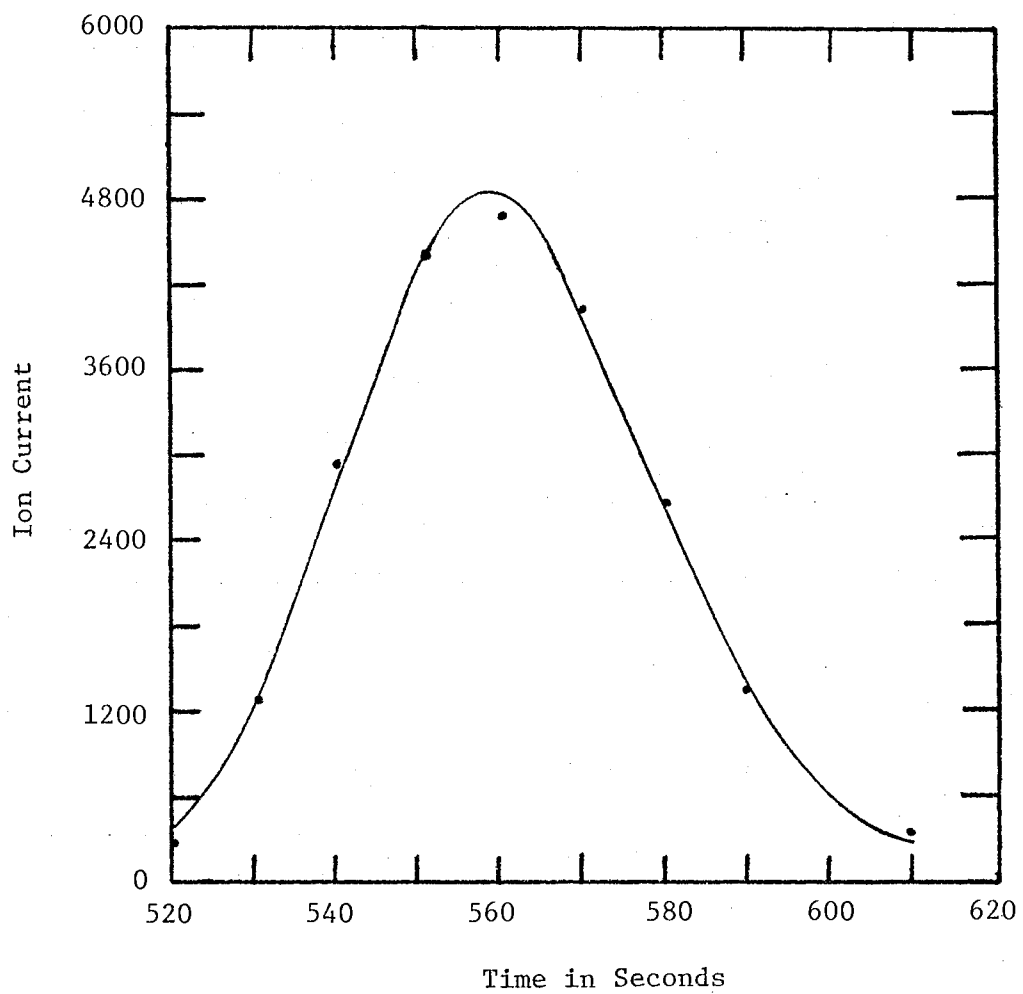
Figure 37. Elution of Mass 286 for ^{13}C Enriched 16:0 FAME (Silar-5CP, 158°C)

TABLE V

^{13}C CONTENT OF FAMES

		Silar-5CP			OV-1		
FAME	Temperature	Number of Scans	% Natural Abundance	Mol % ^{13}C	Number of Scans	% Natural Abundance	Mol % ^{13}C
16:0	142°C	14	2.60	84.96			
	158	10	2.54	85.13	13	2.57	84.48
	168	11	2.55	85.02	9	2.56	84.96
	178	8	2.53	85.01	14	2.55	85.03
	189				9	2.54	85.36
16:1	142°C	8	7.02	75.84			
	158	15	6.02	79.41			
	168	9	6.00	79.72			
	178	7	6.23	79.76			
16:2	142°C	6	2.46	82.39			
	158	13	2.40	83.80			
	168	11	2.43	83.80	10	2.16	84.19
	178	8	2.61	83.65	14	2.06	84.12
	189				9	2.15	84.28
16:3	142°C	13	12.26	65.00			
	158	8	12.23	64.82			
	168	9	12.22	65.34			
	178	12	12.92	64.47			
	189	8	12.21	65.41			
18:1	142°C	13	11.92	73.53			
	158	10	11.32	75.29			
	168	9	11.75	75.47			
	178	7	12.61	76.43			
18:2	142°C	12	1.90	84.07			
	158	16	1.97	84.25			
	168	11	1.88	84.29	14	1.74	84.95
	178	8	1.85	84.42	12	1.77	84.76
	189				16	1.48	85.22
18:3	142°C	18	12.20	65.86			
	158	15	12.34	65.99			
	168	11	12.34	65.88			
	178	12	12.48	65.82			
	189	14	12.69	65.86			

^{13}C content. Even small amounts of impurity (e.g., a methyl substituted FAME) can significantly effect the results if the GC column does not provide complete separation. Consequently, the calculated ^{13}C content for 18:1 shows a steady increase because the resoltuion decreases as the column temperature increases. Also note the higher ^{13}C content for 16:2 and 18:2 FAMEs on the OV-1 column, which did not separate small amounts of impurity. Thus, the preliminary separation (discussed in Chapter III, page 35) is of primary importance to the accurate determination of ^{13}C content.

Secondly, the mol % ^{13}C and percent natural abundance values reflect the effect that nutrient concentration and stage of growth have on fatty acid composition (see Chapter II, page 5). The two liter inoculum in the culture chamber contained natural abundance carbon both as biocarbonate in the medium and as cellular carbon in the algae. Consequently the ^{13}C content of the carbon used in fatty acid synthesis asymptotically approached that of the carbon-^{13}C dioxide supply. Concurrently, the nitrate concentration decreased. Since polyunsaturated fatty acids (especially 16:3 and 18:3) were preferentially synthesized initially, their ^{13}C content is much lower than that of other fatty acids. The values for 16:1 and 18:1 FAMEs are unreliable due to unresolved impurities. Since additional nitrate was added at the midpoint of the growth period, the results for this particular batch of algae are less dramatic than they would otherwise be. Analysis of ^{13}C content and labeling pattern (see Figures 15 and 16) would be a very effective approach to the study of the relative synthesis rates of fatty acids under various growth conditions.

$^{13}C/^{12}C$ Fractionation by Chromatography

Introduction and Literature Review

The chromatographic fractionation of isotopes has been reviewed and evaluated by Klein (151). Fractionation of carbon isotopes has been observed in several separation technqiues (e.g., 152-154), but there have been only a few reports of carbon isotope fractionation by gas chromatography. Blanc et al. (155,156) showed $^{13}C/^{12}C$ fractionation for carbon monoxide on a molecular sieve column. Gunter and Gleason (157) observed $^{13}C/^{12}C$ fractionation for methane on a molecular sieve column and for carbon dioxide on silica gel and Poropak (Q and R) columns. Bayer et al. (158) obtained $^{13}C/^{12}C$ fractionation for tetrafluoromethane on Poropak (Q and S) columns. However, carbon isotope fractionation for larger molecules of biological significance has not been observed. Bentley et al. (159) were unable to detect fractionation for D-glucose-U-^{13}C (50 mol % ^{13}C) on a 3% SE-30 column. Using GC/MS, VandenHeuvel et al. (160,161) could find no $^{13}C/^{12}C$ fractionation with 12-14 mol % ^{13}C amino acids on 2% SE-30 or 2% OV-17. The present study has documented $^{13}C/^{12}C$ fractionation for FAMEs and evaluated the significant parameters that effect the fractionation.

Results and Discussion

As discussed above, $^{13}C/^{12}C$ fractionation was first observed using the SIM mode of operation. In order to perform a detailed study, repetitive scans were taken as the GC peak eluted. Not only does the repetitive scan data provide accurate values for ^{13}C content, but it also

documents the $^{13}C/^{12}C$ fractionation by providing data for two types of plots. The mol % ^{13}C may be plotted versus the time of the spectral scan, or the retention time of each mass number may be plotted versus the number of ^{13}C atoms in the molecule. Figures 38 and 39 show these plots for the same GC peak used to illustrate the curve fitting program.

The data for both types of plots is summarized in Table VI through X. It is readily apparent that the calculated ^{13}C content is dependent on when the spectral scan is taken. Even for small ΔRetention values, there are significant changes in the isotopic content as the GC peak elutes. The four obvious variables that might effect the isotope fractionation are chain length, degree of unsaturation, column temperature and stationary phase. The data shows no apparent relationship between any of these variables and the observed separation factor. However, as seen in Figures 40 and 41 ΔRetention is proportional to the retention time. So, it appears that there is no specific interaction that is responsible for the observed isotope fractionation. Rather a difference in the vapor pressure of the isotopic species seems to be the likely explanation. As has been explained by others (162,163), molecules containing the heavier ^{13}C atoms will have a smaller van der Waals attraction and hence a smaller heat of evaporation. This effect is particularly important for molecules in which the isotopic atoms contribute to intense infrared absorption bands (163). Highly enriched FAMEs have a number of active infrared absorption bands (164).

Two vapor pressure comparisons are useful. There is enough difference (0.8%) in the vapor pressure of carbon-^{12}C monoxide and carbon-^{13}C monoxide that the two isomers may be separated by

TABLE VI

$^{13}C/^{12}C$ FRACTIONATION FOR 16:0 FAME

Temperature	142°C	158°C		168°C		178°C		189°C
GC Column	Silar-5CP	Silar-5CP	OV-1	Silar-5CP	OV-1	Silar-5CP	OV-1	OV-1
Time to First Scan (sec)	1198	520	1313	334	849	206	550	344
Time Between Scans (sec)	10	10	10	5	10	5	5	5
Calculated Mol % ^{13}C for Each Scan	85.36	86.10	84.21	85.67	85.54	86.32	85.74	86.44
	85.40	85.86	84.59	85.59	85.40	85.71	85.58	86.04
	85.40	85.63	84.80	85.48	85.22	85.29	85.44	85.69
	85.36	85.40	84.91	85.32	85.03	84.92	85.30	85.40
	85.29	85.16	14.94	85.14	84.84	84.64	85.17	85.20
	85.18	84.92	84.91	84.93	84.64	84.51	85.05	85.09
	85.05	84.70	84.83	84.72	84.45	84.46	84.94	85.05
	84.90	84.50	84.71	84.52	84.24	84.26	84.85	85.06
	84.74	84.28	84.54	84.33	83.96		84.77	85.09
	84.59	83.99	84.34	84.12			84.70	
	84.46		84.09	83.83			84.64	
	84.34						84.58	
	84.24						84.49	
	84.02						84.37	
			82.56					
			81.87					
Adjusted Retention Time of m/z 270 (sec)	1259.8	563.6	1382.5	357.5	883.9	222.7	579.1	364.3
Adjusted Retention Time of m/z 286 (sec)	1254.9	560.8	1378.6	355.6	881.4	221.3	577.8	363.3
ΔRetention (m/z 270-m/z 286)	4.9	2.8	3.9	1.9	2.5	1.4	1.3	1.0
Separation Factor, (α)*	1.0039	1.0050	1.0028	1.0053	1.0028	1.0063	1.0022	1.0028

*
$$\alpha = \frac{\text{Adjusted Retention Time of } m/z\ 270}{\text{Adjusted Retention Time of } m/z\ 286}$$

TABLE VII

$^{13}C/^{12}C$ FRACTIONATION FOR 16:2 FAME

Temperature	$142^{\circ}C$	$158^{\circ}C$	$168^{\circ}C$		$178^{\circ}C$		$189^{\circ}C$
GC Column	Silar-5CP	Silar-5CP	Silar-5CP	OV-1	Silar-5CP	OV-1	OV-1
Time to First Scan (sec)	1657	713	458	705	288	468	300
Time Between Scans (sec)	15	5	5	10	5	5	5
Calculated Mol % ^{13}C for Each Scan	83.80	84.56	84.36	84.58	84.29	84.92	85.16
	83.80	84.50	84.43	84.75	84.43	84.90	85.05
	83.66	84.42	84.40	84.75	84.27	84.84	84.86
	83.41	84.31	84.29	84.63	83.97	84.74	84.61
	83.07	84.18	84.13	84.40	83.54	84.60	84.31
	82.63	84.03	83.90	84.08	82.94	84.42	83.98
		83.86	83.64	83.70	82.16	84.21	83.62
		83.67	83.34	83.28	81.02	83.96	83.20
		83.47	83.01	82.77		83.68	82.67
		83.26	82.66	82.70		83.38	
		83.04	82.22			83.05	
		82.80				82.68	
		82.56				82.24	
						81.68	
Adjusted Retention Time of m/z 266 (sec)	1707.8	742.8	482.4	749.7	303.8	498.7	320.7
Adjusted Retention Time of m/z 282 (sec)	1701.0	738.2	479.1	746.3	302.2	496.1	319.2
ΔRetention (m/z 266-m/z 282)	6.8	4.6	3.3	3.4	1.6	2.6	1.5
Separation Factor, $(\alpha)^{*}$	1.0040	1.0062	1.0069	1.0046	1.0053	1.0052	1.0050

*

$$\alpha = \frac{\text{Adjusted Retention Time of m/z 266}}{\text{Adjusted Retention Time of m/z 282}}$$

TABLE VIII

$^{13}C/^{12}C$ FRACTIONATION FOR 16:3 FAME

Temperature	142°C	158°C	168°C	178°C	189°C
GC Column	Silar-5CP	Silar-5CP	Silar-5CP	Silar-5CP	Silar-5CP
Time to First Scan (sec)	2059	909	577	354	246
Time Between Scans (sec)	20	10	10	5	5
Calculated Mol % ^{13}C for Each Scan	67.84	66.52	68.99	66.76	68.45
	67.27	66.11	67.65	66.38	66.83
	66.77	65.64	66.55	65.97	65.61
	66.28	65.12	65.59	65.50	64.74
	65.79	64.60	64.76	64.97	64.22
	65.29	64.08	64.11	64.41	64.01
	64.80	63.57	63.65	63.81	63.97
	64.33	63.08	62.77	63.21	63.98
	63.91			62.63	
	63.57			62.02	
	63.29			61.34	
	63.01			60.52	
	62.66				
Adjusted Retention Time of m/z 264 (sec)	2180.9	945.0	614.6	378.8	260.2
Adjusted Retention Time of m/z 280 (sec)	2173.1	941.4	612.0	377.2	259.3
ΔRetention (m/z 264-m/z 280)	7.8	3.6	2.6	1.6	0.9
Separation Factor, (α)*	1.0036	1.0038	1.0042	1.0042	1.0035

*
$$\alpha = \frac{\text{Adjusted Retention Time of m/z 264}}{\text{Adjusted Retention Time of m/z 280}}$$

TABLE IX

$^{13}C/^{12}C$ FRACTIONATION FOR 18:2 FAME

Temperature	142°C	158°C	168°C		178°C		189°C
GC Column	Silar-5CP	Silar-5CP	Silar-5CP	OV-1	Silar-5CP	OV-1	OV-1
Time to First Scan (sec)	3882	1559	971	1644	591	1059	640
Time Between Scans (sec)	30	10	10	15	10	10	5
Calculated Mol % ^{13}C for Each Scan	84.79	85.10	84.20	84.91	84.35	85.17	86.06
	84.79	84.94	84.39	85.22	84.50	85.23	86.01
	84.74	84.78	84.49	85.36	84.52	85.24	85.92
	84.64	84.64	84.52	85.41	84.49	85.21	85.80
	84.49	84.50	84.50	85.39	84.42	85.14	85.67
	84.30	84.38	84.44	85.31	84.34	85.03	85.53
	84.07	84.28	84.34	85.20	84.25	84.88	85.40
	83.49	84.18	84.21	85.04	84.12	84.69	85.26
	83.14	84.10	84.06	84.85		84.44	85.14
	82.73	84.03	83.89	84.63		84.12	85.01
	82.28	83.97	83.69	84.35		83.70	84.89
		83.91		84.02		83.12	84.76
		83.86		83.59			84.62
		83.82		83.01			84.45
		83.77					84.24
		83.73					83.97
Adjusted Retention Time of m/z 294 (sec)	4044.2	1636.7	1019.5	1745.0	622.1	1113.6	678.9
Adjusted Retention Time of m/z 312 (sec)	4022.8	1631.1	1016.2	1738.6	620.4	1108.7	675.2
ΔRetention (m/z 924–m/z 312)	21.4	5.6	3.3	6.4	1.7	4.9	3.7
Separation Factor, (α)[*]	1.0053	1.0034	1.0032	1.0037	1.0027	1.0044	1.0055

[*]
$$\alpha = \frac{\text{Adjusted Retention Time of m/z 294}}{\text{Adjusted Retention Time of m/z 312}}$$

TABLE X

$^{13}C/^{12}C$ FRACTIONATION FOR 18:3 FAME

Temperature	142°C	158°C	168°C	178°C	189°C
GC Column	Silar-5CP	Silar-5CP	Silar-5CP	Silar-5CP	Silar-5CP
Time to First Scan (sec)	4887	1992	1207	709	475
Time Between Scans (sec)	30	10	15	10	5
Calculated Mol % ^{13}C for Each Scan	68.49	67.83	69.40	69.92	70.08
	68.25	67.61	68.30	68.91	68.95
	67.99	67.38	67.42	68.00	67.97
	67.70	67.13	66.66	67.13	67.11
	67.39	66.88	66.00	66.31	66.36
	67.06	66.61	65.44	65.53	65.71
	66.71	66.34	65.00	64.82	65.17
	66.34	66.07	64.68	64.19	64.74
	65.96	65.59	64.47	63.65	64.41
	65.57	65.50	64.31	63.16	64.18
	65.17	65.21	64.14	62.65	64.03
	64.77	64.91		62.10	63.91
	64.37	64.61			63.80
	63.98	64.29			63.69
	63.60	63.97			
	63.20				
	62.78				
	62.33				
Adjusted Retention Time of m/z 292 (sec)	5140.4	2066.4	1281.7	759.9	504.1
Adjusted Retention Time of m/z 310 (sec)	5119.0	2060.8	1276.8	756.0	501.9
ΔRetention (m/z 292–m/z 310)	21.4	5.6	4.9	3.9	2.2
Separation Factor (α)[*]	1.0042	1.0027	1.0038	1.0052	1.0044

[*]
$$\alpha = \frac{\text{Adjusted Retention Time of m/z 292}}{\text{Adjusted Retention Time of m/z 310}}$$
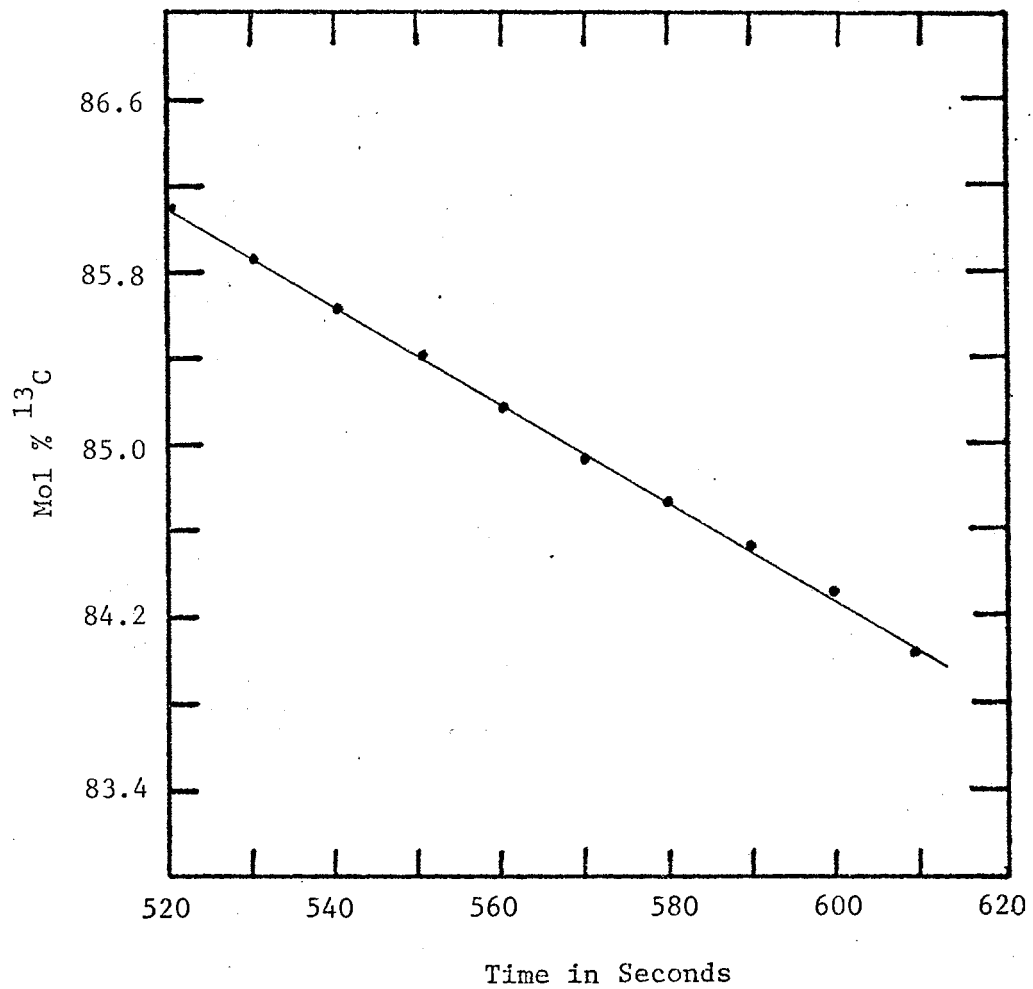
Figure 38.   Change in ^{13}C Content During the
Elution of ^{13}C Enriched 16:0
FAME (Silar-5CP, $158^{o}C$)
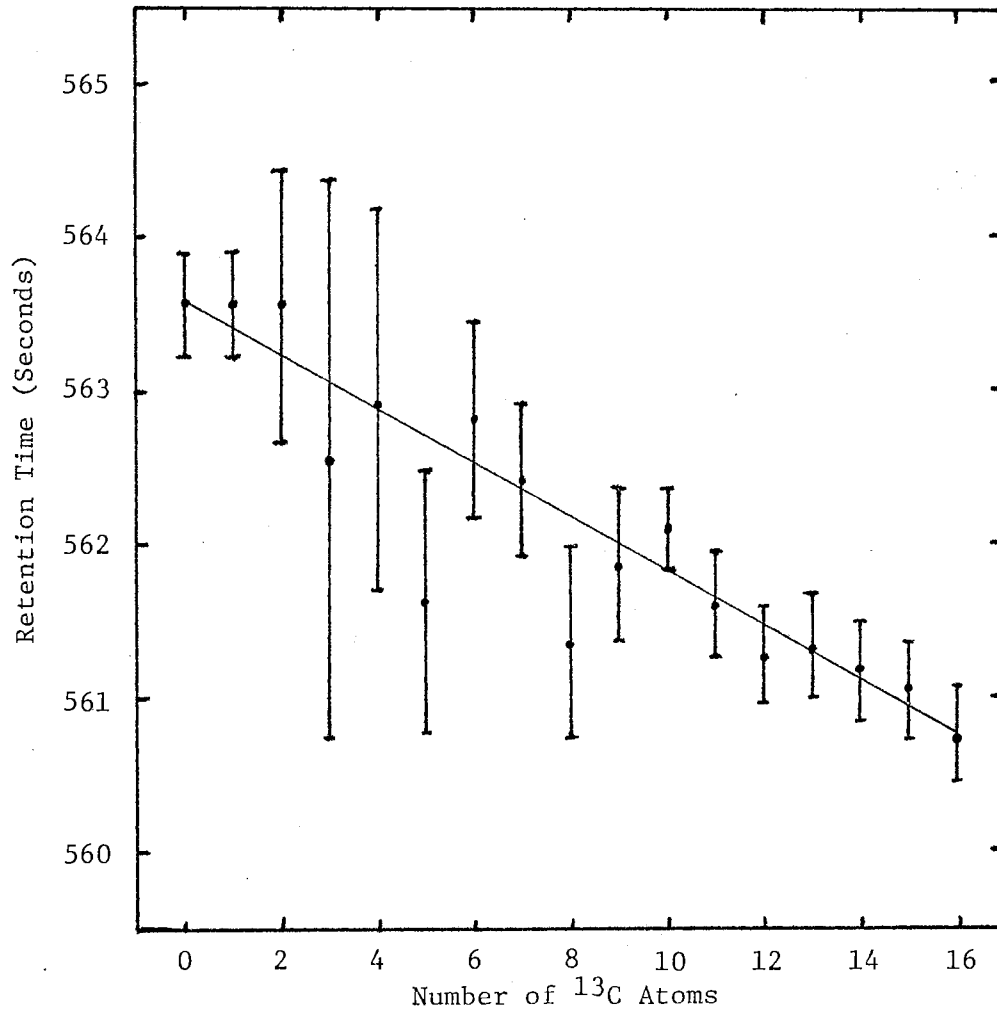
Figure 39. Effect of ^{13}C on Retention Time for
16:0 FAME (Silar-5CP, 158°C)
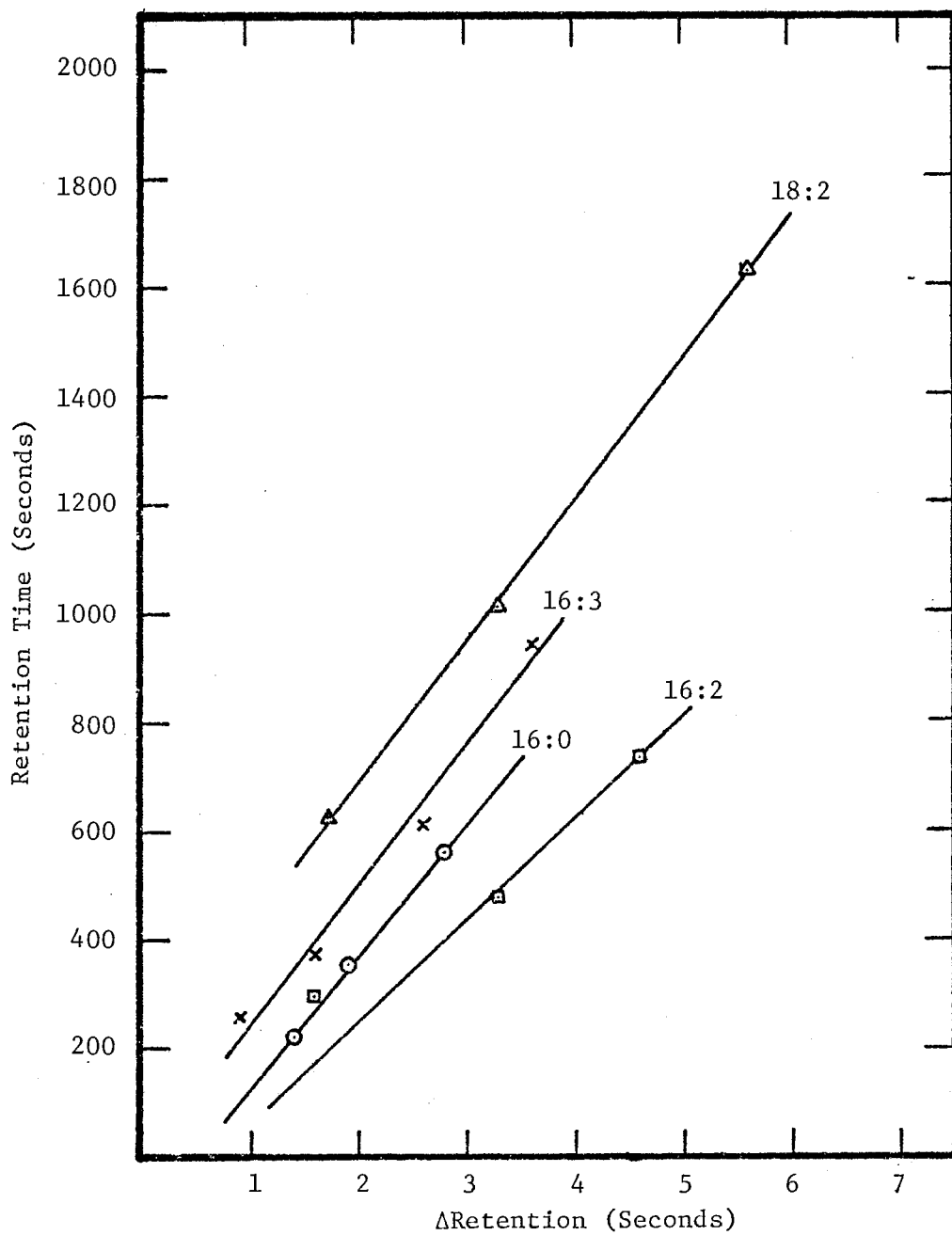
Figure 40. $^{13}C/^{12}C$ Fractionation as a Function of Retention Time on Silar-5CP
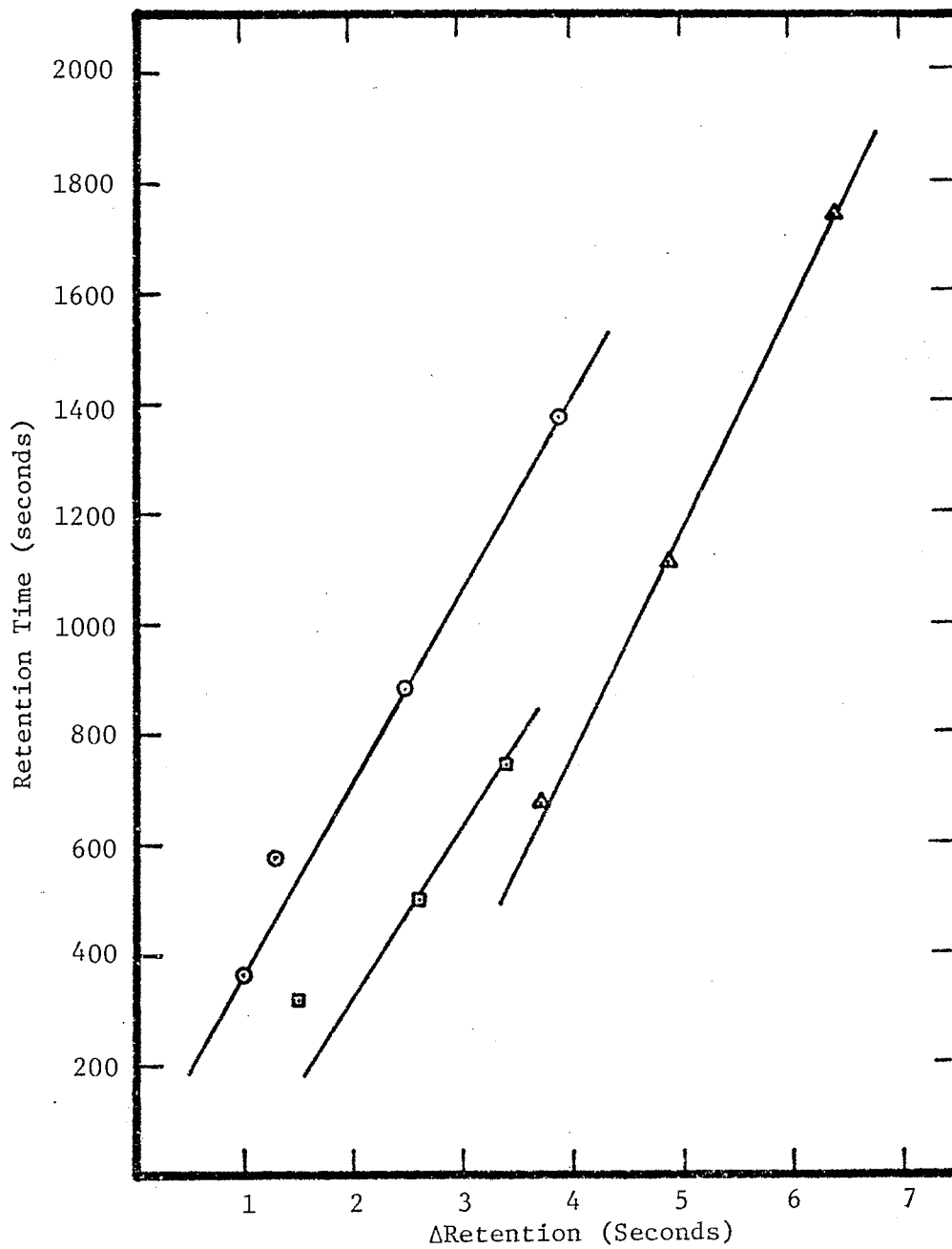
Figure 41. $^{13}C/^{12}C$ Fractionation as a Function of Retention Time on OV-1

distillation (1). The carbon monoxide isomers differ in mass by 3.57%, while for the 16:0 isomers (mass 270 $\underline{vs}$ mass 286) there is 5.92% difference.

The 17:0 FAME has a mass difference of 5.56% compared to the 16:0 FAME. Interpolation of the data of Althouse and Triebold (165) indicates a vapor pressure difference of 5.4 mm at $189^{\circ}C$ for these two FAMEs. Extrapolation of the data in Tables VI, VII and IX indicates that on the OV-1 column at $189^{\circ}C$ there is 156 seconds difference in the adjusted retention times of the two FAMEs and only 1 second ΔRetention for the 16:0 isomers. These values and the values for vapor pressure indicate that there is a 0.2% difference in the vapor pressure of the 16:0 isomers. This agrees quite well with the values for the separation factor.

CHAPTER V

DETERMINATION OF ^{13}C CONTENT USING ^{13}C NUCLEAR

MAGNETIC RESONANCE SPECTROMETRY

Introduction

As seen in the previous chapter mass spectrometry lends itself
very well to the precise determination of overall isotopic enrichment.
However, only for special cases is it possible to determine the isotopic
enrichment at specific sites in a molecule using MS data. This is
especially true in this study since the molecules of each compound
exhibit a wide range of labeling. By contrast ^{13}C nuclear magnetic
resonance spectroscopy (CMR) provides information about the isotopic
enrichment at specific sites, but the calculated enrichment is less
precise. Also, CMR requires several milligrams of enriched sample
(depending on molecular weight and level of enrichment), whereas less
than a microgram is adequate for GC/MS.

Coupling between ^{13}C nuclei and directly bonded protons will pro-
duce "satellite" peaks on either side of the main proton resonance, and
these satellites may be used to calculate ^{13}C enrichments (166,167).
However, the more complex the spectrum, the more difficult it is to
identify and quantitate the satellites. CMR has the advantage of pro-
viding direct information about the molecular carbon skeleton through

chemical shifts and coupling patterns. ^{13}C nuclei have a wide range of chemical shifts (typically up to $\delta = 200$ ppm) so even complex molecules will often produce a natural abundance CMR spectrum with a discrete resonance for each carbon when ^{13}C-^{1}H coupling is absent (168,169). Enrichment results in ^{13}C-^{13}C coupling which can provide valuable information about compounds labeled at specific sites or enriched to low levels. This ^{13}C-^{13}C coupling can even be valuable at high levels of enrichment for simple molecules such as acetic acid (170). But for large molecules that are highly enriched a very complex spectrum results, since each carbon is coupled to one or several other carbons (171).

^{13}C-^{1}H coupling can be eliminated by applying the proton-resonance frequency of one or several protons (selective decoupling) or applying a broad band of frequencies to decouple all protons. The latter produces a "proton noise decoupled" spectrum which provides a gain in sensitivity from two effects. First, by collapsing diffuse multiplets a single sharp line is usually produced. Secondly, a nuclear Overhauser effect (NOE) is induced since the proton spin population is redistributed by the broad band frequency and this produces a change in the ^{13}C energy-level populations (172,173). The NOE leads to an intensity enhancement of up to three-fold for carbons bonded to protons (174). While the NOE beneficially enhances sensitivity, all carbons with attached protons are not enhanced to the same degree, and carbons not bonded to protons normally exhibit an NOE significantly less than 3.0. Thus, intensities do not necessarily correlate with the relative number of carbon atoms when the proton noise decoupling technique is used (175). This also precludes the correlation of intensities to the ^{13}C enrichment of specific carbon atoms.

CMR experiments were conducted to demonstrate that the ^{13}C enrichment at specific molecular sites can be determined when the chemical shifts adequately separate the multiplets produced by ^{13}C–^{13}C coupling. Paramagnetic shift reagents were shown to be useful in separating some overlapping multiplets so that enrichment calculations were possible.

Instruments

Most CMR spectra were obtained using a Varian CFT-20 instrument operating at 20 MHz in the pulsed Fourier transform mode. The proton noise decoupled spectra covered a 4000 Hz bandwidth using 8192 data points in the time domain. The deuterium resonance of chloroform-d was used as internal lock.

Experiments using Eu(fod)$_3$ shift reagent were performed on a Varian XL-100 instrument operating at 25.2 MHz in the pulsed Fourier transform mode and interfaced to a Data General Super-Nova digital computer. Proton noise decoupled spectra were obtained over a 5000 Hz bandwidth using 4096 data points in the time domain. The deuterium resonance of D$_2$O in a capillary was used as lock. All chemical shifts are referenced to TMS (δ = 0) (176).

Results and Discussion

In order to point out the effect of enrichment a natural abundance spectrum (Figure 42) was obtained for 16:0 FAME. The assignments were made by comparison to previous results (177-180) and later were confirmed by the experiments using paramagnetic shift reagents. Note that
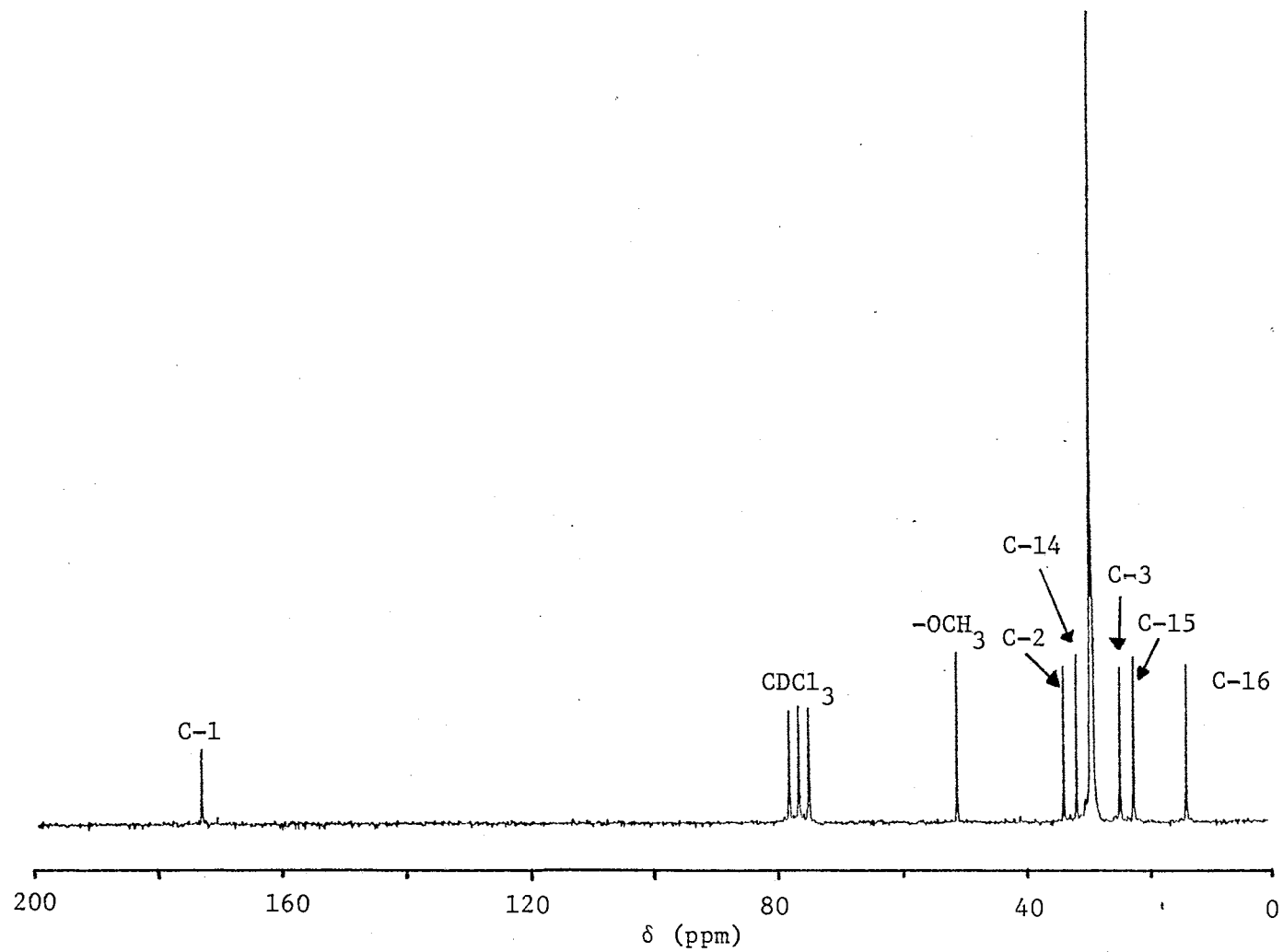
Figure 42. CMR Spectrum of 16:0 FAME (Flip Angle = 75°, 20 Sec Pulse Delay, 2800 Transients)

the resolved peaks illustrate the earlier point that the NOE enhances different carbons to different degrees. Also, carbons with a relatively long relaxation time (e.g., the carboxyl) will exhibit a low intensity when a large flip angle is used without an adequate time delay between pulses.

The CMR spectrum of 16:0 FAME enriched to 85 mol % ^{13}C is shown in Figure 43. The methoxy carbon is not observed since it is natural abundance. ^{13}C–^{13}C coupling causes an obvious loss in relative intensity and resolution. For example, the C-1 resonance is not only coupled to C-2 ($^{1}J_{CC}$) to produce a doublet, but at high levels of enrichment it is also coupled to C-3 ($^{2}J_{CC}$) and C-4 ($^{3}J_{CC}$). Since $^{2}J_{CC}$ and $^{3}J_{CC}$ are both small ($\leq$ 1 Hz and < 5 Hz respectively (181,182), the result is usually line broadening rather than line splitting. Of course, line broadening is more pronounced and line splitting is more complicated for non-terminal carbons. For 16:0 FAME the ^{13}C–^{13}C coupling results in overlap of the C-2 and C-4 multiplets and of the C-3 and C-15 multiplets. Such overlap usually precludes the determination of chemical shifts or enrichment levels.

Figure 44 is the CMR spectrum of 18:2 FAME enriched to 84 mol %. The double bond carbons (δ = ∼128 ppm) are unresolved due to ^{13}C–^{13}C coupling and the C-3 region (δ = ∼24 ppm) is overlapped by C-11. Since the most intense peak (methylene resonance envelope, δ = ∼29 ppm) is produced by fewer carbons (compared to 16:0 FAME), there is an increase in the relative intensity of the other resonances (e.g., the terminal methyl). The chemical shifts from Figures 42, 43 and 44 are tabulated in Table XI. Values from the literature are included for comparison.
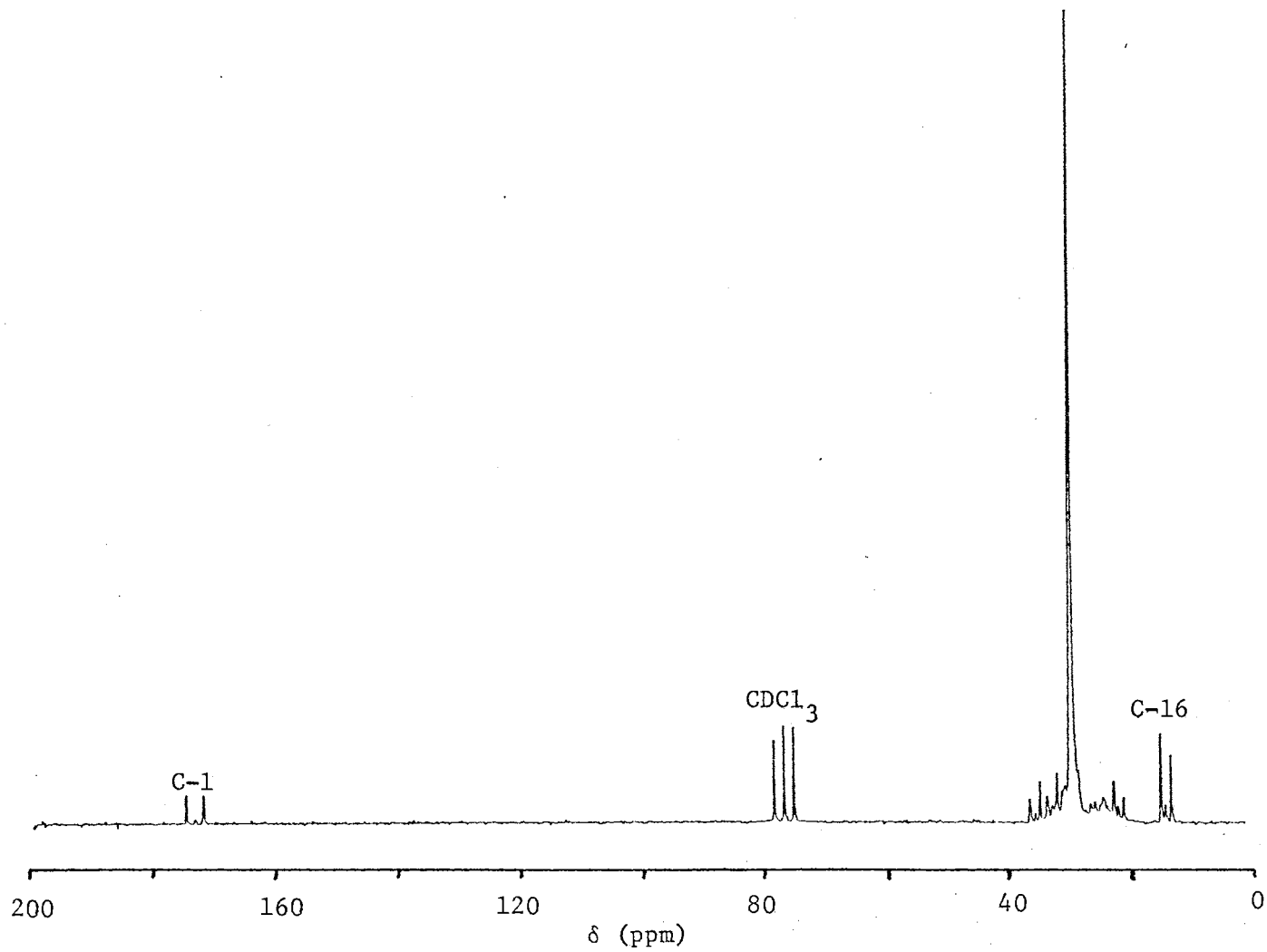
Figure 43. CMR Spectrum of ^{13}C Enriched 16:0 FAME (Flip Angle = 75°, 20 Sec Pulse Delay, 2800 Transients)
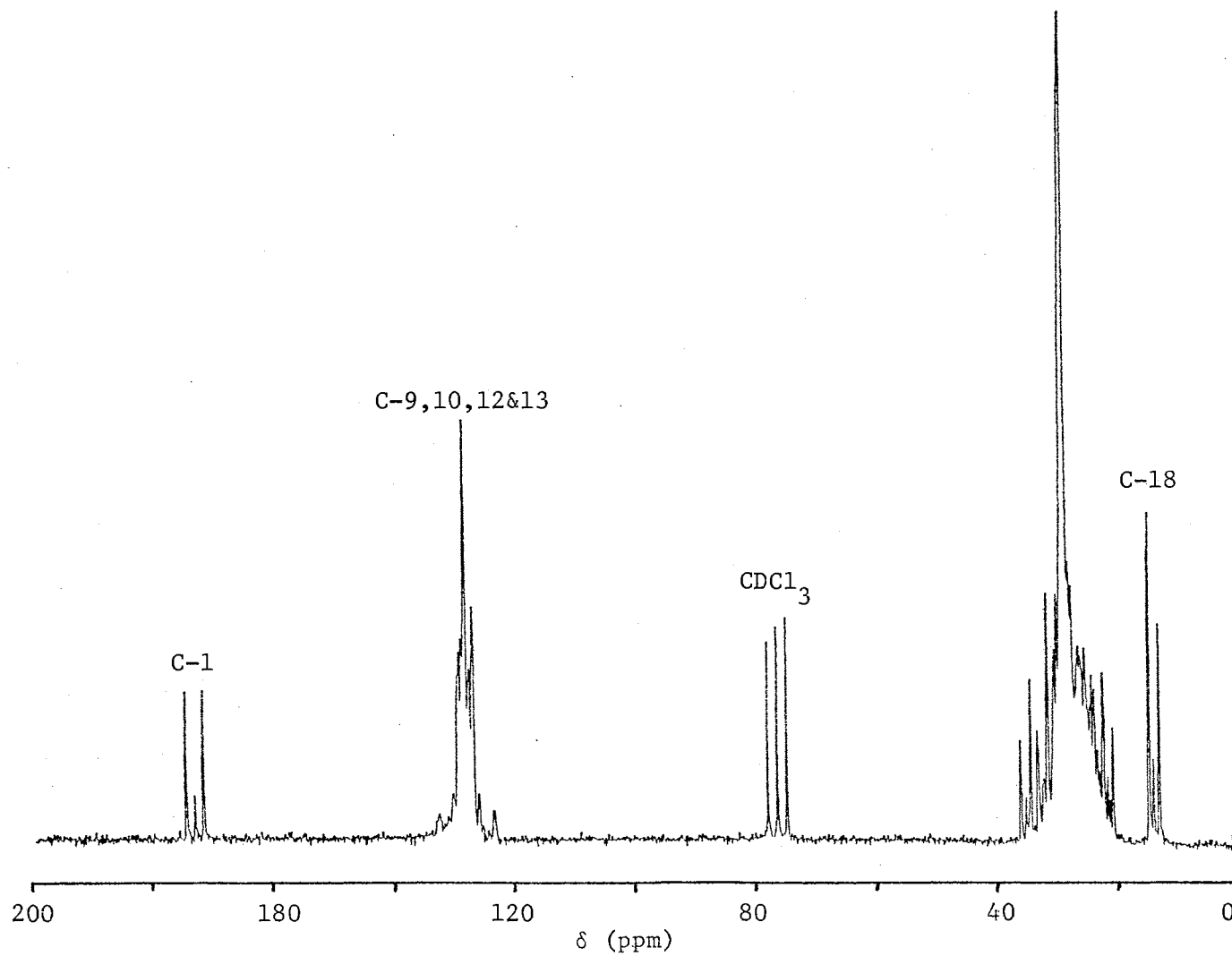
Figure 44. CMR Spectrum of ^{13}C Enriched 18:2 FAME (Flip Angle = 65°, 20 Sec Pulse Delay, 2334 Transients)

TABLE XI

CHEMICAL SHIFTS FOR FAMES

Carbon Position	16:0 FAME	16:0 FAME Enriched	16:1 FAME Ref(1)	18:2 FAME Enriched	18:2 ACID Ref(23)	18:0 Triglyceride Ref(23)
C-1	174.19	(174.3)	174.2	(174.3)	180.2	174.0
C-2	33.91	~33.5	34.0	(34.0)	33.8	34.0
C-3	24.78	*	25.0	*	24.4	24.8
C-4	↑	↑	27.2	↑	28.9	↑
C-5			29.1		28.9	
C-6			29.1	~28.8	28.9	
C-7			29.1	↓	29.4	
C-8	29.0-29.5	~29.5	29.7	*	27.9	
C-9			129.9	127.6-130.1	129.6	29.6
C-10			129.9	127.6-130.1	127.7	
C-11			29.7	*	25.3	
C-12			29.1	127.6-130.1	127.7	
C-13	↓	↓	29.7	127.6-130.1	129.8	
C-14	31.79	*	31.8	*	27.9	
C-15	22.55	~22.5	33.7	~28.8	28.9	↓
C-16	13.98	(13.9)	14.0	*	31.3	31.8
C-17				~22.4	22.4	22.5
C-18				14.06	13.8	13.9
OCH$_3$	51.27		51.4			

* Peak overlap precluded chemical shift assignment.
( ) Value is midpoint between doublet peaks.

While it is sometimes possible to calculate the enrichment from an unresolved multiplet (183), in Figures 43 and 44 only the resonances of the terminal carbon atoms permit enrichment calculations. In Figure 45 the multiplets of the terminal carbons are compared. The comparatively low sensitivity of the carboxyl carbon is due to a combination of partial saturation resulting from the large flip angle with an insufficient delay between pulses and the absence of NOE enhancement. The non-equal intensity of the doublet in the methyl resonances is the result of residual AB character (184) and must be taken into account when enrichment calculations are necessary for unresolved multiplets (183). The $^1J_{C-C}$ values shown in Figure 45 are in agreement with values for similar molecular structures (185,186).

A multiplet contains two types of information. First, the sum of the intensities of all the multiplet peaks is a function of the ^{13}C enrichment at the site producing the resonance. (As noted earlier, the intensity is also a function of other factors.) Secondly, the intensity pattern of the multiplet is a function of the ^{13}C enrichment of the carbon atoms bonded to the carbon producing the resonance. Thus, for the carboxyl resonance in Figure 45a the sum of the doublet intensity divided by the total intensity corresponds to the enrichment at the C-2 position. So, for FAME highly enriched in ^{13}C proton noise decoupled spectra will directly yield the enrichment for only two sites, namely, the C-2 carbon and the carbon adjacent to the terminal methyl. Since these sites are at opposite ends of the molecule, it can be tentatively concluded from the calculated enrichments (see Figure 45) that within experimental error the labeling is uniform. Peak areas were

$^1J_{CC}$ = 56.8 hz

(a)

Mol % ^{13}C at C-2 = 88.4%

$^1J_{CC}$ = 34.3 hz

(b)

Mol % ^{13}C at C-15 = 89.7%

$^1J_{CC}$ = 56.7 hz

(c)

Mol % ^{13}C at C-2 = 87.3%

$^1J_{CC}$ = 33.9 hz

(d)

Mole % ^{13}C at C-17 = 88.4%
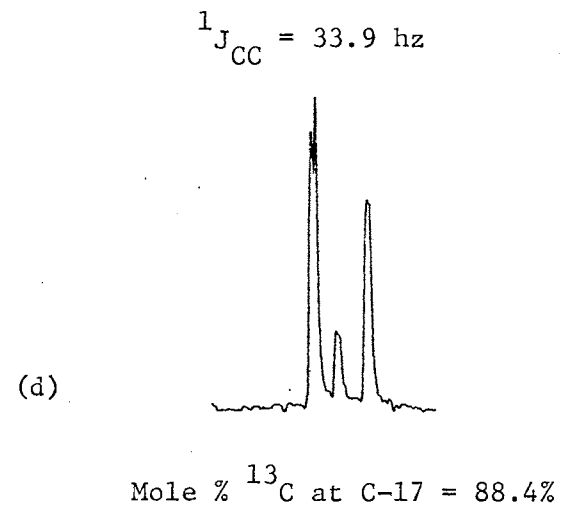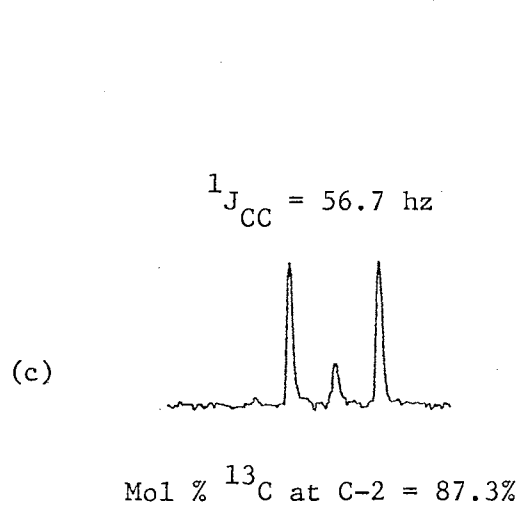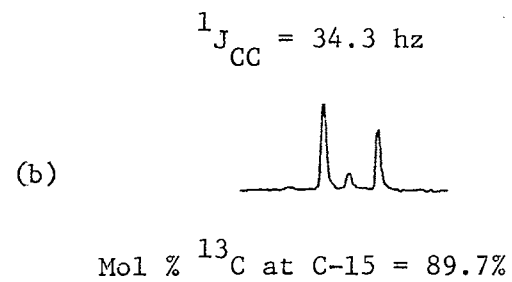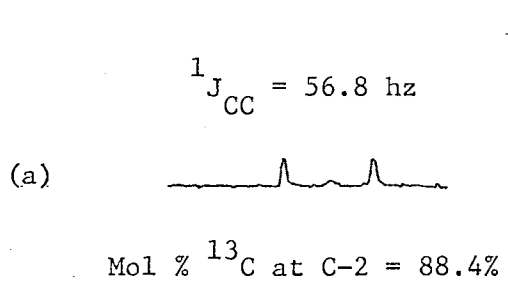
Figure 45. Multiplets of the Terminal Carbons of ^{13}C Enriched 16:0 (a and b) and 18:2 (c and d) FAMEs

determined by carefully cutting and weighing each peak from Xerox

copies of expanded spectra (187).

Admittedly, highly enriched FAME are a "worst case" for determining

enrichment by CMR, but obtaining the enrichment of only two positions

out of sixteen (or more) is not very satisfactory. Selective homonuclear

decoupling of ^{13}C resonances can be used to assist in the assignment of

peaks (188,189) and might be used in certain cases to eliminate multi-

plet overlap (190). However, this decoupling must be in addition to

proton noise decoupling and instruments capable of such triple resonance

experiments are not generally available. Indeed, neither of the instru-

ments used in this study have this feature.

Another peak assignment technique did lend itself to the purposes

of this study; namely, the use of a paramagnetic shift reagent (PSR).

The PSR is usually a chelate compound of a lanthanide element. Europium

or praseodymium are usually the elements of choice because they pro-

duce large shifts with a minimum of line broadening (191). For use

in organic solvents the two ligands used most often are 2,2,6,6-tetra-

methyl-3,5-heptanedione (thd) and 2,2-dimethyl-6,6,7,7,8,8,8-hepta-

fluoro-3,5-octanedione (fod). Figure 46 is a diagram of metal complexes

formed by these ligands (192). These metal complexes can coordinate

with polar groups on a substrate molecule, and the internal field pro-

duced by the unpaired electrons coordinated to the metal ion induces

a change in the chemical shift for carbon positions near the polar

group. The magnitude of the induced shift depends on the functional

group and decreases in the order $-NH_2$ < $-OH$ < $>C=O$ < $-O-$ < $-CO_2R$ < $-CN$

(193). Of course, variables that affect the stability of the
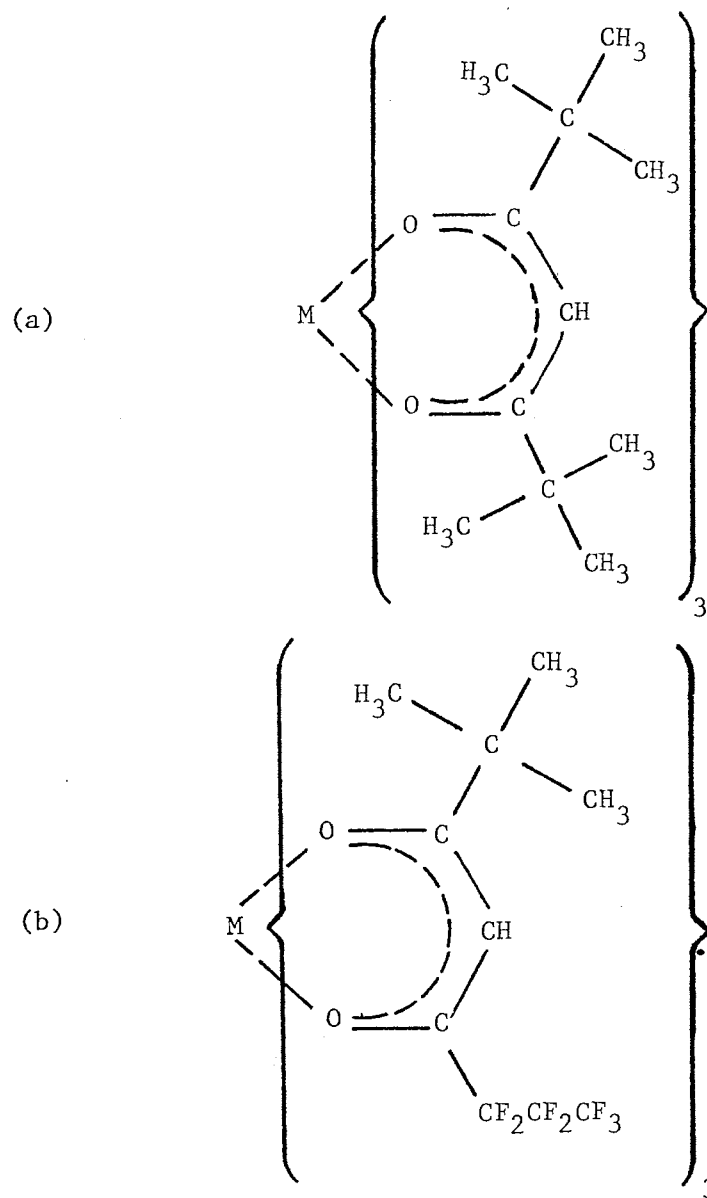
Figure 46.   Structure of Paramagnetic Shift
             Reagents, (a) $M(dpm)_3$ and (b)
             $M(fod)_3$

PSR-substrate complex (e.g., temperature, concentration and solvent) will also affect the magnitude of the induced shift. Hence, reproducing the same shift is quite difficult. To obviate this difficulty the induced shift is usually plotted vs the mole ratio of the PSR to substrate, and the induced shift is extrapolated to a ratio of one (e.g., 194).

Since their introduction (195) PSRs have been widely used in proton magnetic resonance and recently have received some use in CMR. Most CMR applications have been directed toward the assignment of peaks (194,196-199). The nature of the PSR-substrate interaction has also been probed (200). In the biosynthesis of hirsutic acid C from acetate labeled at a single position $Eu(fod)_3$ was used to demonstrate labeling at a specific molecular site (201).

In this study the intent was to shift the C-2 multiplet enough so that the enrichment at C-1 and C-3 could be claculated. For this purpose an europium PSR was selected in order to produce a downfield shift (202) and minimize the magnitude of the required shift. A preliminary investigation was conducted in which small increments of $Eu(thd)_3$ were added to 1.5 ml chloroform-d containing 16:0 FAME. The first addition shifted the C-2 multiplet completely away from the C-14 multiplet and shifted the C-3 multiplet enough to leave the C-15 multiplet completely resolved. However, subsequent additions produced only minor increases in the induced shift, probably because of a failure to ensure anhydrous conditions (i.e., solvent and storage of the PSR) (203).

In an effort to resolve additional multiplets several changes were
made. Eu(fod)$_3$ was obtained, since it is a stronger Lewis acid and forms
a stronger complex (204). Also, fod compounds are more soluble than thd
compounds (192). Carbon tetrachloride was used, since the hydrogen
bonding characteristic of chloroform competes with complex formation
(198). The carbon tetrachloride was dried over Linde molecular sieve
(5X) and the PSR was stored in vacuo over DrieRite between additions.
A Varian XL-100 was used to obtain improved sensitivity and resolution,
and the probe temperature was lowered to 15°C.

Figure 47 through Figure 51 illustrate the effects of Eu(fod)$_3$ on
the CMR spectrum of enriched 16:0 FAME. Several features are readily
apparent from these spectra. It is obvious by comparing the other
spectra to Figure 47 that the PSR induces quite large shifts. Indeed,
the C-1 multiplet is shifted beyond the spectral width and appears as
a fold-over resonance in Figures 49 through 51. Even the C-4 multiplet
is completely separated from the methylene envelope at high PSR-substrate
ratios (Figure 51).

However, line broadening limits the quantitative information that
can be obtained by using PSRs. The multiplet structure for C-1 and C-2
is lost at relatively low PSR-substrate ratios (see Figure 49). When
enough PSR is added to shift C-3 and C-4 away from the methylene enve-
lope, the multiplet lines are broadened so much that a quantitative
calculation is impossible. Also, at high PSR concentrations field
homogeneity deteriorates, and this results in side bands such as those
for the carbon tetrachloride resonance (δ = 96 ppm) in Figure 51.
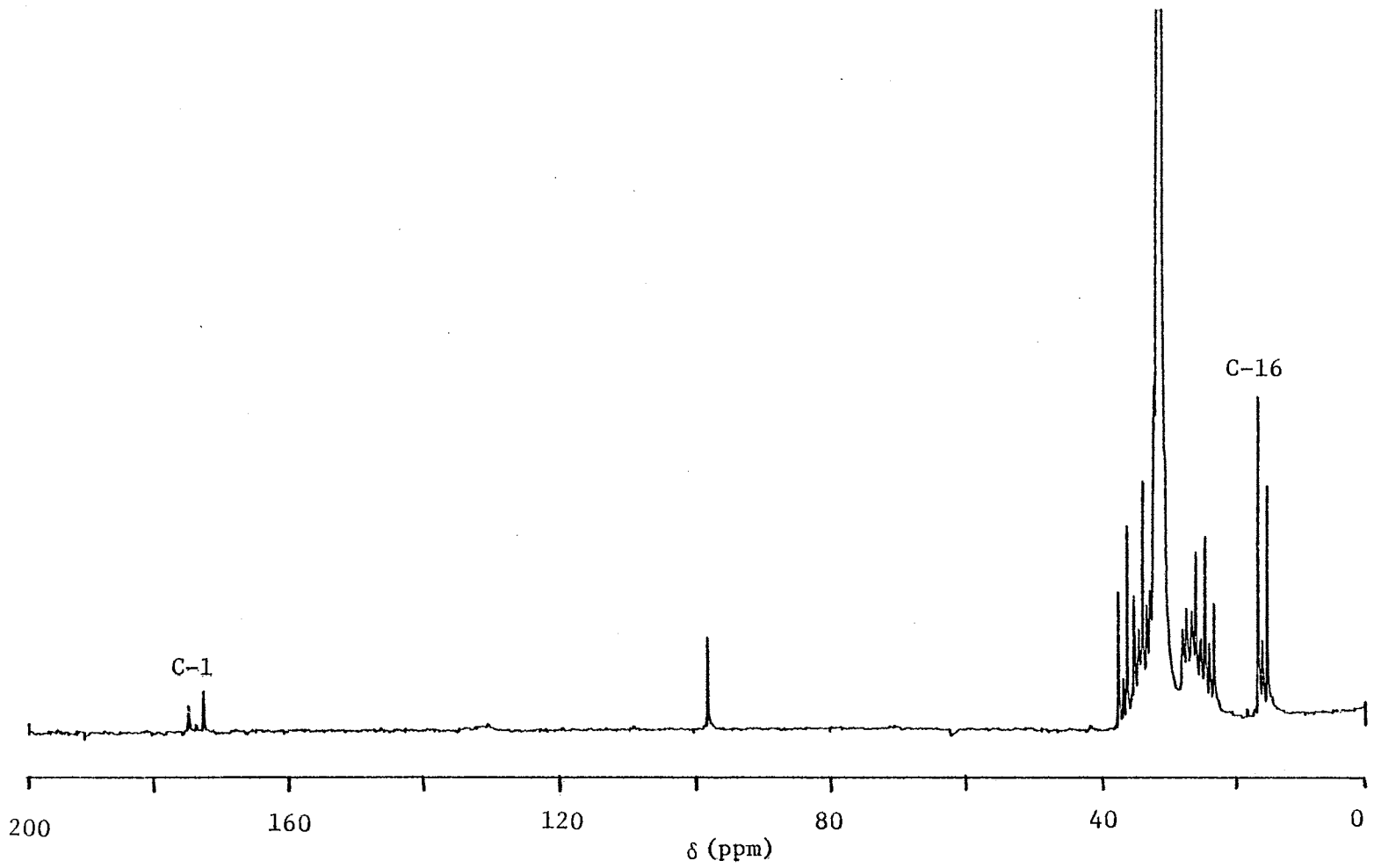
Figure 47. CMR Spectrum of ^{13}C Enriched 16:0 FAME (Flip Angle = 45°)
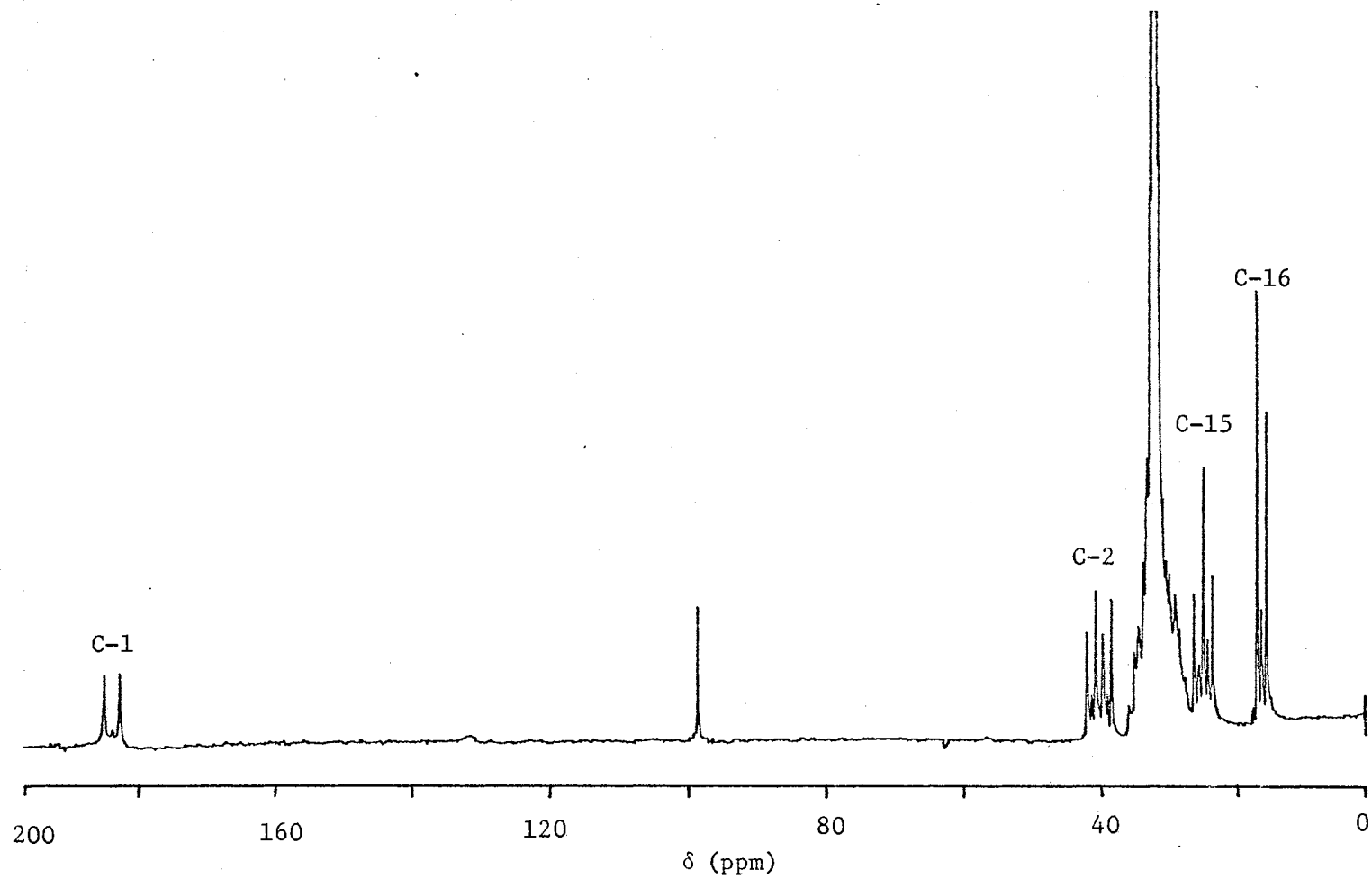
Figure 48.   CMR Spectrum of ^{13}C Enriched 16:0 FAME with $Eu(fod)_3$ (PSR/FAME Mole Ratio is 0.128, Flip Angle = 45°)
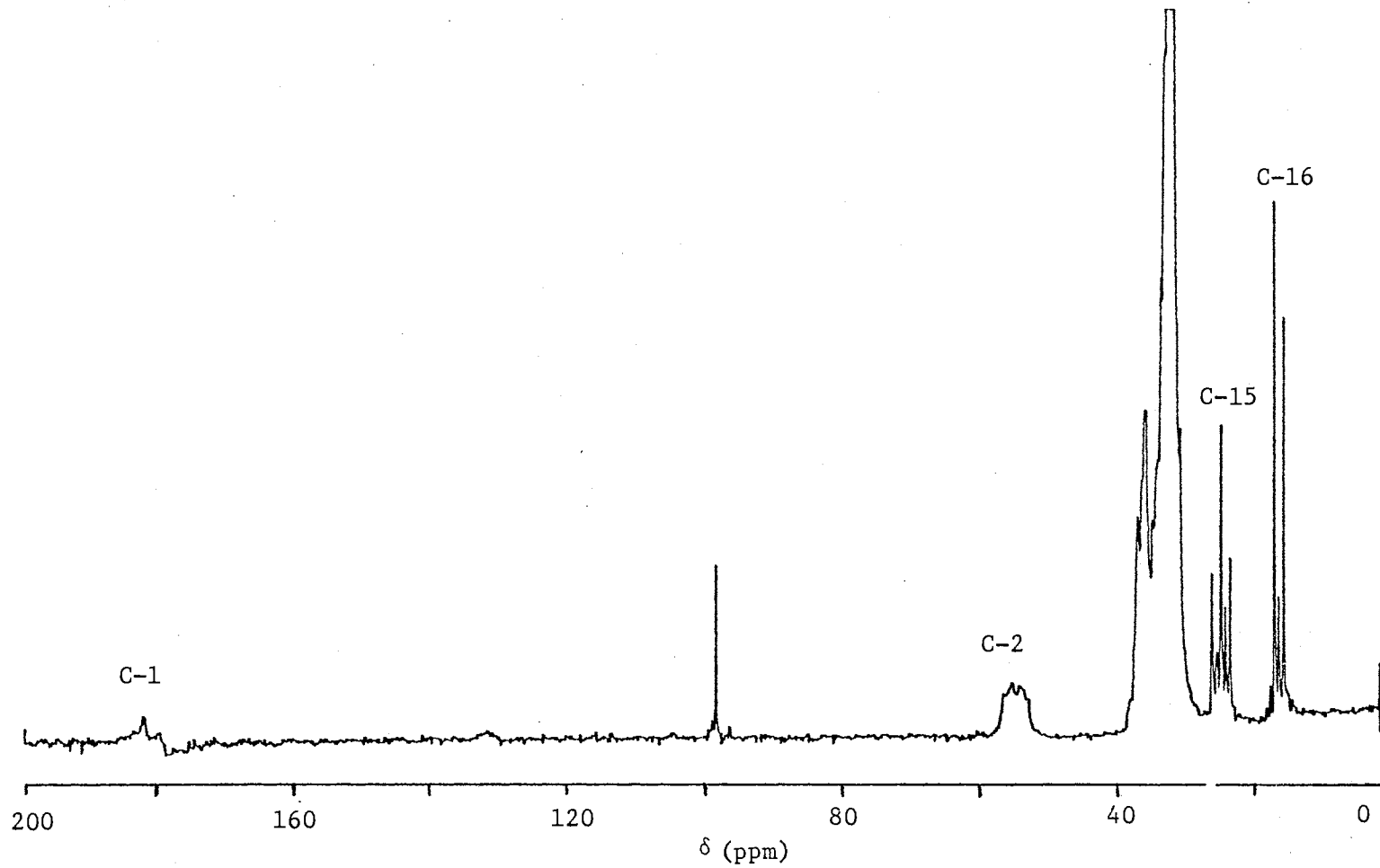
Figure 49. CMR Spectrum of ^{13}C Enriched 16:0 FAME with Eu(fod)$_3$ (PSR/FAME Mole Ratio is 0.638, Flip Angle = 45°)
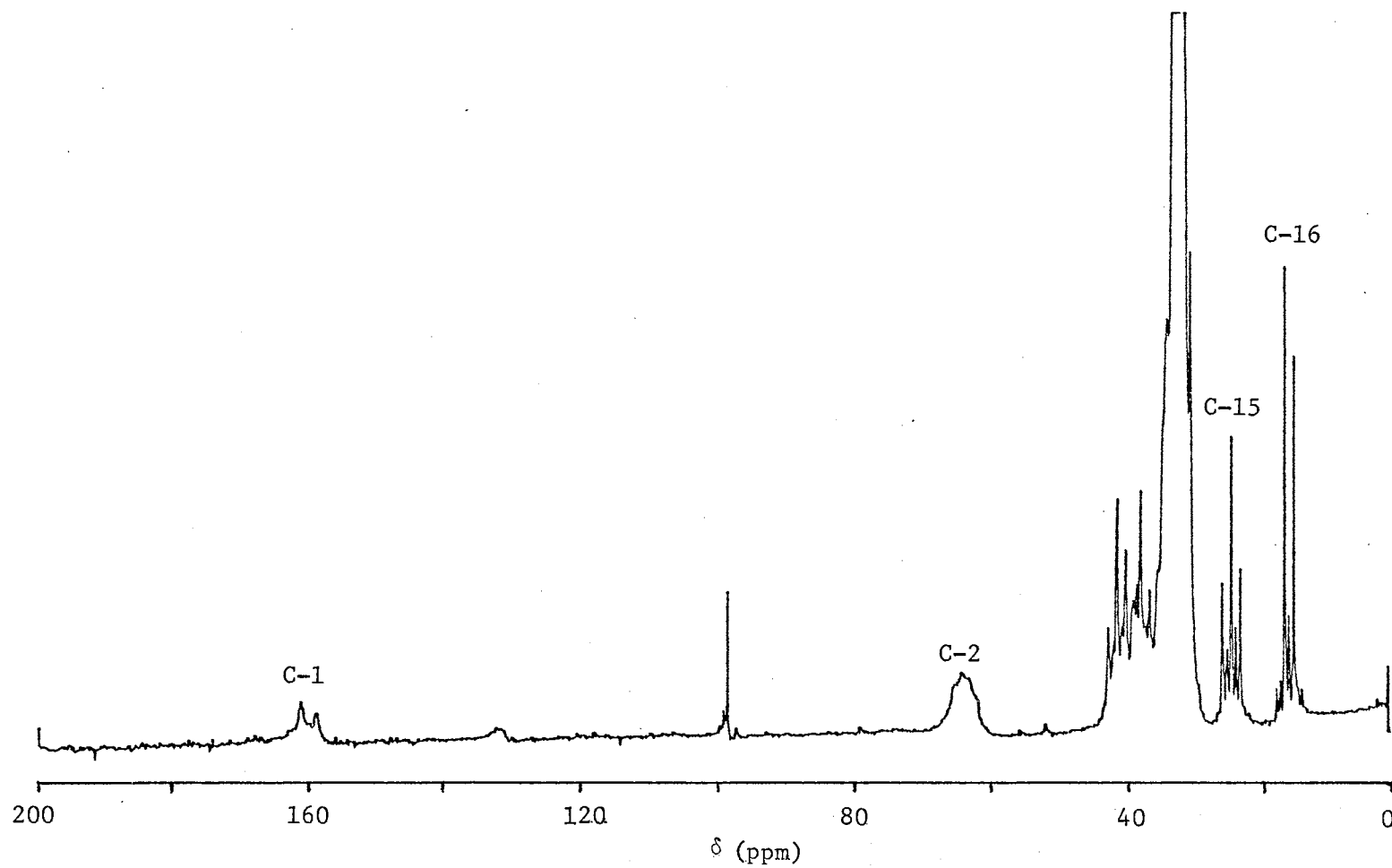
Figure 50. CMR Spectrum of ^{13}C Enriched 16:0 FAME with $Eu(fod)_3$ (PSR/FAME Mole Ratio is 1.11, Flip Angle = $45°$)
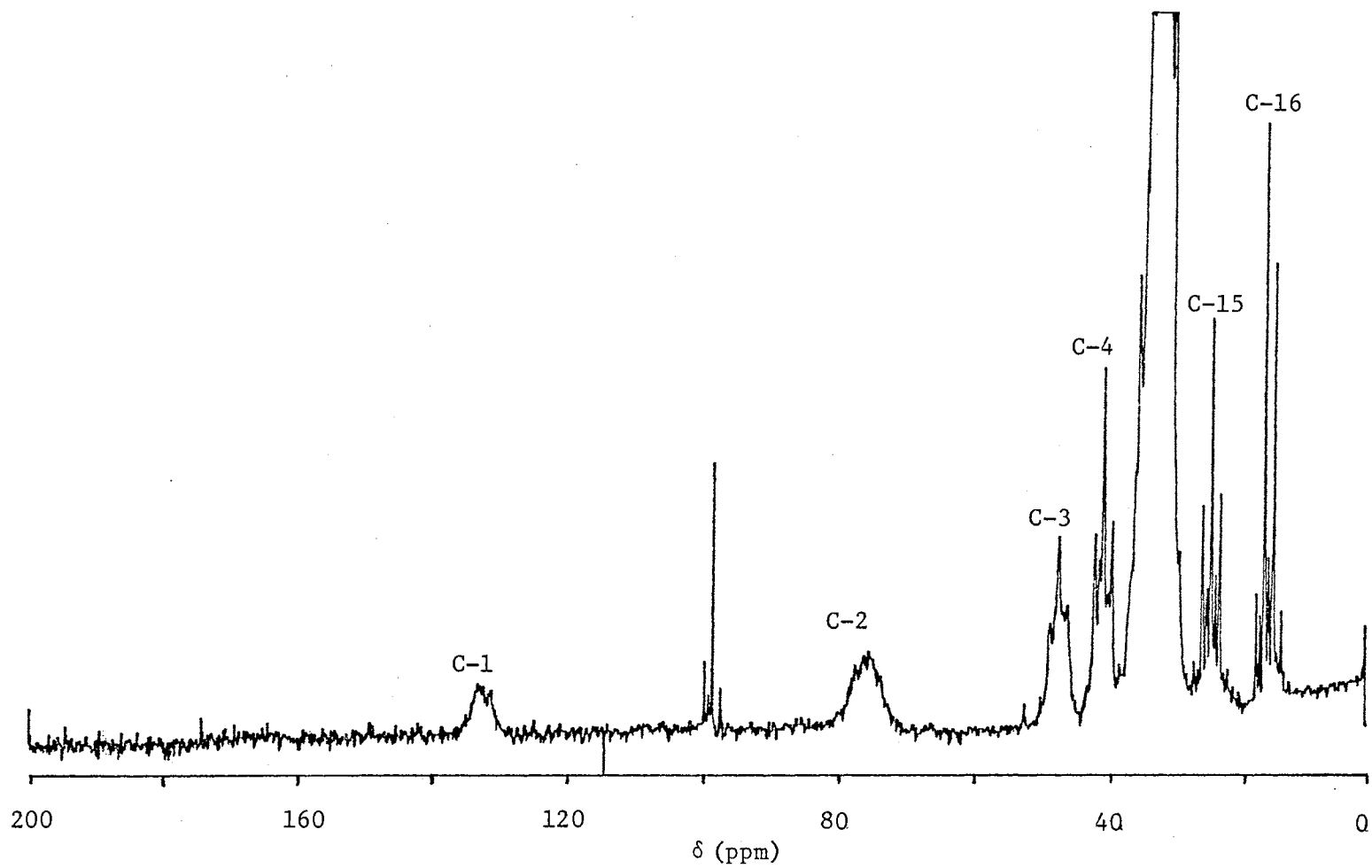
Figure 51. CMR Spectrum of ^{13}C Enriched 16:0 FAME with Eu(fod)$_3$ (PSR/FAME Mole Ratio is 1.66, Flip Angle = 45°)

Conspicuously absent in Figures 48 through 51 are intense reso-
nances due to the PSR. Since the PSR ligand is natural abundance, it
comprises a minor portion of the ^{13}C atoms present. The alkyl carbon
resonances are obscured by the methylene envelope (198). The small broad
resonance at δ = 130 ppm is probably due to the fluorinated carbons
(205).

The use of PSRs with substrates having a high ^{13}C content proved
to be beneficial in several ways. A substrate that is highly enriched
has a minimum of interference from PSR ligand resonances. Also, rather
than extrapolating to a ratio of one, it was possible to measure induced
shifts at a ratio greater than two (see Figure 52). The limited solu-
bility of PSRs (53) usually restricts experiments to relatively low
ratios, since natural abundance spectra require much more substrate.
For highly enriched substrates line broadening rather than PSR solu-
bility imposes a limit on the PSR-substrate ratio. Although the large
ratios failed to provide additional information for the purposes of
this study, they would be quite valuable for peak assignment studies.

As expected (194,198,202) the magnitude of the induced shift falls
off sharply for carbon atoms not adjacent to the site of complexation.
Also as expected (194,198,202,204) the induced shift is nearly linear
for small ratios. The formation of PSR dimers (207) contributes to non-
linearity at higher ratios. Substrate saturation by the PSR might also
be expected to contribute to nonlinearity at higher ratios (204).

When a carbon is coupled to two adjacent carbons, enrichment
calculations become more involved. Figure 53 diagrams the splitting
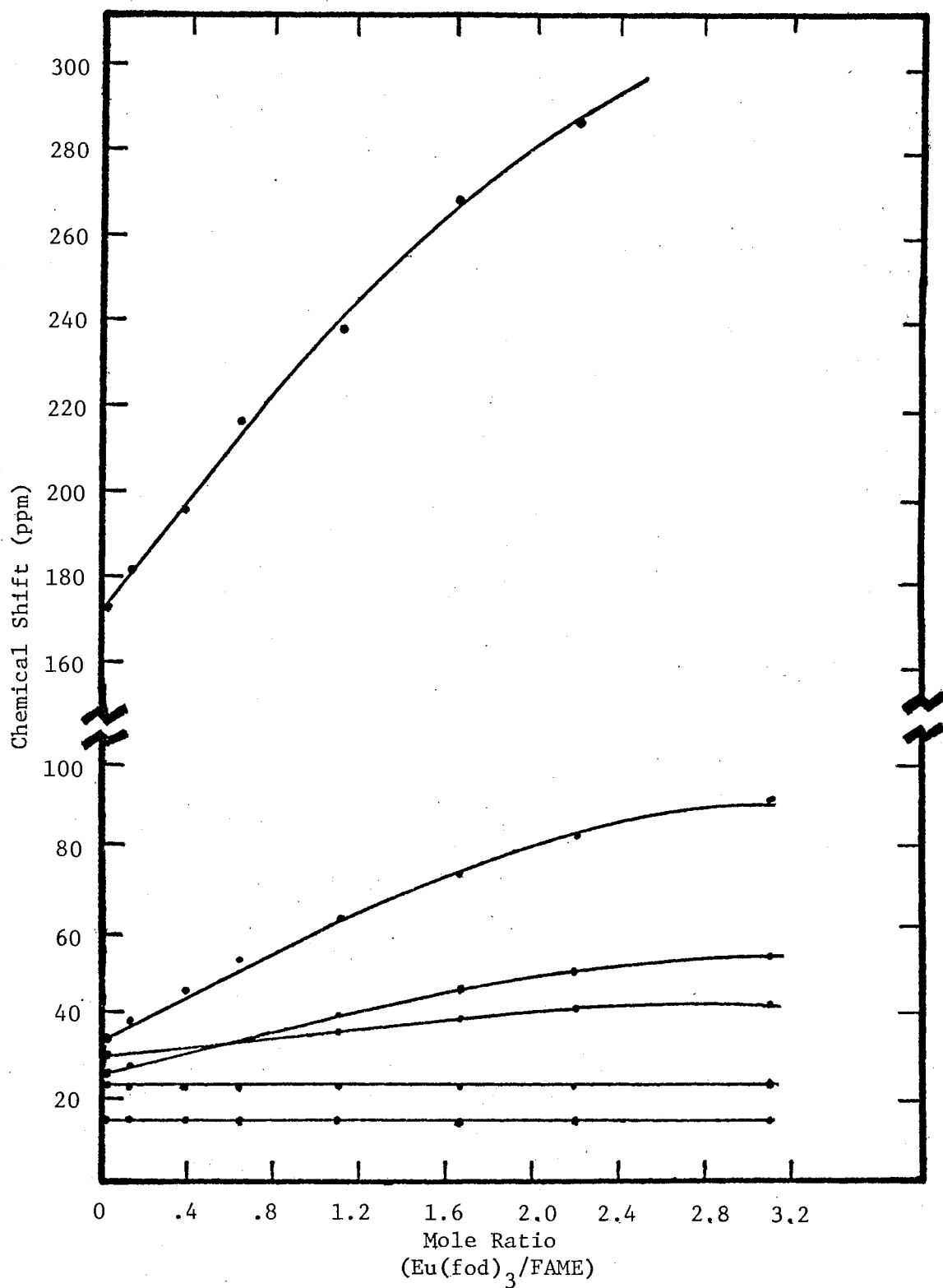
Figure 52. Change in Chemical Shift Values for ^{13}C
Enriched 16:0 FAME as a Function of
Eu(fod)$_3$ Concentration

$^1J_{CC} = \sim 57$ hz

a   b   a

$^1J_{CC} = \sim 33$ hz

c   d   ec   f   ce   d   c
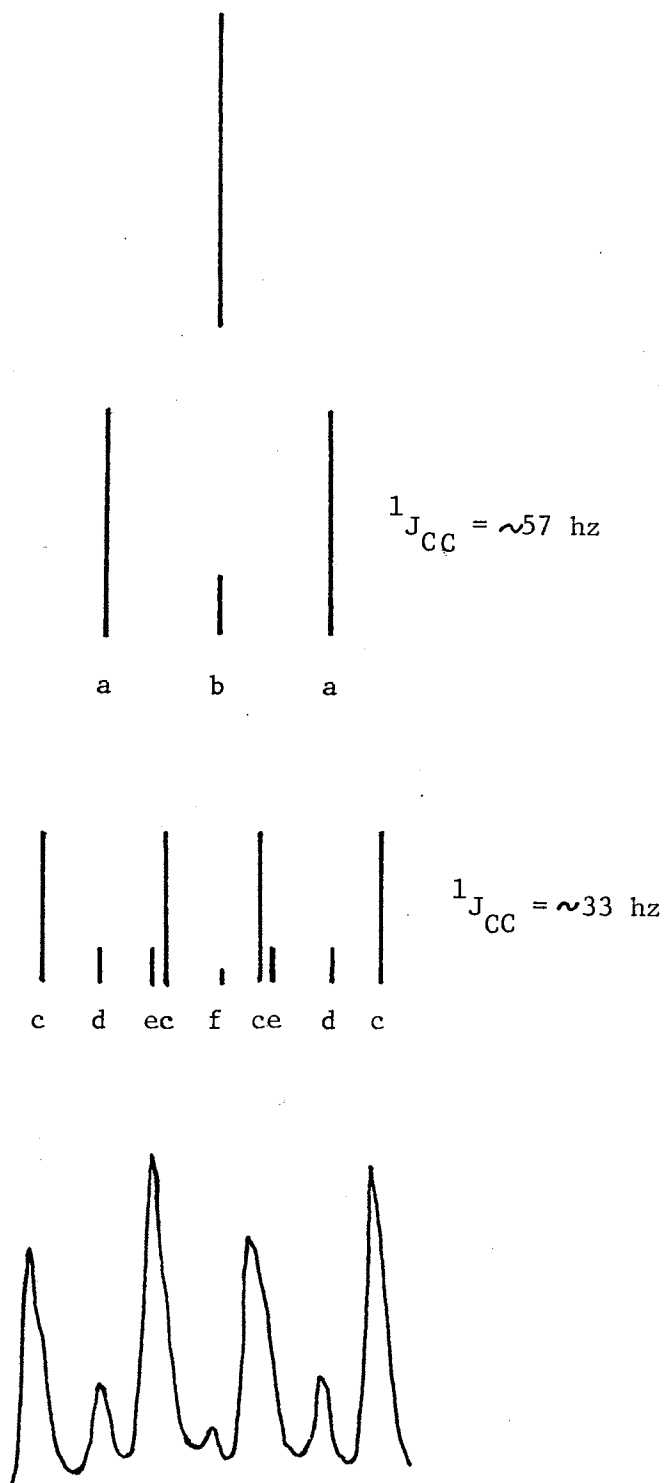
Figure 53.   C-2 Multiplet of ^{13}C Enriched 16:0 FAME

pattern that produces the C-2 multiplet and it is seen that only the

e lines and center c lines are not resolved.

When the C-1 enrichment is α and the C-3 enrichment is β, the

line intensities are related to enrichment values as follows:

$$a = 1/2 \; \alpha$$

$$b = 1-\alpha$$

$$c = 1/2 \; \alpha \cdot 1/2 \; \beta$$

$$d = 1/2 \; \alpha \cdot (1-\beta)$$

$$e = (1-\alpha) \cdot 1/2 \; \beta$$

$$f = (1-\alpha) \cdot (1-\beta)$$

The measured peak intensities produce a set of equations that permit

the calculation of enrichment values of $\alpha = .850 \pm .013$* and $\beta = .860$

$\pm .005$.*

Figure 54 diagrams the splitting pattern that produces the C-15

multiplet. Since the two $^{1}J_{C-C}$ values are nearly equal, lines e and d

overlap and line f overlaps the two center c lines. When the C-16

enrichment is α and the C-14 enrichment is β, the line intensities

and enrichments are related as above. However, there is too much line

overlap to calculate separate values for α and β. If it is assumed

that α equals β, then a set of quadratic equations is produced. Solu-

tion of these equations gives an enrichment value of .864 $\pm$ .004.*

These values confirm the earlier conclusion that the molecules are

uniformly labeled. This is not surprising since the methyl palmitate

was derived from algae that had been grown for five generations

on carbon-^{13}C dioxide.

---

* The standard deviation was determined by measuring the area at least
    three times.

$$^1J_{CC} \cong\ ^1J_{CC} = \sim 33\ hz$$
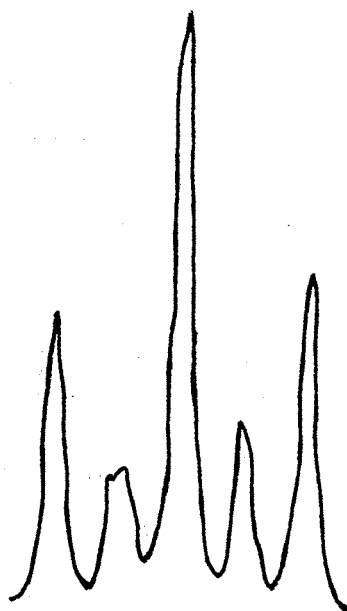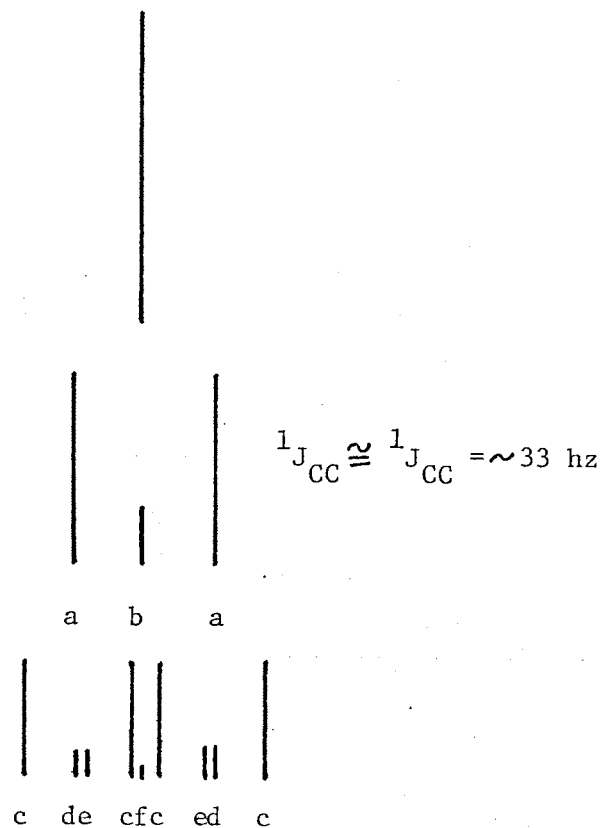
Figure 54. C-15 Multiplet of ^{13}C Enriched 16:0 FAME

CHAPTER VI

SUMMARY

The primary objective of this study was to develop the procedures and delineate the calculations necessary to fully characterize bio-synthesized materials having a high ^{13}C content. The biosynthesis described in Chapter II provided the FAMEs, each of which had a unique ^{13} content.

HPLC was used to purify the transesterified lipid extract. Silica columns effectively separated the FAMEs from pigments and other lipid material, but did not have the selectivity needed to separate the FAME mixture. For GC/MS analysis the FAME mixture was separated on an ion exchange column in the silver form (argentation chromatography) to effect a separation by the degree of unsaturation. To obtain pure, individual FAMEs for CMR analysis, the FAME mixture was separated on a reverse phase column (µBondapak-C18).

AVA experiments confirmed that there was ^{13}C/^{12}C fractionation occurring on the GC colunn, so repetitive scans were taken as each GC peak eluted. Computer programs were written to integrate all molecular ions over the entire GC peak. In this way an accurate measure of the total ^{13}C content was obtained.

CMR spectrometry was used to measure the ^{13}C concentration at particular sites in the molecules. The use of paramagnetic shift reagents permitted quantative calculations for several resonances that could not

have otherwise been analyzed. Within experimental error the FAMEs are uniformly labeled with ^{13}C.

The curve fitting and calculations discussed in Chapter IV are applicable to GC/MS data for any compound that exhibits a molecular ion, and in some fortuitous cases may be applicable to fragment ions. The computer programs could be stored in a GC/MS-computer system to provide virtually real-time analysis of ^{13}C-enriched compounds.

The unique ^{13}C content of each FAME suggest that ^{13}C labeling would be a useful method to study the relative rates of synthesis of fatty acids and other classes of compounds. Using short culture times it should be possible to observe significant differences in the ^{13}C concentration at various molecular sites.

REFERENCES

1. Schreiber, R. E. (ed.), Los Alamos Scientific Laboratories, Report LA-4759-MS (1971).

2. Armstrong, D. E., et al., Los Alamos Scientific Laboratories, Report LA-4391 (1970).

3. Jung, Gunther and Friedrich Juttner, Chemiker-Zeitung 96, 603 (1972), LA-TR-73-22.

4. Matwiyoff, N. A. and D. G. Ott, Science 181, 1125 (1973).

5. Ricci, Enzo, Anal. Chem. 43, 1866 (1971).

6. Close, D. A., J. J. Malanify and C. J. Umbarger, Los Alamos Scientific Laboratories, Report LA-UR-73-1615 (1973).

7. McDowell, Robin S., Anal. Chem. 42, 1192 (1970).

8. Caprioli, Richard M., in Biochemical Applications of Mass Spectrometry, George R. Waller (ed.), Wiley-Interscience, New York (1972).

9. Caprioli, R. M., W. F. Fies and M. S. Story, Anal. Chem. 46, 453A (1974).

10. Waller, G. R. and O. C. Dermer (eds.), First Supplementary Volume to Biochemical Applications of Mass Spectrometry, Wiley-Interscience, New York, in press.

11. Sweeley, C. C., et al., in First Supplementary Volume to Biochemical Applications of Mass Spectrometry, G. R. Waller and O. C. Dermer (eds.), Wiley-Interscience, New York, in press.

12. Nichols, B. W., and B. J. B. Wood, Lipids 3, 46 (1968).

13. Parker, Patrick L., C. Van Baalen and Larry Maurer, Science 155, 707 (1967).

14. Schneider, H., et al., Phytochem. 9, 613 (1970).

15. Holton, Raymond, W., Harry H. Blecker and Timothy S. Stevens, Science 160, 545 (1968).

16. Pohl, P., T. Passig and H. Wagner, Phytochem. 10, 1505 (1971) (Ger.).

17. Otsuka, Hama and Yuji Morimura, Plant Cell Physiol. $\underline{7}$, 663 (1966).

18. Burlew, John S., in Algal Culture from Laboratory to Pilot Plant, John S. Burlew (ed.), Institute of Washington, Washington, DC (1953), Chapter 1.

19. Myers, Jack, in Algal Culture from Laboratory to Pilot Plant, John S. Burlew (ed), Carnegie Institute of Washington, Washington, DC (1953), Chapter 3.

20. Tamiya, Hiroshi, Ann. Rev. Plant Physiol. $\underline{8}$, 309 (1957).

21. Sorokin, Constantine and Jack Myers, Science $\underline{117}$, 330 (1953).

22. Sorokin, Constantine, Nature $\underline{184}$, 613 (1959).

23. Sorokin, Constantine and Robert W. Krauss, Proc. Natl. Acad. Sci., USA $\underline{45}$, 1740 (1959).

24. Buchholz, J. R., et al., Los Alamos Scientific Laboratory, Report LA-4902, 1972.

25. Milner, Harold W., J. Biol. Chem. $\underline{176}$, 813 (1948).

26. Spoehr, H. A. and Harold W. Milner, Plant Physiol. $\underline{24}$, 120 (1949).

27. Pratt, Robertson and Evelyn Johnson, J. Pharmac. Sci. $\underline{52}$, 979 (1963).

28. Reitz, Ronald C., James G. Hamilton and Francis E. Cole, Lipids $\underline{2}$, 381 (1970).

29. Patterson, Glenn W., Lipids $\underline{5}$, 597 (1970).

30. Matthern, Robert O. and Robert B. Koch, Food Technol. $\underline{18}$, 58 (1964).

31. Myers, Jack, in Algal Culture from Laboratory to Pilot Plant, John S. Burlew (ed.), Carnegie Institute of Washington, Washington, DC (1953), Chapter 4.

32. Fogg, G. E., Algal Cultures and Phyloplankton Ecology, 2nd Edition, University of Wisconsin, Madison, WI (1975), Chapter 2.

33. Folch, Jordi, M. Lees and G. H. Sloane-Stanley, J. Biol. Chem. $\underline{226}$, 497 (1957).

34. Bligh, E. G. and W. J. Dyer, Can. J. Biochem. Physiol. $\underline{37}$, 911 (1959).

35. Gellerman, J. L. and H. Schlenk, J. Protozool. $\underline{12}$, 178 (1965).

36. Chuecas, L. and J. P. Riley, J. Mar. Biol. Assoc. U.K. <u>49</u>, 97 (1969).

37. Nichols, B. W. and R. S. Appleby, Phytochemistry <u>8</u>, 1907 (1969).

38. Allen, C. Freeman, Pearl Good and Raymond W. Holton, Plant Physiol. <u>46</u>, 748 (1970).

39. Paschke, R. F. and D. H. Wheeler, J. Am. Oil Chem. Soc. <u>31</u>, 81 (1954).

40. Collyer, Dorothy M. and G. E. Fogg, J. Exp. Botany <u>6</u>, 256 (1955).

41. Vereshchagin, A. G. and G. L. Klyachko-Gurvich, Biokhimiya <u>30</u>, 469 (1965) (Eng. trans.).

42. Ast, Herbert J., Anal. Chem. <u>35</u>, 1539 (1963).

43. Schmid, Peter and Edward Hunter, Physiol. Chem. Phys. <u>3</u>, 98 (1971).

44. Schmid, Peter, Physiol. Chem. Phys. <u>5</u>, 141 (1973).

45. Handbook of Chemistry and Physics, 48th Edition, Chemical Rubber Company, Cleveland, Ohio (1967), p. D-7.

46. Schlenk, Hermann and Joanne L. Gellerman, Anal. Chem. <u>32</u>, 1412 (1960).

47. Vorbeck, Marie L., Leonard R. Mattick, Frank A. Lee and Carl S. Pederson, Anal. Chem. <u>33</u>, 1512 (1961).

48. Christie, W. W., Topics in Lipid Chemistry <u>3</u>, 171 (1972).

49. Metcalfe, L. D. and A. A. Schmitz, Anal. Chem. <u>33</u>, 363 (1961).

50. Metcalfe, L. D., A. A. Schmitz and J. R. Pelka, Anal. Chem. <u>38</u>, 514 (1966).

51. American Oil Chemists Society, Instrumental Committee, J. Am. Oil Chem. Soc. <u>45</u>, 103 (1968).

52. Fulk, Winifred Knuese and Mary S. Shorb, J. Lipid Res. <u>11</u>, 276 (1970).

53. Morrison, William R. and Lloyd M. Smith, J. Lipid Res. <u>5</u>, 600 (1964).

54. Lough, A. K., Biochm. J. <u>90</u>, 4C (1964).

55. Tove, S. B., J. Nutrition <u>75</u>, 360 (1961).

56. Mason, Michael E. and George R. Waller, Anal. Chem. 36, 583 (1964).

57. Huston, Charles K. and Phillip W. Albro, J. Bacteriol. 88, 425 (1964).

58. Cowan, J. C., in Fatty Acids, 2nd Ed., Part 5, Klare S. Markley (ed.), Interscience, New York (1968), Chapter XIV-A.

59. Lundberg, W. O., in Fish Oils, M. E. Stansby (ed.), Avi Publishing Company, Westport, CT (1967), Chapter 9.

60. Olcott, H. S., in Fish Oils, M. E. Stansby (ed.), Avi Publishing Company, Westport, CT (1967), Chapter 11.

61. Scott, Gerald, Atmospheric Oxidation and Antioxidants, Elsevier Publishing Company, Amsterdam (1965).

62. Holton, R. W., H. H. Blecker and M. Onore, Phytochemistry 3, 595 (1964).

63. Rosenberg, Abraham, Biochemistry 2, 1148 (1963).

64. Rosenberg, Abraham and Marc Pecker, Biochemistry 3, 254 (1964).

65. Nichols, B. W. and R. Moorhouse, Lipids 4, 311 (1969).

66. Halasz, I. and P. Walking, J. Chromatogr. Sci. 7, 129 (1969).

67. Kirkland, J. J., J. Chromatogr. Sci 7, 7 (1969).

68. Kirkland, J. J., Anal. Chem. 41, 218 (1969).

69. Majors, Ronald E., Am. Lab. 4, 27 (1972).

70. Majors, Ronald E., Am. Lab. 7, 13 (1975).

71. Majors, Ronald E., Anal. Chem. 44, 1722 (1972).

72. Williams, R. C., et al., Am. Lab. 5, 45 (1973).

73. Locke, David C., J. Chromatogr. Sci. 11, 120 (1973).

74. Novotny, Milos, et al., Anal. Chem. 45, 971 (1973).

75. Grushka, Eli and Edward J. Kikta, Jr., Anal. Chem. 1004A (1977).

76. Kirkland, J. J., Anal. Chem. 43, 36A (1971).

77. Leitch, R. E. and J. J. DeStefano, J. Chromatogr. Sci. 11, 105 (1973).

78. Berry, Laverne and Barry L. Karger, Anal. Chem. 45, 819A (1973).

79. Jackson, M. T. and R. A. Henry, Am. Lab. 6, 41 (1974).

80. Bombaugh, Karl J. and Robert F. Levangie, J. Chromatogr. Sci. 8, 560 (1970).

81. Conlon, R. D., Anal. Chem. 41, 107A (1969).

82. McNair, Harold M., Chromatographia 7, 161 (1974).

83. Fallick, Gary J. and James L. Waters, Am. Lab. 4, 21 (1972).

84. Majors, Ronald E., J. Chromatogr. Sci. 8, 338 (1970).

85. Hadden, Nina, et al., Basic Liquid Chromatography, Varian Aerograph (1971), Appendix TWO.

86. Martin, Michel, et al., J. Chromatogr. Sci. 12, 438 (1974).

87. Grushka, Eli, Anal. Chem. 46, 510A (1974).

88. Waters Associates, "WALCEP Resource Material", CS-11.

89. Snyder, L. R., Anal. Chem. 39, 698 (1967).

90. Knox, J. H., and M. J. Saleem, J. Chromatogr. Sci. 7, 614 (1969).

91. Majors, Ronald E., J. Chromatogr. Sci. 11, 88 (1973).

92. Wittmer, D. P., Waters Associates Inc., private communication.

93. Kirkland, J. J., J. Chromatogr. Sci. 10, 129 (1972).

94. Haer, Frederick C., An Introduction to Chromatography on Impregnated Glass Fiber, Gelman Instrument Company, Ann Arbor, MI (1969), Chapter 5.

95. Schlenk, Herman, in Fatty Acids, 2nd edition, Part 3, Klare S. Markley (ed.), Interscience, New York (1964), Chapter XX.

96. Mangold, Helmut K., J. Am. Oil Chem. Soc. 41, 762 (1964).

97. Rouser, George, J. Chromatogr. Sci. 11, 60 (1973).

98. Carroll, K. K. and B. Serdarevich, in Lipid Chromatographic Analysis, Vol. 1, Guido V. Marinetti (ed.), Marcel Dekker, (1967), Chapter 6.

99. Snyder, Lloyd R., Principles of Absorption Chromatography, Marcel Dekker, New York (1968).

100. Scott, Charles D. and Norman E. Lee, J. Chromatog. 83, 383 (1973).

101. Korn, Edward D., J. Lipid Res. 5, 352 (1964).

102. Mulder, J. L. and F. A. Buytenhuys, J. Chromatog. 51, 459 (1970).

103. Johnson, K. M., D. J. Stern and A. C. Waiss, Jr., J. Chromatog. 33, 539 (1968).

104. Waters Associates, "Chromatography" catalog (1970), p. 20.

105. Hendrickson, J. G., Anal. Chem. 40, 49 (1968).

106. Trowbridge, J. R., A. B. Herrick and R. A. Bowman, J. Am. Oil Chem. Soc. 41, 306 (1964).

107. Hirsch, Jules, J. Lipid Res. 4, 1 (1963).

108. Beijer, Karin and Ernst Nystrom, Anal. Biochem. 48, 1 (1972).

109. Privett, O. S. and E. Christense Nickell, J. Am. Oil Chem. Soc. 40, 189 (1963).

110. Schlenk, Herman and Joanne L. Gellerman, J. Am. Oil Chem. Soc. 38, 555 (1961).

111. Morris, L. J., J. Lipid Res. 7, 717 (1966).

112. Hogue, M., Amitabha Ghosh and J. Dutta, J. Am. Oil Chem. Soc. 50, 29 (1973).

113. DeVries, B., J. Am. Oil Chem. Soc. 40, 184 (1963).

114. Morris, L. J., D. M. Wharry and E. W. Hammond, J. Chromatog. 31, 69 (1967).

115. Emken, E. A., C. R. Scholfield and H. J. Dutton, J. Am. Oil Chem. Soc. 41, 388 (1964).

116. Wurster, C. F., Jr., J. H. Copenhaven, Jr. and P. R. Shafer, J. Am. Oil Chem. Soc. 40, 513 (1963).

117. McGaughey, Stepehn M., Brian A. Bidlingmeyer and William A. Dark, Waters Associates, private communication, 1976.

118. Pei, Patrick T-S., Robert S. Henly and S. Ramachandran, Lipids 10, 152 (1974).

119. Scholfield, C. R., J. Am. Oil Chem. Soc. 52, 36 (1975).

120. Scholfield, C. R., Anal. Chem. 47, 1417 (1975).

121. Locke, David D., J. Chromatogr. Sci. 12, 433 (1974).

122. Jamieson, George R., Topics in Lipid Chemistry 1, 107 (1970).

123. Landowne, R. A. and S. R. Lipsky, Biochim. Biophys. Acta 47, 589 (1961).

124. Lipsky, S. R., R. A. Landowne and J. E. Lovelock, Anal. Chem. 31, 852 (1959).

125. Oro, J., T. G. Tornabene, D. W. Nooner and E. Gelpi, J. Bacteriol. 93, 1811 (1967).

126. Jaeger, H., H. Klor, G. Blos and H. Ditschuneit, J. Lipid Res. 17, 185 (1976).

127. Onuska, F. I. and M. E. Comba, J. Chromatog. 126, 133 (1976).

128. Ackman, R. G. and J. D. Castell, Lipids 1, 341 (1966).

129. Gunstone, F. D., I. A. Ismail and M. Lie Ken Jie, Chem. Phys. Lipids 1, 376 (1967).

130. Litchfield, Carter, Raymond Reiser, A. F. Isbell and G. L. Feldman, J. Am. Oil Chem. Soc. 41, 52 (1964).

131. Panos, Charles, J. Gas Chromatog. 3, 278 (1964).

132. Ackman, R. G., J. Am. Oil Chem. Soc. 40, 558 (1963).

133. Miwa, Thomas K. et al., Anal. Chem. 32, 1739 (1960).

134. Woodford, F. P. and C. M. van Gent, J. Lipid Res. 1, 188 (1960).

135. Kovats, E., in Advances in Chromatography, Vol. 1, J. Calvin Giddings and Roy A. Keller (eds.), Marcel Dekker, New York (1965), p. 229.

136. Odham, Goran and Einar Stenhagen, in Biochemical Applications of Mass Spectrometry, George R. Waller (ed.), Wiley-Interscience, New York (1972), p. 211.

137. McCloskey, James A., Topics in Lipid Chemistry 1, 369 (1970).

138. Ryhage, Ragnar and Einar Stenhagen, J. Lipid Res. 1, 361 (1960.

139. Stenhagen, Einer, in Analysis and Characterization of Oils, Fats and Fat Products, Vol. 2, H. A. Boekenoogen (ed.), Interscience, New York (1968), p. 1.

140. Myher, J. J., L. Marai and A. Kuksis, Anal. Biochem., 62, 188 (1974).

141. Ryhage, Ragnar, and Einar Stenhagen, Ark. Kemi 13, 523 (1959).

142. McLafferty, F. W., Anal. Chem. 31, 82 (1959).

143. Hallgren, Bo, Ragnar Ryhage and Einar Stenhagen, Acta Chem. Scand. 13, 845 (1959).

144. Ryhage, Ragnar and Einar Stenhagen, Ark. Kemi 15, 291 (1960).

145. Matucha, M., L. Zilka and K. Svihel, J. Chromatog. 65, 371 (1972).

146. Waller, Geroge R., Proc. Okla. Acad. Sci. 47, 271 (1968).

147. Beynon, J. H., Mass Spectrometry and Its Applications to Organic Chemistry, Elsevier, Amsterdam (1960), Chapter 8.

148. Boone, Barbara, Ronald K. Mitchum and Stuart E. Scheppele, Int. J. Mass Spectrom. Ion Phys. 5, 21 (1970).

149. Biemann, Klaus, Mass Spectrometry: Organic Chemical Applications, McGraw-Hill, New York (1962), Chapter 5.

150. Heron, Elaine Jones, Finnigan Corporation, unpublished data.

151. Klein, Peter D., Adv. Chromatog. 3, 4 (1966).

152. Marshall, Lawrence M. and Delors Magee, J. Chromatog. 15, 97 (1964).

153. Davidson, Charles N., Charles K. Mann and Raymond K. Sheline, J. Phys. Chem. 67, 1519 (1963).

154. Piez, K. A. and Harry Eagle, Science 122, 968 (1955).

155. Blanc, Claude, Chanh-Trung Huynk and Lucien Espagno, J. Chromatog. 28, 177 (1967). LA-TR-74-18.

156. Blanc, Claude, Chanh-Trung Huynk and Lucien Espagno, J. Chromatog. 28, 194 (1967). LA-TR-74-19.

157. Gunter, B. D. and J. D. Gleason, J. Chromatogr. Sci. 9, 191 (1971).

158. Bayer, E., G. Nicholson and R. E. Sievers, J. Chromatogr. Sci. 8, 467 (1970).

159. Bentley, Ronald, Nripendra C. Saka and Charles C. Sweeley, Anal. Chem. 37, 1118 (1965).

160. VandenHeuvel, W. J. A. and Jack S. Cohen, Biochim. Biophys. Acta. 208, 251 (1970).

161. VandenHeuvel, W. J. A., J. L. Smith and J. S. Cohen, J. Chromatogr. Sci. 8, 567 (1970).

162. Herzfeld, Karl F. and Edward Teller, Phys. Rev. 54, 912 (1938).

163. Baertschi, P. and W. Kuhn, in Proc. Int. Symp. Isotope Separation, 1957, J. Kistenaker, J. Bizeleisen and A. O. C. Nier (eds.), North-Holland, Amsterdam (1958), Chapter 5.

164. Casal, Jorge, Steven Danyluk and Ralph T. Holman, unpublished results.

165. Althouse, Paul M. and Howard O. Triebold, Ind. Eng. Chem., Anal. Ed. 16, 605 (1944).

166. Desaty, D., A. G. McInnes, D. G. Smith and L. C. Vining, Can. J. Biochem. 46, 1293 (1968).

167. Tanabe, M. and G. Detre, J. Am. Chem. Soc. 88, 4515 (1966).

168. Matwiyoff, N. A. and T. E. Walker, in Stable Isotopes in the Life Sciences, International Atomic Energy Agency, 1977, p. 252.

169. Simpson, T. J., Chem. Soc. Rev. 4, 497 (1975).

170. Matwiyoff, N. A. and B. F. Burnham, Ann. N.Y. Acad. Sci. 206, 365 (1973).

171. Wehrli, F. W. and T. Wirthlin, The Interpretation of Carbon-13 NMR Spectra, Heyden (London), 1976, p. 123.

172. Breitmaier, Eberhard, Gunther Jung and Wolfgang Voelter, Angew. Chem., Int. Edn. 10, 673 (1971).

173. Levy, George C. and Gordon L. Nelson, Carbon-13 Nuclear Magnetic Resonance for Organic Chemists, Wiley-Interscience, New York (1972), p. 8.

174. Kuhlmann, Karl F. and David M. Grant, J. Am. Chem. Soc. 90, 7355 (1968).

175. McInnes, A. G., et al., in Topics in Carbon-13 NMR Spectroscopy, Vol. 2, George C. Levy (ed.) Wiley-Interscience, New York (1976), p. 132.

176. Standard E 386-76, American Society for Testing and Materials, 1976.

177. Burlingame, A. L., et al., J. Chem. Soc., Chem. Comm., 1972, 318.

178. Stoffel, W., O. Zierenburg and B. D. Tunggal, Hoppe-Seyler's Z. Physiol. Chem. 354, 1962 (1972).

179. Wenkert, Ernest, et al., in Topics in Carbon-13 NMR Spectroscopy, Vol. 2 George C. Levy (ed.), Wiley-Interscience, New York (1976), p. 82.

180. Kanohta, Kenzoh, Eisei Shikensho Hokoku, 1971, 1 (Japan).

181. Leyden, D. E. and R. H. Cox, Analytical Applications of NMR, Wiley Interscience, New York (1977), p. 228.

182. Marshall, James L., et al., Acct. Chem. Res. 7, 333 (1974).

183. London, Robert E., V. H. Kollman and N. A. Matwiyoff, J. Am. Chem. Soc. 97, 3565 (1975).

184. Wiberg, Kenneth B. and Bernard J. Nist, The Interpretation of NMR Spectra, W. A. Benjamin, Inc., New York (1962), p. 3.

185. Marshall, J. L. and D. E. Miller, J. Am. Chem. Soc. 95, 8305 (1973).

186. Weigert, F. J., and J. D. Roberts, J. Am. Chem. Soc. 94, 6021 (1972).

187. London, Robert E., Nicholas A. Matwiyoff and Delbert D. Mueller, J. Chem. Phys. 63, 4442 (1975).

188. McInnes, A. Gavin, et al., J. Chem. Soc., Chem. Comm., 1975, 66.

189. Dorn, Harry C. and Gary E. Maciel, J. Phys. Chem. 2972 (1972).

190. Schaefer, Jacob, J. Magn. Reson. 6, 670 (1972).

191. Crump, D. R., J. K. M. Sanders and Dudley H. Williams, Tetrahedron Letters 50, 4419 (1970).

192. Arduini, Anita, et al., Carbohydrate Res. 31, 255 (1973).

193. Sanders, Jeremy K. M., and Dudley H. Williams, J. Am. Chem. Soc. 93, 641 (1971).

194. Gansow, Otto A., M. R. Willcott and R. E. Lenkinski, J. Am. Chem. Soc. 93, 4295 (1971).

195. Hinckley, C. C., J. Am. Chem. Soc. 91, 5160 (1969).

196. Ammon, Herman L., Paul H. Mazzocchi and Elena J. Colicelli, Org. Mag. Res. 11, 1 (1978).

197. Bose, Ajay K. and R. J. Brambilla, Proc. First Intern. Conf. Stable Isotopes in Chem., Biol. and Medicine, 1973, p. 431.

198. Wenkert, R., et al., J. Am. Chem. Soc., 93, 6271 (1971).

199. Almqvist, S. O., C. R. Enzell and F. W. Wehrli, Acta Chem. Scand. B29, 695 (1975).

200. Chadwick, Derek J. and Dudley H. Williams, J. Chem. Soc., Perkin II, 1974, 1202.

201. Feline, Timothy, et al., J. Chem. Soc., Chem. Comm., 1974, 63.

202. Horrocks, William DeW., Jr. and James P. Sipe, III, J. Amer. Chem. Soc. 93, 6800 (1971).

203. Crump, D. R., J. K. M. Sanders and Dudley H. Williams, Tetrahedron Letters, 1970, 4949.

204. Rondeau, Roger E. and Robert E. Sievers, J. Am. Chem. Soc. 93, 1522 (1971).

205. Breitmaier, E. and W. Voelter, ^{13}C NMR Spectrometry: Methods and Applications, Verlag Chemie, Weinheim, West Germany (1974), p. 134.

206. Ahmad, Naseer, et al., J. Am. Chem. Soc. 93, 2564 (1971).

207. Descreax, Jean F., Lloyd E. Fox and Charles N. Reilley, Anal. Chem. 44, 2217 (1972).

APPENDIX A

CURVE FITTING PROGRAM LSMFT

LSMFT is a collection of Fortran programs combined into a system that permits a general approach to least squares problems. A complete description may be obtained from the Program Library or C. R. McInteer, S-1, P. O. Box 1663, Los Alamos Scientific Laboratories, Los Alamos, New Mexico 87545. Only a brief, simplified description is presented here.

For NPTS pairs of data points, (x_i, y_i), a curve of fitted if the general form

$$Y = F(X, P_1, P_2, \ldots, P_{NPARAM}).$$

The user may select from a number of pre-written functions (F012 = shewed Gaussian) or supply a function written for the particular problem.[*] The program determines values of $P_1, P_2, \ldots, P_{NPARAM}$ so as to minimize the difference function

$$\sum_{i=1}^{NPTS} (F(x_i, P_1, P_2, \ldots, P_{NPARAM})^2.$$

In order to do this, initial values (supplied by the user) for the parameters are incremented until the percent change in all of the parameters is less than the value of TEST (specified by the user).

The control cards used to fit the GC/MS data are listed on the following pages.

---

[*] If a user-supplied function is used, the partial derivative of F with respect to each parameter must also be supplied.

```
$OPEN(FS=Z05LSQS,TYPE=SP,OAC=ZD0)
$IF.
$OPERM(FS=Z05LSQS,OAC=ZD0,FSI=ZFSI)
$COPYF(I=Z05LSQS,O=NCCD)
$REWIND(NCCD)
$SETQ(KEY=KCCF,Q=NCCD)
$FM.
*IDENT AWH
*I,HERE.2
```

Subroutines for GS/MS
Calculations, see
Appendix B

```
$FM.
SET NPTS=30 NPARAM=5 NV=2 $
SET FIXPAR=5 PROPT=0 $
SET ALGOR=MARQUAR FUNC=F012 DFUNC=DF012   $
READ INPUT=LABELX $
          TIME IN SECONDS
READ INPUT=LABELY $
             ION CURRENT
READ INPUT=TEST $
   1.000E-3
CALL SUB=ISOTOPE $
```

Data Input

```
CALL SUB=SWITCH $
FIT ALGOR=MARQUAR $
PLOT PLTDATA=TRUE PLTCF=TRUE IYVAR=1 IXVAR=2 $
CALL SUB=KEEP $
CALL SUB=SWITCH $
CALL SUB=CORREC $
CALL SUB=ATOMS $
SET NPARAM=2 NV=2 FUNC=F001 DFUNC=DF001 $
READ INPUT=LABELX $
     TIME OF SCAN (IN SECONDS)
READ INPUT=LABELY $
         PER CENT OF MOLECULAR IONS
READ INPUT=TEST $
   1.000E-3
CALL SUB=CYCLE $
FIT ALGOR=PACKALG $
READ INPUT=LABELY $
         ATOM PER CENT CARBON-13
PLOT PLTDATA=TRUE PLTCF=TRUE IYVAR=1 IXVAR=2 $
SET NPARAM=2 NV=3 WOPT=2 NWOPT=3 $
READ INPUT=TEST $
```

```
   1.000C0E-5
SET FUNC=F002 DFUNC=DF002 $
READ INPUT=LABELX $
    NUMBER OF C13 ATOMS IN MOLECULE
READ INPUT=LABELY $
                    RETENTION TIME
CALL SUB=SLOPE $
FIT $
PLOT PLTDATA=TRUE PLTCF=TRUE IYVAR=1 IXVAR=2 $
FIT FUNC=F001 DFUNC=DF001 $
PLOT PLTDATA=TRUE PLTCF=TRUE IYVAR=1 IXVAR=2 $
SET LCHPLT=TRUE $
PLOT PLTDATA=TRUE PLTCF=TRUE IYVAR=1 IXVAR=2 $
STOP $
$FM,
SEJ,
```

APPENDIX B

FORTRAN PROGRAM FOR MASS SPECTRAL CALCULATIONS

```
C
      SUBROUTINE SLOPE
C
*CALL COMMON
      COMMON /EXTRA/DATA(25,99),M(25),PT(25,99),TIM1(99),N,NC,NP,NO,
     2NPEAK,CATOM,HATOM,OATOM,AC,AH,AO,AOX,PREP(99,9),N1,HEAD(8,25),
     3SKEEP(25),TKEEP(99),SP1(25),P2(25),SP2(25),P4(25),SP4(25),BKG(99),
     4 FRAC(25,99),COM(4),CPER(99),NVERG(25)
      DIMENSION XLOGC(99),XENR(99),TLOG(99),TLOGK(25),TLOGUP(25)
     2,TLOGD(25),XNAT(99)
      IX = 0
      IT = NC+3
      DO 2 I=3,II
      IX = IX+NVERG(I)
    2 CONTINUE
      JT = NC+1
      NPT = NC+1-IX
      NPTS = NC+1-IX
      JX = 0
      JJ = 0
      DO 30 J=1,JT
      JX = JX+1
      JJ = JJ+1
      IF(NVERG(J+2).EQ.1) GO TO 20
      X(JJ,1) = TKEEP(JX+2)
      XJ = JX-1
      X(JJ,2) = XJ+TEST
      X(JJ,3) = SKEEP(JX+2)
      GO TO 30
   20 CONTINUE
      JJ = JJ-1
   30 CONTINUE
      PG(1) = TKEEP(3)
      PG(2) = -.001
      PRINT 460, PG(1),PG(2),NPT
  460 FORMAT(/////2X,2(E14.7,4X),I4//)
      PRINT 470, (X(I,2),X(I,1),X(I,3),I=1,NPT)
  470 FORMAT(4X,F6.0,4X,F8.2,4X,F6.3)
      RETURN
      END
```

```
C
      SUBROUTINE CYCLE
*CALL COMMON
      COMMON /EXTRA/DATA(25,99),M(25),PT(25,99),TIM1(99),N,NC,NP,NO,
     2NPEAK,CATOM,HATOM,OATOM,AC,AH,AO,AOX,PREP(99,9),N1,HEAD(8,25),
     3SKEEP(25),TKEEP(99),SP1(25),P2(25),SP2(25),P4(25),SP4(25),BKG(99),
     4 FRAC(25,99),COM(4),CPER(99),NVERG(25)
      DIMENSION XLOGC(99),XENR(99),TLOG(99),TLOGK(25),TLOGUP(25)
     2,TLOGD(25),XNAT(99)
      EXTERNAL F001,DF001
      IYVAR = 1
      PLTDATA = 1
      NPTS = NO
      IXVAR = 2
      PLTCF = 1
      NPT = NC+1
   10 CONTINUE
      NCYCLE = NCYCLE+1
      IF(NVERG(NCYCLE+2).EQ.1) GO TO 10
      IF(NCYCLE.GT.NPT) GO TO 30
      DO 20 IK=1,NO
      X(IK,1) = FRAC(NCYCLE,IK)*100.
      X(IK,2) = TIM1(IK)
       K = NCYCLE+2
       DO 15 J=1,4
       PTITLE(J) = HEAD(J,K)
       TITLE(J) = HEAD(J,K)
   15  CONTINUE
   20 CONTINUE
      PG(1) = X(1,1)
      PG(2) =   (X(NO,1)-X(1,1))/(X(NO,2)-X(1,2))
      CALL PACKALG(F001,DF001)
      CALL OUTPACK
      CALL PLTPACK(F001)
      PRINT 222
  222 FORMAT(//)
      GO TO 10
   30 CONTINUE
      DO 35 J=1,NO
      X(J,1) = CPER(J)
      X(J,2) = TIM1(J)
   35 CONTINUE
       DO 40 J1=1,4
       TITLE(J1) = COM(J1)
       PTITLE(J1) = COM(J1)
   40  CONTINUE
      PG(1) = CPER(1)
      PG(2) = (CPER(NO)-CPER(1))/(TIM1(NO)-TIM1(1))
   50 CONTINUE
      RETURN
      END
```

```
C
      SUBROUTINE ATOMS
C
C  SUBROUTINE ATOMS USES THE CORRECTED SPECTRUM TO CALCULATE THE PERCENT
C  OF NATURAL ABUNDANCE MATERIAL, THE OVERALL ATOM PERCENT OF CARBON-13,
C  AND THE PERCENT OF EACH ISOTOPE ISOMER.
C
      COMMON /EXTRA/DATA(25,99),M(25),PT(25,99),TIM1(99),N,NC,NP,ND,
     2NPEAK,CATOM,HATOM,OATOM,AC,AH,AO,AOX,PREP(99,9),N1,HEAD(8,25),
     3SKEEP(25),TKEEP(99),SP1(25),P2(25),SP2(25),P4(25),SP4(25),BKG(99),
     4 FRAC(25,99),COM(4),CPER(99),NVERG(25)
      DIMENSION XLOGC(99),XENR(99),TLOG(99),TLOGK(25),TLOGUP(25)
     2,TLOGD(25),XNAT(99)
      NSPEC = 0
      DO 1 K=1,99
      XNAT(K) = 0.
      CPER(K) = 0.
      DO 1 L=1,25
   1  FRAC(L,K) = 0.
   5  NSPEC = NSPEC + 1
      IF(NSPEC.GT.NP) GO TO 100
      TOTAL = 0.
      C13 = 0.
      NX = NC+3
      DO 10 NN=3,NX
  10  TOTAL = TOTAL + PT(NN,NSPEC)
      ANAT = PT(3,NSPEC)*(1.+AC*(CATOM)+(AC*AC/2.)*CATOM*(CATOM-1.))
      XNAT(NSPEC) = (ANAT/TOTAL)*100
      XENR(NSPEC) = ((TOTAL-ANAT)/TOTAL)*100
      ND = NC+1
      DO 20 KK=1,ND
      KP = KK+2
      FRAC(KK,NSPEC) = PT(KP,NSPEC)/TOTAL
      AKK = KK-1
  20  C13 = C13 +FRAC(KK,NSPEC)*AKK
      CPER(NSPEC) = (C13/CATOM)*100
      XLOGC(NSPEC) = ALOG10(CPER(NSPEC))
      GO TO 5
 100  CONTINUE
      TIM1(NP) = 0.
      DO 15 K1=3,NX
      K = K1-2
  15  TIM1(NP) = TIM1(NP) + (TKEEP(K)*PT(K1,NP)/TOTAL)
      K2 = 0
  30  K2 = K2+1
      IF(K2.GT.NP) GO TO 31
      IF(TIM1(K2).EQ.0.) GO TO 30
      TLOG(K2) = ALOG10(TIM1(K2))
      GO TO 30
  31  CONTINUE
      PRINT 400
 400  FORMAT(///9X,*C13 ATOMS--*,2X,*0*,8X,*1*,8X,*2*,8X,*0*,8X,*4*,8X,
     2 *5*,8X,*6*,8X,*7*,8X,*8*,8X,*9*,8X,*10*//1X,*SPECTRUM NO.*/)
      DO 101 NSPEC=1,NP
 101  PRINT 401, NSPEC,(FRAC(KK,NSPEC),KK=1,11)
 401  FORMAT(5X,I2,12X,11(F6.5,3X)/)
      PRINT 402
 402  FORMAT(//8X,*C13 ATOMS--*,2X,*11*,7X,*12*,7X,*13*,7X,*14*,7X,*15*,
     2 7X,*16*,7X,*17*,7X,*18*,7X,*19*,7X,*20*//1X,*SPECTRUM NO.*/)
      DO 103 NSPEC=1,NP
```

```
103 PRINT 403, NSPEC,(FRAC(KK,NSPEC),KK=12,21)
403 FORMAT(5X,I2,12X,10(F6.5,3X)/)
    PRINT 404
404 FORMAT(//1X,*SPECTRUM NO.*,4X,*PERCENT NATURAL*,3X,*PERCENT ENRICH
   2ED*,3X,*ATOM PERCENT C13*,3X,*LOG10 ATOM*,6X,*TIME TO*,8X,*LOG10 T
   3IME*)
    PRINT 405
405 FORMAT(15X,*ABUNDANCE MATERIAL*,7X,*MATERIAL*,24X,*PERCENT C13*,
   26X,*POINT*)
    DO 106 NSPEC=1,NP
106 PRINT 406, NSPEC,XNAT(NSPEC),XENR(NSPEC),CPER(NSPEC),XLOGC(NSPEC),
   2TIM1(NSPEC),TLOG(NSPEC)
406 FORMAT(/5X,I2,14X,F6.3,12X,F6.3,11X,F7.3,11X,F7.4,7X,F6.0,8X,F7.5)
    DO 47 IND=1,N
    IF(TKEEP(IND).EQ.0.) GO TO 50
    TLOGK(IND) = ALOG10(TKEEP(IND))
 50 CONTINUE
    TUP = TKEEP(IND)+SKEEP(IND)
    IF(TUP.EQ.0.) GO TO 52
    TLOGUP(IND) = ALOG10(TUP)
 52 CONTINUE
    TDOWN = TKEEP(IND)-SKEEP(IND)
    IF(TDOWN.EQ.0.) GO TO 54
    TLOGD(IND) = ALOG10(TDOWN)
 54 CONTINUE
 47 CONTINUE
    PRINT 407
407 FORMAT(////2X,*NOMINAL MASS*,3X,*MEAN TIME*,3X,*STD. DEV.*,8X,
   2 *LOG10*,7X,*LOG10*,7X,*LOG10*/44X,*MEAN TIME*,3X,*LIMIT UP*,3X,
   3 *LIMIT DOWN*/)
    DO 108 NEW=1,N
108 PRINT 408, M(NEW),TKEEP(NEW),SKEEP(NEW),TLOGK(NEW),TLOGUP(NEW),
   2 TLOGD(NEW)
408 FORMAT(/6X,I3,8X,F8.2,4X,F7.3,9X,F7.5,4X,F7.5,4X,F7.5)
    PRINT 460
460 FORMAT(//19X,*AREA UNDER*,3X,*STD. DEV.*,6X,*SIGMA*,3X,*STD. DEV.*
   2 /21X,*CURVE*,7X,*OF AREA*,15X,*OF SIGMA*//)
    DO 70 NIP=1,N
 70 PRINT 470, HEAD(1,NIP),PT(NIP,NP),SP1(NIP),P2(NIP),SP2(NIP)
470 FORMAT(1X,A10,4X,F13.2,2X,F9.3,4X,F8.3,3X,F8.4)
    NCYCLE = 0
    RETURN
    END
```

```
C
      SUBROUTINE CORREC
C
C  SUBROUTINE CORREC SUBTRACTS THE CONTRIBUTION OF H2, O17, AND O18
C  FROM EACH PEAK TO PRODUCE A CORRECTED SPECTRUM. IT ALSO SUBTRACTS THE C13
C  CONTRIBUTION OF THE METHOXY CARBON.
C
      COMMON /EXTRA/DATA(25,99),M(25),PT(25,99),TIM1(99),N,NC,NP,NO,
     2NPEAK,CATOM,HATOM,OATOM,AC,AH,AO,AOX,PREP(99,9),N1,HEAD(8,25),
     3SKEEP(25),TKEEP(99),SP1(25),P2(25),SP2(25),P4(25),SP4(25),BKG(99),
     4 FRAC(25,99),COM(4),CPER(99),NVERG(25)
      DIMENSION XLOGC(99),XENR(99),TLOG(99),TLOGK(25),TLOGUP(25)
     2,TLOGD(25),XNAT(99)
      PRINT 401
  401 FORMAT(///2X,*NOMINAL MASS*,10X,*CALCULATED FROM CURVES*/)
      J2 = 0
    4 J1 = J2+1
      J2 = J1+9
      IF(J2.GT.NO) J2=NO
      DO 6 I=1,N
    6 PRINT 406, (M(I),(PT(I,J),J=J1,J2))
  406 FORMAT(5X,I3,8X,10(F7.1,3X))
      PRINT 407
  407 FORMAT(///)
      IF(J2.NE.NO) GO TO 4
      PRINT 408, (M(I),PT(I,NP),I=1,N)
  408 FORMAT(5X,I3,8X,E15.6)
      CF1 = AH*HATOM+AO*OATOM+AC*1.
      A1 =OATOM*(AOX+(OATOM-1.)*AO*AO/2.)
      A2 = HATOM*(HATOM-1.)*AH*AH/2.
      A3 = OATOM*AO*HATOM*AH
      A4 = AC*1.*(AH*HATOM+AO*OATOM)
      CF2 = A1+A2+A3+A4
      DO 13  J=1,NP
      DO 13  I=3,N
      IN = I-1
      IM = I-2
      CN = PT(IN,J)*CF1
      CM = PT(IM,J)*CF2
      IF(PT(I,J).EQ.0.) GO TO 13
      PT(I,J) = PT(I,J)-CN-CM
   13 CONTINUE
      PRINT 410
  410 FORMAT(///2X,*NOMINAL MASS*,10X,*CORRECTED PEAK INTENSITIES*/)
      J2 =0
   40 J1 = J2+1
      J2 = J1+9
      IF(J2.GT.NO) J2=NO
      DO 41 I=1,N
   41 PRINT 411, (M(I),(PT(I,J),J=J1,J2))
  411 FORMAT(5X,I3,8X,10(F7.1,3X))
      PRINT 412
  412 FORMAT(///)
      IF(J2.NE.NO) GO TO 40
      PRINT 413, (M(I),PT(I,NP),I=1,N)
  413 FORMAT(5X,I3,8X,E15.6)
      RETURN
      END
```

```
C
C
      SUBROUTINE KEEP
C
*CALL COMMON
      COMMON /EXTRA/DATA(25,99),M(25),PT(25,99),TIM1(99),N,NC,NP,NO,
     2NPEAK,CATOM,HATOM,DATOM,AC,AH,AO,AOX,PREP(99,9),N1,HEAD(8,25),
     3SKEEP(25),TKEEP(99),SP1(25),P2(25),SP2(25),P4(25),SP4(25),BKG(99),
     4 FRAC(25,99),COM(4),CPER(99),NVERG(25)
      DIMENSION XLOGC(99),XENR(99),TLOG(99),TLOGK(25),TLOGUP(25)
     2,TLOGD(25),XNAT(99)
      IF(.NOT.CONVERG) GO TO 40
      CHECK1 = PREP(N1,1)/P(1)
      IF(CHECK1.LT..01.OR.CHECK1.GT.100.) GO TO 40
      CHECK2 = PREP(N1,2)/P(2)
      IF(CHECK2.LT..01.OR.CHECK2.GT.100.) GO TO 40
      CHECK3 = PREP(N1,3)/P(3)
      IF(CHECK3.LT..01.OR.CHECK3.GT.100.) GO TO 40
      DO 50 JJ=1,NO
      PT(N1,JJ) = CF(JJ)
  50  CONTINUE
      PT(N1,NP) = P(1)
      TKEEP(N1) = P(3)
      SKEEP(N1) = SIGMAP(3)
      SP1(N1) = SIGMAP(1)
      P2(N1) = P(2)
      SP2(N1) = SIGMAP(2)
      P4(N1) = P(4)
      SP4(N1) = SIGMAP(4)
      GO TO 60
  40  CONTINUE
      NVERG(N1) = 1
      DO 30 IK=1,NO
      PT(N1,IK) = DATA(N1,IK)
  30  CONTINUE
      PT(N1,NP) = 0.
      TKEEP(N1) = 0.
      SKEEP(N1) = 0.
  60  CONTINUE
      RETURN
      END
```

```
C
      SUBROUTINE SWITCH
C
*CALL COMMON
      COMMON /EXTRA/DATA(25,99),M(25),PT(25,99),TIM1(99),N,NC,NP,NO,
     2NPEAK,CATOM,HATOM,OATOM,AC,AH,AO,AOX,PREP(99,9),N1,HEAD(8,25),
     3SKEEP(25),TKEEP(99),SP1(25),P2(25),SP2(25),P4(25),SP4(25),BKG(99),
     4 FRAC(25,99),COM(4),CPER(99),NVERG(25)
      DIMENSION XLOGC(99),XENR(99),TLOG(99),TLOGK(25),TLOGUP(25)
     2,TLOGD(25),XNAT(99)
      EXTERNAL F012,DF012
      PLTDATA = 1
      PLTCF = 1
      IYVAR = 1
      IXVAR = 2
      IKEY = 0
      NPTS = NO
      IF(N1.EQ.0) GO TO 10
      IF(.NOT.CONVERG) NVERG(N1) = 1
   10 N1 = N1+1
      IF(N1.GT.N) GO TO 55
      DO 20 IN=1,NO
      X(IN,1) = DATA(N1,IN)
      X(IN,2) = TIM1(IN)
   20 CONTINUE
      DO 30 LN=1,NPARAM
   30 PG(LN) = PREP(N1,LN)
      DO 40 I=1,8
   40 TITLE(I) = HEAD(I,N1)
      PRINT 400, TITLE
  400 FORMAT(///2X,*/////////////////////*,6X,8A10)
      DO 44 I=1,4
   44 PTITLE(I) = HEAD(I,N1)
      IF(N1.EQ.1.AND.IKEY.EQ.0) GO TO 99
      CALL MARQUAR(F012,DF012)
      IF(.NOT.CONVERG.AND.IKEY.EQ.0) CALL PLTPACK(F012)
      IF(.NOT.CONVERG) NVERG(N1)=1
      IF(IKEY.EQ.0.AND.NVERG(N1).EQ.1) GO TO 10
      CALL KEEP
      IF(IKEY.EQ.0) GO TO 10
      CALL OUTPACK
      CALL PLTPACK(F012)
      GO TO 10
   55 CONTINUE
      IF(IKEY.NE.0) GO TO 99
      PRINT 457
  457 FORMAT(///4X,*NOMINAL MASS*,4X,*SKEW FACTOR*,4X,*STD DEV OF S.F.*)
      N1 = N-1
      PRINT458, (M(IK),P4(IK),SP4(IK),IK=3,N1)
  458 FORMAT(8X,I3,11X,F6.4,12X,F6.4)
      WS = 0.
      WSKEW = 0.
      IDO = NC+1
      DO 60 K=1,IDO
      IF(NVERG(K+2).EQ.1) GO TO 60
      WX = 1./(SP4(K+2)*SP4(K+2))
      WS = WS+WX
      WSKEW = WSKEW+WX*P4(K+2)
   60 CONTINUE
      WSKEW = WSKEW/WS
```

```
      DO 70 J=1,N
      PREP(J,4) = WSKEW
      IF(NVERG(J).EQ.1) GO TO 65
      PREP(J,1) = PT(J,NP)
      PREP(J,2) = P2(J)
      PREP(J,3) = TKEEP(J)
   65 CONTINUE
      NVERG(J) =0
   70 CONTINUE
      DO 29 INN=1,N
      PRINT 209,(PREP(INN,J),J=1,NPARAM),NVERG(INN)
   29 CONTINUE
  209 FORMAT(F10.0,F5.1,F5.0,F7.4,F3.0,I10)
      FIXPAR(4) = 4
      TEST = 1.00000E-5
      N1 = 0
      IKEY = 1
      GO TO 10
   99 CONTINUE
      RETURN
      END
```

```
C
      SUBROUTINE ISOTOPE
C
*CALL COMMON
      COMMON /EXTRA/DATA(25,99),M(25),PT(25,99),TIM1(99),N,NC,NP,NO,
     2NPEAK,CATOM,HATOM,OATOM,AC,AH,AO,AOX,PREP(99,9),N1,HEAD(8,25),
     3SKEEP(25),TKEEP(99),SP1(25),P2(25),SP2(25),P4(25),SP4(25),BKG(99),
     4 FRAC(25,99),COM(4),CPER(99),NVERG(25)
      DIMENSION XLOGC(99),XENR(99),TLOG(99),TLOGK(25),TLOGUP(25)
     2,TLOGD(25),XNAT(99)
      AC = 1.080E-02
      AH = 1.6003E-04
      AO = 3.9093E-04
      AOX = 2.0048E-03
      READ 200, NPEAK,NO,CATOM,HATOM,OATOM,(COM(I),I=1,4)
  200 FORMAT(I3,1X,I2,2X,3(F2.0,1X),6A10)
      PRINT 450, (COM(I),I=1,4)
  450 FORMAT(////*===========*,2X,4A10,8X,*===========================*)
      NC = CATOM
      N = 4+NC
      READ 202, (BKG(J),J=1,N)
      READ 201, (TIM1(L),L=1,NO)
  201 FORMAT(12F6.0)
      DO 22  JJ=1,NO
   22 READ 202,(DATA(II,JJ),II=1,N)
  202 FORMAT(14F5.0)
      DO 25 JD=1,NO
      DO 25 ID=1,N
      IF(DATA(ID,JD).LT.1000.) GO TO 33
      IF(DATA(ID,JD).LT.2000.) GO TO 34
      GO TO 35
   33 DATA(ID,JD) = DATA(ID,JD)/10.
      GO TO 25
   34 DATA(ID,JD) = DATA(ID,JD)-1000.
      GO TO 25
   35 DATA(ID,JD) = (DATA(ID,JD)-2000.)*10.
   25 CONTINUE
      DO 26 J=1,N
      DO 26 K=1,NO
      DATA(J,K) = DATA(J,K)-(BKG(J)/10.)
      IF(DATA(J,K).LT.0.) DATA(J,K)=0.
   26 CONTINUE
      M(1)=NPEAK-2
      DO 27 II=2,N
   27 M(II) = M(II-1)+1
      HED = 6H MASS
      HD = 1H,
      HEAD(6,1) = 10H///////////
      HEAD(7,1) = 10H//////////
  128 FORMAT(A6,I3,A1)
      DO 28 II=1,N
      NVERG(II) = 0
      HEAD(6,II) = HEAD(6,1)
      HEAD(7,II) = HEAD(7,1)
      ENCODE(10,128,HEAD(1,II)) HED,M(II),HD
      DO 28 J=2,4
      HEAD(J,II) = COM(J)
   28 CONTINUE
      PRINT 451
  451 FORMAT(//2X,*NOMINAL MASS*,10X,*INPUT DATA FOR PEAK INTENSITIES*/)
```

```
      J2 =0
  50 J1 = J2+1
     J2 = J1+9
     IF(J2.GT.NO) J2=NO
     DO 52 II=1,N
  52 PRINT 452, (M(II),(DATA(II,JJ),JJ=J1,J2))
 452 FORMAT(5X,I3,8X,10(F7.1,3X))
     PRINT 453
 453 FORMAT(///)
     IF(J2.NE.NO) GO TO 50
     NNO = NO/2
     TIM2 = (TIM1(NO)-TIM1(1))/4.
     DO 29 INN=1,N
     PREP(INN,1) = DATA(INN,NNO)*60.
     IF(DATA(INN,NNO).EQ.0.) PREP(INN,1) = 60.
     PREP(INN,2) = TIM2
     PREP(INN,3) = TIM1(NNO)
     PREP(INN,4) = .001
     PREP(INN,5) = 0.
     PRINT 209,(PREP(INN,J),J=1,NPARAM)
  29 CONTINUE
 209 FORMAT(F10.0,F5.1,F5.0,F7.4,F3.0)
     NP = NO+1
     N1 = 0
     RETURN
     END
```

VITA

Anthony Wayne Harmon

Candidate for the Degree of

Doctor of Philosophy

Thesis: GAS CHROMATOGRAPHY/MASS SPECTROMETRY AND NUCLEAR MAGNETIC
RESONANCE ANALYSIS OF ^{13}C LABELED FATTY ACIDS

Major Field: Chemistry

Biographical:

Personal Data: Born in Donelson, Tennessee, February 18, 1943,
the son of Mr. and Mrs. J. Wilson Harmon, Rockmont, Georgia.

Education: Graduated from Campbell High School, Smyrna, Georgia
May, 1961; received the Bachelor of Science degree from
Bethany Nazarene College, Bethany, Oklahoma, May, 1965, with
a major in Chemistry; received the Master of Science degree
from Purdue University, West Lafayette, Indiana, June, 1967,
with a major in Analytical Chemistry; completed requirements
for the Doctor of Philosophy degree at Oklahoma State Uni-
versity, May, 1979.

Professional Experience: Student Assistant, Chemistry Department,
Bethany Nazarene College, 1962-1965; Graduate Assistant,
Chemistry Department, Purdue University, 1965-1967; Assistant
Professor, Bethany Nazarene College, 1967-1970; Graduate
Assistant, Chemistry Department, Oklahoma State University,
1970-1972; Associated Western Universities Fellowship at
Los Alamos Scientific Laboratories, 1972-1975; Graduate
Research Assistant, Los Alamos Scientific Laboratories,
Summer, 1975; Staff Member, Los Alamos Scientific Labora-
tories, 1976-1979.

Professional Organization: American Chemical Society.